Strategies for antibiofouling membranes

By William Joseph Cloete

Dissertation presented in partial fulfilment of the requirements for the degree of PhD (Polymer Science)

Supervisor: Prof. Bert Klumperman
Co-supervisor: Prof. Thomas Eugene Cloete

Department of Chemistry and Polymer Science

Stellenbosch University

March 2015

Declaration

By submitting this thesis electronically, I declare that the entirety of the work contained therein is my own, original work, that I am the sole author thereof (save to the extent explicitly otherwise stated), that reproduction and publication thereof by Stellenbosch University will not infringe any third party rights and that I have not previously in its entirety or in part submitted it for obtaining any qualification.

William Joseph Cloete December 2014

Abstract

Membrane filtration is increasingly used for municipal and industrial wastewater treatment because it is an effective way to filter out bacteria and organic compounds. One of the largest problems is biofouling of the membranes, which may lead to blockage of the membrane with organic biofilms. Such blockages require expensive interruptions to the filtration process for periodic cleaning and cause a decrease in membrane lifespan. The ideal solution to the biofouling problem would be the production of novel polymeric membranes that do not biofoul. Theoretically, this can be accomplished in two ways: (1) provide membrane surfaces to which bacteria and organic material are incapable of adhering, and (2) introduce reactive compounds on the membrane surface that degrade the biofilm.

In four data chapters written in the format of stand-alone publications, techniques were explored for the production of inherently anti-fouling membranes using the most current strategies of polymer synthesis and characterization. Specifically, Reversible Addition Fragmentation Chain Transfer (RAFT) polymerization is employed to graft an anti-adhesive layer of hydrophilic copolymer chains onto the surface of regenerated cellulose membranes. Then, the mechanism of control of the polymerization reaction of the hydrophilic copolymers was investigated in enable design of an optimized anti-adhesive surface layer. In the following two chapters, immobilization of different combinations of biomolecule-degrading enzymes on high surface area non-woven nanofibrous mats, produced via electrospinning, was investigated. The retention of their enzymatic activity was tested in order to first prove the principle that enzymes can retain activity once immobilized on a substrate. In the subsequent chapter two additional enzymes commonly used for biofilm remediation in clean-in-place (CIP) processes were immobilized on the nanofibers, on their own as well as in combination with each other.

Surface modification of regenerated cellulose membranes to introduce zwitterionic hydrophilic copolymers revealed that grafting of copolymers of *N*-vinylpyrrolidone (NVP) and maleic anhydride (MAnh) could be achieved through an R-group approach of RAFT-mediated polymerization. The MAnh contained in the polymer backbone or as end-groups of the polymer were converted to zwitterionic compounds. Upon exposure to bacteria, these membranes prevented adhesion of extracellular polymeric substances (EPS) and bacteria

cells to the membrane surface. An investigation into the underlying kinetics of RAFT-mediated polymerization showed that no control was achieved for 1:1 monomer ratios of NVP/MAnh for two types of RAFT agents. The lack of control was due to the acid-catalyzed dimerization of NVP occurring at a very large extent. Copolymerization was affected at even small amounts of MAnh but, once consumed, an initialization step for NVP was observed. This provides a means of incorporating short segments of the functional MAnh monomer in the copolymer whilst maintaining reasonable control over the polymerization using RAFT chain transfer agents.

As an alternative to anti-cell adhesive surfaces, immobilization of enzymes on nanofibrous mats holds promise for the *in situ* degradation of organic biofilms. First, horseradish peroxidase and glucose oxidase were immobilized via nucleophilic addition of primary amines of the enzyme to reactive maleic anhydride residues in the copolymer backbone to prove the principle and illustrate that cascade reactions can be performed with catalytically active immobilized enzymes. Next, the combined immobilization of protease and α-amylase, two enzymes commonly used for biofilm remediation, enabled the degradation of protein and starch solutions. Co-immobilization led to an unexpected increase in activity of the α-amylase, but at the same time a significant decrease in protease activity.

The results obtained from the strategies explored in this thesis bode well for the future of manufacturing inherently anti-biofouling membranes and may very well lead to making membrane filtration economically more feasible to produce safe potable water, especially in the developing world.

Acknowledgements:

I would like to acknowledge and thank my supervisor Prof Bert Klumperman for all the support and research freedom, not only during this project but ever since I joined the group more than 6 years ago. The support of all members of Klumperman-group was crucial in completing this project.

I would like to acknowledge and thank my co-supervisor, Prof Eugene Cloete, for all his encouragement and, "mentoring by means of storytelling". In turn, I would like to thank his personal assistant, Inge-Rae Scholtz, as well as the members of his microbiology research group for their assistance and support.

I would like to thank Prof Pieter Swart, Craig Adriaanse and Stefan Hayward for all their support in developing and executing the enzyme immobilization studies.

I am grateful to Prof Christopher Barner-Kowollik , Dr Anja Goldmann and the rest of his research group for accommodating me on a research stay at their laboratories at Karlsruhe Institute of Technology (KIT).

I am also extremely grateful for the research scholarships and support I received from the DAAD-NRF.

The following people are acknowledged for their excellent support in either assisting with some of the analyses or discussions around the characterization of the materials produced in this project:

Elsa Malherbe, Dr Jaco Brand (*NMR, SU*)

Dr Nadine Pretorius (*SEC, SU*)

Prof Gideon Wolfaardt and Dr Elana Bester (*Biofilm evaluations, SU*)

Dr. Thomas Tischer (*FT-IR Microscopy, KIT*)

Vanessa Trouillet (*XPS, KIT*)

Research assistance: Lehani Verwey, Jason Daniels, Linda Scholtz, Ben van der Westhuizen

The staff of the Department of Polymer Science, Stellenbosch University

I would like to thank my parents, Tommy and Ingrid, for all their support and encouragement throughout my life and essentially for the education and guidance that led up to the completion of this project. To my family and friends, thank you for always believing in me and accepting my seemingly endless 'rain checks' when it came to lighting fires and the braaing of saddle chops.

Finally I would like to thank Corey for all her encouragement and for always being there when I sometimes relied on her to be 109 % of my support system. Your love and support made all the difference!!!

Table of Contents:

List of figures

List of schemes:

List of tables:

Chapter 1: Prologue

1.1 Introduction

Approximately 1.1 billion people worldwide lack access to potable water and as many as 2.6 billion people lack access to proper sanitation[1]. Desalination and other filtration processes are becoming increasingly vital for production of potable water and residential and commercial waste water remediation. Rapid advances in Thin Film Composite (TFC) membrane technology and its implementation are leading to the widespread application of reverse osmosis (RO) and ultrafiltration (UF) processes to provide a solution to water purification. The efficiency of these processes, however, is reduced due to biofouling of the polymeric membranes by aggregates of microorganisms. Cells initially adhere to the membrane surface and then to each other, leading to the formation of a gel-like matrix that grows on the surface and blocks membrane pores. This in turn leads to a large decrease in volumes of purified water produced and the lifespan of the membrane.

At present, thin biofilms can be removed by back washing and scrubbing with surfactant/soap solutions. Alternatively, biofouling can be inhibited and controlled by two methods: by pre-treating feed water to reduce the amount of nutrients or with the use of biocides blended into membranes to kill bacteria and prevent biofilms from maturing. These methods, however, do not prevent cell adhesion or accumulation of dead bacterial cells. At present, none of these methods are completely effective, economically feasible or environmentally friendly. Pre-treatment and backwashing are expensive, while excessive use of surfactants and biocides that leach from membranes over time, leads to large scale environmental problems. The degradation products of some surfactants (alkyl phenol ethoxylates) are known endocrine disrupters and long term retention of surfactants and biocides in the environment leads to residual toxicity as well as biocide-resistant bacteria.

With recent emphasis on the importance of membrane filtration for the supply of potable water to communities, any development towards the efficacy of membrane filtration is highly important. The main focus of this study is to improve the sustainability and cost effectiveness of

membrane filtration and doing so in a way that will have little to zero negative impact on the environment. Improving the ease of application and cost-effectiveness of membrane technology will increase the lifespan of the individual membranes, making the process more sustainable and ensure increased availability of membrane processes for clean and safe drinking water. This will allow the treatment process to be available to even remote communities that in the past could not benefit from membrane technologies due to high initial and maintenance costs. The study aims to make membrane filtration, as a means to clean drinking water, accessible to people of all walks of life by providing technologies that can be adopted with minimal research and development (R&D) efforts.

The study seeks to provide a facile means for surface modification of already commercially available filtration membranes. The materials that these membranes are made of, such as cellulose acetate and nylon, contain reactive functional groups on their surfaces. Using specific surface chemistry, the functional groups are activated and used as initiation site to grow polymer chains from. These so-called grafted polymer chains are hydrophilic and will render the surface anti-adhesive towards bacteria cells. In the case of polyethersulfone (PES) membranes that do not contain these reactive groups, these can easily be introduced via corona treatment of the surface. As a proof of principle, commercially available regenerated cellulose membranes were used to demonstrate the effective surface modification making use of reactive hydroxyl functional groups on the membranes surface. Successful surface modification for antifouling membranes using hydroxyl groups as a starting point will lead to a universal technique for surface modification of filtration membranes. In addition, functional electrospun nonwoven membranes (ENMs) were evaluated as a support for immobilizing enzymes known for biofilm remediation. The development of ENMs as ultrafiltration media has increased over the last decade and functionalized with immobilized enzymes as inherently anti-biofouling membranes may find this technology more readily implemented as alternative to conventional membranes in the near future.

The present study will have a large scale impact on the manufacturing cost of desalinated and ultra-filtrated water, making it a more feasible means of producing potable water in arid

regions. Without the cost of expensive pre-treatment and increased lifespan of membranes, filtration can be used more widely as a means to provide potable water to communities.

1.2 Objectives

The main objective of this study was the introduction of anti-bioufouling properties to biomaterials for potential use as filtration media. Surface grafting of regenerated cellulose with hydrophilic polymers was conducted using RAFT polymerization to obtain anti-cell adhesive membrane surfaces containing antimicrobial and zwitterionic functionalities.

ENMs containing immobilized protease and α-amylase for the degradation of proteins and starch were developed for future use as high surface area filtration media with inherent anti-bioufouling properties.

1.3 Thesis outline

Chapter 1 – Prologue

This chapter briefly highlights the importance for the development of efficient membrane technologies for the production of potable water. The motivation for the study is presented in light of the problems associated with biofouling of TFC membranes decreasing the feasibility of widespread use of membrane filtration as a means for the production of potable water.

Chapter 2 – Literature review

This chapter gives a brief overview of the use of membrane filtration for the remediation of waste water and the production of potable water. Here the problems associated with membranes filtration in particular biofouling is covered as well as current strategies for biofouling remediation and prevention in water treatment processes. The review also covers alternative materials to be used as TFC membranes and surface modification techniques to introduce inherent anti-biofouling properties to these materials. In order to supplement the background related to each strategy discussed in this thesis, each subsequent chapter also

contains relevant background information related to that section in the form of a short introduction.

Chapter 3 - Surface modification of regenerated cellulose for improved anti-biofouling properties

Chapter 3 describes the production of inherently anti-fouling regenerated cellulose membranes through the use of an R-group approach of RAFT polymerization. Surface grafting of hydrophilic poly(*N*-vinyl pyrrolidone) (PVP) and copolymers with antimicrobial and zwitterionic derivatives of maleic anhydride (MAnh) is described and evaluated for the anti-fouling properties it bestows on the cellulose membranes.

Chapter 4 - Initialization behavior of RAFT-mediated copolymerization of *N*-vinylpyrrolidone (NVP) and maleic anhydride (MAnh)

Little is known about the kinetics and underlying mechanisms of copolymerization of NVP and MAnh using RAFT polymerization. This chapter seeks to establish whether control over the copolymerization of NVP and MAnh is achieved employing two types of RAFT agents known to control the copolymerization of these monomers in combination with other monomers, respectively. Controlled polymerization of a hydrophilic monomer such as NVP in combination with a functional monomer such as MAnh will go a long way in producing functional copolymers for surface grafting and modification of filtration membranes.

Chapter 5 - Facile immobilization of enzymes on electrospun poly(styrene-*alt*-maleic anhydride) nanofibres

This chapter comprises of a manuscript published in the journal *Polymer Chemistry* on the use of electrospun nanofibers for the immobilization of enzymes, horse radish peroxidase (HRP) and glucose oxidase (GOX)[2]. The publication is included to serve as background and motivation for the work done on enzyme immobilization in Chapter 6.

Chapter 6 - Degradation of proteins and starch by combined immobilization of protease and α-amylase on a single electrospun nanofibrous membrane

Protease and α-amylase are commonly used in clean-in-place (CIP) treatment processes of membrane filtration systems as a means for biofilm remediation and control. These processes are often not economically feasible due to the fact that the enzymes used cannot be recovered and recycled. This chapter provides a means of immobilizing these enzymes on high surface area nanofibrous materials for potential use as inherently antibiofouling membranes.

Chapter 7

A comprehensive summary of the main findings is presented along with detailed strategies to extend these concepts for the development of inherently anti-biofouling filtration media.

Bibliography

(1) Montgomery, M. A.; Elimelech, M. *Environ. Sci. Technol.* **2007**, 17.

(2) Cloete, W. J.; Adriaanse, C.; Swart, P.; Klumperman, B. *Polym. Chem.* **2011**, *2*, 1479.

Chapter 2: Literature Review

The worldwide lack of clean and safe drinking water has driven widespread research into the development of membrane filtration processes as a means to increase the capacity of treating industrial and municipal effluent. Membrane filtration and membrane bioreactors for the treatment of waste water effluent are increasingly used in combination or as alternative to conventional sedimentation and activated sludge processes to remove organic and particulate matter from waste water[1]. In spite of its wide applicability and numerous advantages, membranes used for filtration suffer from biofouling causing significant operational problems. This leads to an ever-increasing demand for the development of inherently anti-biofouling materials to be used in these processes. In this review, the major problems observed with biofouling (specifically related to membrane filtration) are discussed along with ways of remediation and ongoing research into strategies to control biofilm formation.

2.1 Membrane filtration

Membrane filtration is a process by which soluble and insoluble matter is excluded or separated from a solution, based on size, as it passes through a physical barrier subjected to a driving force across the membrane. In water treatment, the feed is separated into two streams, the permeate, containing solutes that pass through the membrane and the concentrate containing particles and dissolved matter that are excluded or rejected by the membrane. Filtration processes are classified based on the size of the particulates they exclude and are coined RO (Reverse Osmosis), NF (Nanofiltration), UF (Ultrafiltration), MF (Microfiltration) and MCF (Membrane Cartridge Filtration) based on the pore sizes of the membranes used[2].

2.2 Membranes for water treatment

Membranes for water treatment are characterized based on their molecular weight cut-off (MWCO) which is defined as the molecular weight of the smallest molecules the filter is able to separate from the permeate. In municipal wastewater from domestic waste streams, UF

membranes are often employed due to their capability of filtering proteins, starches, various microorganisms, bacteria and viruses. In the case of desalination of sea water, RO membranes have a much lower MWCO for the rejection of salts and have a MWCO smaller than 100 Daltons.

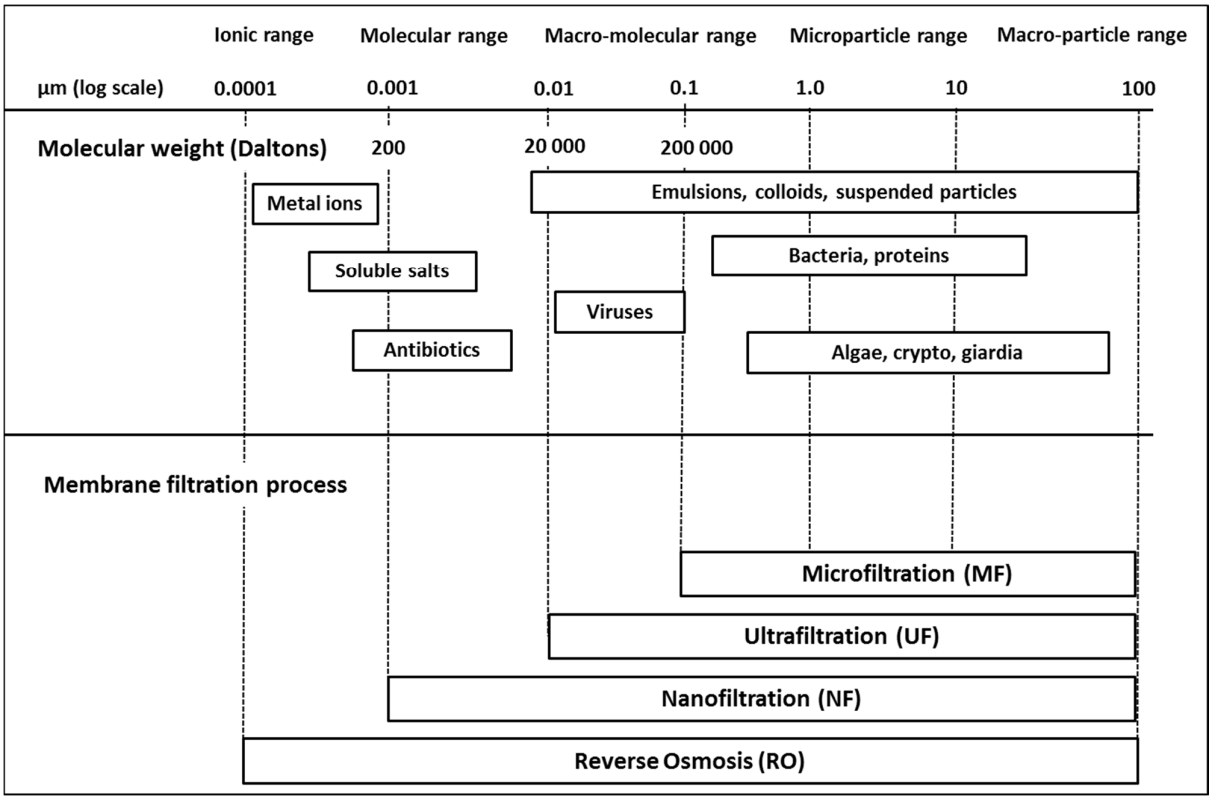

Figure 2.1 Diagram showing the various MWCO ranges and type of impurities that can be filtered using different kind of membranes (reproduced with permission[2]).

Membranes for water filtration are generally manufactured through phase inversion after solvent casting. Hollow-fiber UF and RO membranes are also produced through extrusion into water baths. The type of membrane, hollow-fiber or flat sheets, determines their assembly into filtration modules. Flat sheet membranes are typically assembled in spiral wound modules or cartridges, whereas tubular membranes are bunched together in bundles and configured in tubular modules. Cartridge configuration often makes use of pleated flat sheet membranes to increase the membrane surface area for filtration. Synthetic membranes for filtration are made from a wide range of polymers, cellulose acetate (CA), polyvinylidene fluoride (PVDF), polyacrylonitrile (PAN), polypropylene (PP), polysulfone (PS), and polyethersulfone (PES), amongst others[3]. Synthetic polymer membranes are preferentially

used in water filtration processes due to their considerably lower cost compared to other types of membranes such as ceramics[4].

Membranes for filtration are becoming an increasingly viable means for treatment of waste water, municipal and industrial. Since they are predominantly made up from synthetic materials, it is important to develop membranes from more sustainable sources. In addition, it is vital to increase the antifouling nature of membrane surfaces to increase their lifespan and reduce operating costs.

2.3 Biofouling

Biofouling can be seen as the deposition and irreversible attachment of microorganisms and bacteria on a surface, which subsequently grow into large colonies called biofilms[5]. Ship hulls and materials used in water treatment processes are especially susceptible to biofouling, and biofouling is even known to occur in biomedical devices and oral cavities[6,7]. Membranes used in filtration processes are susceptible to various kinds of fouling such as scaling, colloidal fouling and organic fouling, but biofouling is considered to cause the most serious damage and is also the most difficult to control[1]. Biofouling not only leads to a decrease in permeate flux, but also has implications in terms of membrane lifespan. This is due to the blocking of the membrane pores due to the presence of mature biofilms, which in turn requires cleaning with harsh oxidizing chemicals that not only degrade the biofilm, but oxidizes the outer layer of the membranes which is crucial to achieve separation[8]. Biofouling readily occurs on membrane surfaces due to inherent properties such as surface roughness and their hydrophobic nature and reduction of these can potentially make membranes less susceptible to biofouling. Investigations using atomic force microscopy (AFM) to evaluate the extent and fouling rate of smooth vs. rough membrane surfaces found that fouling more readily occurs on membranes with a slightly rougher surfaces[9]. The rough surfaces have valleys in which particles and foulants can accumulate, leading to irreversible attachment and clogging of membrane pores.

2.4 Bacterial biofilms

Bacterial biofilms form in a series of distinct phases. During the first stage, single cells associate loosely with the membrane surface during which it is covered by a conditioning film of proteins and macromolecules or extracellular polymeric substances (EPS). The onset of this

"slimy" layer during the initial stages of biofilm formation can take place within a matter of seconds. In the next stage there is irreversible attachment, usually over a time scale of minutes, during which the cells express proteins and exopolymers that adhere to the membrane surface. Over the hours and days that follow proliferation of bacteria cells leads to the formation of micro colonies which constitute a biofilm that can continue to mature over time. In the period that follows, dissolution of the micro colonies leads to dispersion of the biofilm and attachment to other sections of the membrane surface whilst leaving remnant structures of the biofilm behind[1]. The three main stages in bacterial biofilm formation are illustrated in Figure 2.2.

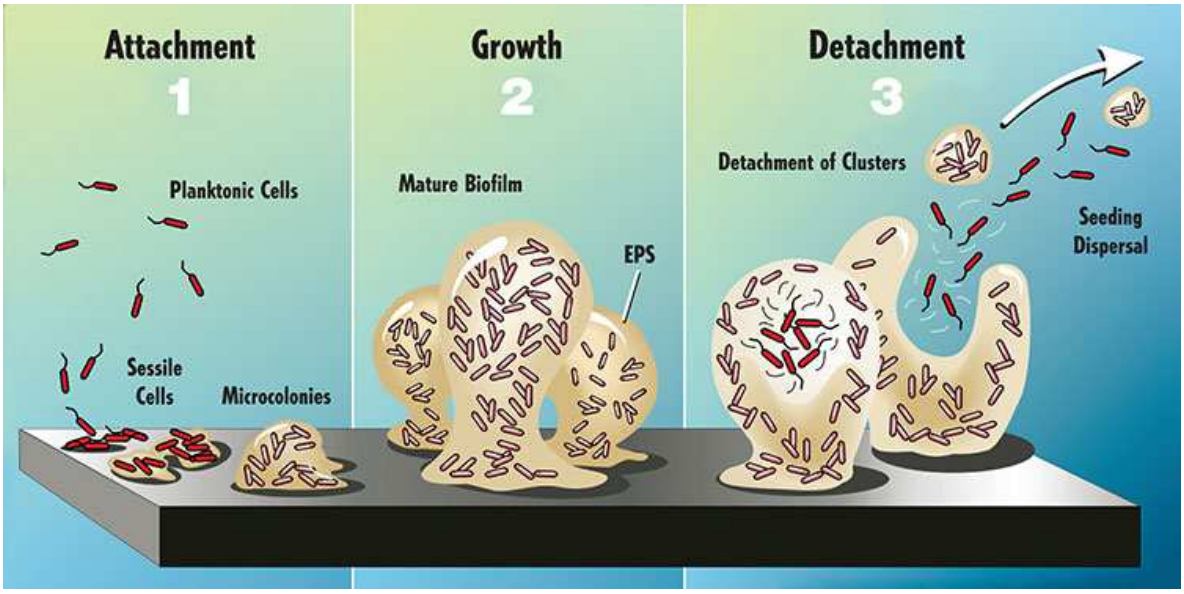

Figure 2.2 Illustration of the main stages of biofilm formation (reproduced with permission) [10]

2.5 Why is biofouling such a big problem?

Biofouling is an extremely costly problem in many industrial processes[11]. How costly, is however difficult to assess due to its ubiquitous nature and the many factors that need to be taken into account.. Besides leading to decreases in process performance as a result of down time and shortened life-time of equipment it also impacts on product quality and quantity. Biofilms are essentially hydrogels that grow to sizes where they physically block membrane pores. This implies that increased pressure is needed to obtain a decent flux of clean water as permeate and as a result leads to increased energy costs to operate the process.

Control of biofouling in membrane filtration is especially difficult, since it cannot always be reduced by pre-treatment of the feed to the filter. Pre-treatment of feed water usually involves the coagulation and precipitation of natural organic materials by addition of suitable flocculants followed by slow sand filtration or a course filter to trap the colloids. This process removes materials that can reversibly or irreversibly adhere to membranes which can act as nutrients for growing biofilms. They can, however, not effectively remove bacteria and other microorganisms. As a result of ineffective removal and due to the self-replicating nature of microorganisms capable of forming mature biofilms, as little as a single microorganism can lead to the formation of a mature biofilm. Thus, for pre-treatment to be successful it would in essence require the absolute removal of bacteria and microorganisms which cannot easily be achieved with conventional forms of pre-treatments that are currently employed. For the purpose of desalination using RO membranes, which are very expensive, it is however essential to remove microorganisms that can potentially foul the membranes. To this end UF filtration is used as pre-treatment of the feed to the RO membrane modules. This significantly increases the cost of desalinated water through the addition of an upstream filtration processes and equipment where the membranes themselves are essentially also susceptible to biofouling and require cleaning programs and periodic replacement of the filters. The costs incurred as a result of biofouling was assessed for an RO plant in Orange County, California[12]. Here it was found that membranes had a lifetime of only 4 years as opposed to the expected theoretical lifespan of 8 years. The decrease in lifespan was believed to be as a result of damage to the membranes by chemical cleaning agents to remove biofilms. Energy consumption due to biofouling also increased significantly due to the increased hydraulic resistance caused by the biofouling layer. This meant that the plant needed to operate at pressures roughly a 150% higher than the initial operating pressure for more than 80% of the lifetime (4 years) of the membrane. Due to decreased lifespan of membranes, additional energy requirements as well as chemicals required for cleaning and inhibition of biofilms the total costs incurred as a result of biofouling amounted to 30 % of the total operating costs for the plant[12].

2.6 Common strategies to prevent biofouling

Control of biofilm formation on membranes is complicated by the many factors that can influence biofilm formation. These factors include the specific operating conditions such as shear and pressure, the nature of the bacteria in the feed, the surface roughness and hydrophobicity of the membrane surface as well as environmental factors such as pH, ionic strength of and ion species contained in the feed[13].

2.6.1 Biocide doping

It is common practice to kill biofilms by the addition of a biocide to the feed[14]. Biocides are capable of killing the bacteria and essentially the biofilm, but is not effective in removing the biofilm altogether. However, killing the biofilm is often not a trivial exercise since the EPS matrix of the biofilm provides some form of protection to bacteria and microorganisms that are embedded deep within this matrix [15]. Effective killing of the biofilm also does not prevent the surface from being recolonized with biofilm-forming bacteria and the dead biofilm may even accelerate the process by providing the ideal niche and nutrients needed for bacterial colonization. In addition, bacteria build up resistance to the biocides used for routine control of biofilms. Since they are not effectively removed from the permeate stream and invariably end up in waste water streams , the residual toxicity of biocidesmay have large scale environmental impacts, besides the problems already caused by the residual toxicity of biocides, [16]. Biofouling control through the use of biocides is largely ineffective due to the careless nature in which they are applied[17]. Often, little consideration is given to the nature of the bacteria and biofilms that need to be killed and whether the biocide used is in fact able to kill the organisms involved. In terms of biofouling control it is also necessary to use the biocide at specific frequencies to achieve total destruction of the biofilm as well as preventing re-colonization. Another problem is the slow release of biocides from membranes. The release from the membrane does not happen in a controlled fashion and this may lead to a sub-lethal dose of the biocide constantly administered to the bacteria in the biofilm. Biocide dosing below the minimum inhibition concentration (MIC) or minimum bactericidal concentration (MBC) is one of the major contributors leading to the proliferation of biocide-resistant bacterial strains.

Different classes of biocides have different modes of operation which require different time scales and concentrations for effective killing. For example, polymeric biguanides as biocide

has activity against Gram-negative bacteria. These biocides are able to readily attach to the negatively charged cell surfaces and is active under pH neutral or alkaline conditions. They act by rupturing the cell wall, resulting in leaking of cytoplasmic constituents that leads to cell death. This process is not instantaneous, but requires a few minutes for the killing of a bacteria cell to take place. Two biguanides commonly used in industrial processes are polyhexamthylene biguanide (PHMB) and 1,6-di(4-chlorophenyldiguanido)-hexane or chlorhexidine. Although highly effective, they are also extremely corrosive. This limits their use and is especially not suited for use in cooling water systems. The fact that the mode of action is not instantaneous begs the need to apply a sufficient amount to make sure that all the bacteria are killed before they can attach to any surfaces.

Aldehyde-based biocides, such as formaldehyde and gluteraldehyde, are popular and have activity against a wide range of bacteria. These highly polar compounds with their high nucleophilic reactivity react with free amino groups to form methylolamines that react with vital cellular components. Reactions with cell components such as membrane porins adversely affects their transport properties and leads to a decrease in the rate of protein uptake and enzyme synthesis. Formaldehyde has been classified as a human carcinogen and its use for most applications has been banned along with other toxic compounds such as tributyltin (TBT), which were previously widely used to kill bacteria and prevent biofouling. Oxidizing agents such as hypochlorous acid and hydrogen peroxides are also widely used for biofilm remediation. These chemical species are by nature destructive not only towards biofilms and their components, but as a non-selective oxidant they can react with all biological molecules as well as the membrane surfaces destroying the surface and corroding system components. Although careful consideration and well thought out biocide treatment programs may make this process more effective, the negative aspects of biocide use far outweighs the benefits.

2.6.2 Backwashing, surfactants and clean-in-place (CIP)

Cleaning of membranes often involve the use of alkaline and acidic solutions ($NaOH_{(aq)}$, $HCl_{(aq)}$), metal chelating agents (EDTA), strong oxidising agents ($NaOCl_{(aq)}$)and surfactants such as SDS[18]. Alkaline solutions hydrolyze polysaccharides, sugars and proteins, and are mainly used for the removal of organically-fouled membranes. . Extensive use of alkaline solutions, however, leads to damage to the membrane itself, as well as corrosion problems upstream and downstream of the filtration system. Organic fouling layers are often bound together by

means of divalent cations and the use of chelating agents cause a breakdown of the stable layer by solubilizing and removing the cations. The large-scale use of chelating agents, however, can lead to the solubilisation and contamination of drinking water by toxic heavy metals. Surfactants also lead to residual toxicity and downstream contamination of water bodies due to the fact that many of them in themselves or their degradation products are classified as endocrine disruptors affecting marine life and humans[19,20]. Enzymes such as proteases and amylases have been evaluated for the CIP of membrane systems and bioreactors with the advantage of causing no degradation to the filtration system or membranes[21]. The disadvantage of using enzymes for biofilm remediation is that multiple cycles are necessary for the effective cleaning and the costly enzymes cannot be recovered for future use. Avoiding the use of any cleaning agents in CIP processes is possible, but are expensive ost due to the fact that additional energy is required for backwashing and scrubbing with compressed air. This strategy also invariably requires downtime and effective loss in production during backwashing and scrubbing.

2.6.3 Protein-degrading films, antimicrobial coatings and surface modifications

A number of recent developments centred around producing surface active films that are capable of killing bacteria and degrading biofilms[22]. These typically involve the impregnation of biocides that can be released over time to kill bacteria on the membrane surface and surroundings. Due to the mode of operation requiring leaching from the membrane, the antimicrobial activity is invariably lost over time. The covalent attachment of polycationic species such as quaternary ammonium compounds (QACs) is considered to provide surfaces that are inherently, and thus permanently, antimicrobial. The exact mode of operation and how they bring about cell death is not fully understood, but the proposed mechanism is that the positive charge on the nitrogen atom is capable of attracting and immobilizing bacterial cells. Bacteria typically have a negatively charged cell wall and after immobilization by the positively charged QAC, one or more of the long aliphatic chains of the quaternary ammonium salt are capable of penetrating the cell to cause cell lysis[23]. The area of research to introduce QACs to achieve functional polymers is growing and with the advent of controlled surface grafting of membrane surfaces may see this strategy adopted widely as a means to permanently antimicrobial membrane surfaces[23,24].

Surfaces modified with polymers containing zwitterionic functionality have been shown to possess improved antifouling properties. Kostina *et al*. demonstrated that surface grafting of copolymers containing different ratios of carboxybetaine monomers and 2-hydroxyethyl methacrylate resulted in non-fouling surfaces[25]. The reason for the fouling resistance is attributed to the enhanced wettability. As little as 10 mol % of carboxybetaine acrylamide, complete resistance against fouling with blood plasma was achieved. In another study, Rodriguez-Emmenegger *et al.* demonstrated that a 90 % reduction against fouling of blood plasma was achieved and zero fouling from single protein solutions by employing a substrate-independent surface modification with zwitterionic graft polymers[26]. The surface modification method does not rely on availability of reactive groups on the surface and can be used for a wide range of surfaces, including inert surfaces such as polypropylene. All surfaces in this study were first "activated" with a functional layer of Nylon 6,6 through plasma sputtering of the polymer. Through this Nylon 6,6 layer, an ATRP initiator could be introduced through acylation of the amide groups in the polymer backbone using α-bromoisobutyrate bromide. Grafting of carboxybetaine acrylamide subsequently led to copolymer brushes containing zwitterionic functionality that are able to resist fouling from complex biological fluids.

2.6.4 Self-cleaning and anti-adhesive surfaces[27]

Nature contains a number of examples where surfaces possess both antifouling and self-cleaning properties and allow for living systems to sustain important and diverse functions. One of the most popular examples of this is the Lotus leaf, which shows remarkable resistance to fouling by dirt and microorganisms[28]. Mimicking the "Lotus effect" in synthetic materials is an area of continuous refinement and led to the development of ultra-hydrophobic surfaces as well as surfaces containing self-assembled monolayers (SAMs). These strategies borrowed from the Lotus leaf are based on the fact that water droplets simply slide off from the hydrophobic surfaces, taking with it the dust and dirt that would otherwise accumulate on the surface. In addition SAMs are used to mimic the surface roughness of the leaf which further increases the contact angle of water leading to ultra-hydrophobic surfaces[29]. Surface modification employing SAMs is, however, not limited to increasing the hydrophobicity of membranes surfaces, but a reduction in fouling has also been shown for surfaces with increased hydrophilicity[30].

Surfaces coated with derivatives of poly(ethylene glycol) (PEG) have been widely adopted for surface modification of filtration membranes due to the ability of PEG to provide anti-cell adhesive properties to the coated surfaces. The polymer is hydrophilic and the chains stick out from the surface into the water layer due to the polar ethylene glycol groups that lower the interfacial tension between the water and the polymer chains. It subsequently leads to steric hindrance for attachment of other macromolecules on the surface.

PEG, however is not suitable in long term applications due to its limited oxidative stability in the presence of O_2 and heavy metals[31,32]. When exposed to complex media, PEG undergoes oxidation over time. Once oxidized to form functional groups such as aldehydes it results in a surface that is readily able to covalently bind to proteins since the aldehydes on the surface are able to react with primary amines contained in the protein structure[22].

2.6.5 Disadvantages and future challenges

The number one concern with biofilm remediation through biocide doping and washing with surfactants is the residual toxicity that these species pose once released into the environment[33,34]. One of the major challenges facing biofouling control is thus to move away from using costly surfactants, biocides and oxidizing agents as a means of remediation of biofilm growth. Surface functionalization of membranes with immobilized enzymes, surface grafting with hydrophilic polymers and covalent attachment of antimicrobial compounds are good alternatives. However, these techniques are often either in their infancy as far as development is concerned or are not economically feasible at this point in time. Development of a universal technique of surface functionalizing membranes made of various polymeric materials would change the face of membrane production as we know it and is at the core of many research projects related to surface modification of polymeric materials.

2.7 Cellulose (and regenerated cellulose) Membranes

Cellulose is the most abundant natural polymer. In various forms such as wood, hemp, cotton, linen, etc. it has made its way into applications to improve our standard of living for hundreds of years. Wood pulp is one of the most important sources of cellulose and is extensively used in the paper industry. Annual total production of cellulose is roughly 1.5×10^{12} tons, of that only about 2% of the major source, wood pulp, is used to produce regenerated cellulose fibers[35]. The production of Rayon through the viscose process is an example of producing

regenerated cellulose from naturally occurring cellulose. The viscose process entails the dissolution of wood pulp in $NaOH_{(aq)}$ after which it is treated with CS_2 (xanthation) and finally, subsequent to treatment with a strong acid solution during spinning/stretching the so-called regenerated cellulose fibers are obtained washed and dried. Rayon is considered to be a semi-synthetic fiber used in cellophane film production as well as in textiles[36]. In addition to the viscose process, the Lyocell process has the potential of increasing the inclusion of Tencel as replacement for Rayon and other synthetic fibers[37]. The Lyocell process involves the treatment and dissolution of wood pulp in N-methylmorpholine-N-oxide (NMMO) hydrate at high temperature. The treated cellulose is then filtered off and subsequently spun/stretched before washing and drying to obtain regenerated cellulose fibers. Although Tencel is ultimately not superior to Rayon, the Lyocell process by which it is produced is more eco-friendly and a more sustainable alternative to the viscose process by which Rayon is manufactured. Increased environmental awareness is the main driver behind the substantial interest in replacing synthetic oil-based materials with renewable raw materials such as cellulose. In turn this has led to a number of investigations to increase the functionality and scope of cellulose and its application. Since, despite all its well-known properties and advantages, cellulose still lacks the versatility obtained from synthetic polymers.

Focus is thus on increasing the understanding of cellulose in terms of its nature and that of derivatives, composites, copolymers and blends that contain cellulose. Rapid increase in the number of synthetic tools in polymer synthesis and surface modification has seen the manufacturing of an ever-increasing number of functional and sustainable materials based on cellulose. As most membranes, those made from cellulose and its derivatives suffer from biofouling. Surface modification to increase the anti-biofouling properties of cellulose membranes will increase its use and provide a good alternative to synthetic membranes synthesized from oil derivatives.

A commonly used technique for producing functional materials through the modification of cellulose is polymer grafting, which is discussed in the following section. One of the major applications of regenerated cellulose would be to use it in ultrafiltration processes for separation and water treatment.

2.7.1 Surface grafting of cellulose

Grafting onto cellulose derivatives has been achieved using a variety of synthetic techniques. Surface grafting of cellulose in solution has been achieved by redox initiation in water and in organic solvent systems via ATRP-, NMP-, ROP- and RAFT processes respectively. All of these processes require some means of "activating" the available hydroxyl groups on the cellulose backbone[38–42]. This can be done by hydrolysis or simple esterification reactions with functional molecules. It is also possible to form radicals directly on the cellulose surface by oxidation with ceric (IV) ions. Through a single electron-transfer process, radicals are generated on the cellulose backbone which in turn are capable of initiating the graft polymerization of vinyl monomers from the surface[43,44].

ATRP is a technique that allows for the control over the polymerization of a wide range of monomers and due to the ease of introducing an ATRP initiator on solid surfaces has been used for grafting polymers from various surfaces including cellulose[45]. Permanently, non-leaching antimicrobial surfaces have been achieved through the grafting of 2-(dimethylaminino)ethyl methacrylate (DMAEMA) from the surface of Whatman #1 filter paper[46]. The ATRP initiator was introduced to the surface by the reaction of the hydroxyl groups available on the cellulosic surface with 2-bromoisobutyryl bromide. The surface grafting of DMAEMA was subsequently done at 30 ^{o}C in the presence of Cu(I)Br and 2,2'-bipyridine in 1,2-dichlorobenzene. This polymer contains tertiary amine groups all along the backbone and these can easily be quaternized by reaction with aliphatic bromides as a means of increasing the antimicrobial efficacy. Grafting of cellulose has also been achieved through a combination of ring-opening polymerization (ROP) and ATRP. Grafting of cellulose can be done via ROP due to the fact that the available hydroxyl groups on the surface of cellulose can act as initiation site for the polymerization. The surface initiated ring-opening polymerization (SI-ROP) from cellulose fibres was demonstrated by Carlsson *et al.*[47] for norbornene. This was achieved after the immobilization of a suitable catalyst on the fiber surface employing the available hydroxyl functionalities. The combination of ATRP and ROP was achieved by partially converting the hydroxyl groups on cellulose diacetate to ATRP initiators. The remaining hydroxyl groups were used for the ring opening polymerization of ε-caprolactone using tin(II) 2-ethylhexanoate ($SnOct_2$) as catalyst[48]. After grafting of poly(ε-caprolactone), the grafting of styrene, methyl methacrylate and butyl actrylate was subsequently achieved through ATRP.

One of the first reported grafting studies on cellulose employing living radical polymerization techniques was reported by Daly *et al.*[49] who made use of nitroxide mediated polymerization

(NMP). They reported the controlled grafting of carboxymethyl and hydroxypropyl cellulose after modification with Barton esters in the presence of TEMPO. This process was however limited to the grafting of styrene and has the additional drawback that the reaction needs to be done at relatively high temperatures (130 ^{o}C).

Despite the above-mentioned examples, not many studies have been conducted into grafting on reconstituted cellulose (solid membranes) such as filter paper and especially not on regenerated cellulose membranes. Facile ways of modification of reconstituted cellulose membranes would open the gate for increasing the functionality of existing membranes for a wider range of applications or improving the properties in the applications they are already used in. Surface grafting via RAFT polymerization is especially attractive since it leads to polymers with a low dispersity (*Đ*) whilst a predetermined chain length can be targeted. Discoloration of the membrane due to the presence of a thiocarbonyl thio group at the end of each chain is disadvantageous but can be overcome by removing this moiety with relative ease. Chain end modification can be achieved by reduction, thermolysis, aminolysis, exposing the membrane to ultraviolet radiation and oxidising agents such as peroxides or sodium hypochlorite[50,51]. During these treatments the thiocarbonyl thio and its associated colour are removed whilst a wide range of functional end groups are obtained. Through the resulting thiol, aldehyde, amine or hydroxyl functionalities additional conjugation reactions or chemistry can be conducted. The grafted polymer chains are understood to grow at the same rate as polymer chains in solution and thereby having the same low *Đ* and similar chain length when employing living radical polymerization techniques such as ATRP[42]. This has been trusted to be the case in studies where a sacrificial RAFT agent was employed for surface-grafting from cellulose [23]. However, grafting of polystyrene from Whatman filter paper using RAFT polymerization by Roy *et al*. show that although excellent control was achieved for the grafted polymer chains (*Đ* = 1.11), a monomer conversion of 20 % implied that a to a much shorter chain length was achieved than the targeted DP = 1000 (monomer : CTA = 1000 : 1)[52]. So despite being a powerful tool for surface grafting, screening and optimization of RAFT agents, monomers and reaction conditions are crucially important.

In short, the reactive nature of cellulose allows for the effective surface grafting with a variety of monomers to improve its properties and will lead to increased use of this sustainable biopolymer in current and novel applications of polymeric materials. On-going research

improving our understanding of surface grafting is continuously broadening the scope for this sustainable polymer's widespread use.

2.8 Functionalized Electrospun Nonwoven Membranes (ENMs)

The last decade has seen widespread use of the electrospinning process for the production of nanofibers from polymer solutions or melts. Parameter investigations into particularly solution electrospinning have led to an ever increasing number of synthetic and natural polymers to be spun from solution into nanofibers[53]. As a result, a number of technological advances have been made for the up scaling of the process in the form of high throughput electrospinning equipment becoming commercially available[54].

In short and its most basic form, electrospinning is a technique where a polymer solution is fed by gravity through a glass pipette or by means of a syringe pump through a needle. A large positive charge is applied to the end of the pipette or needle tip and fibers are collected on a grounded or negatively charged collector plate, typically aluminium foil. As the polymer leaves the needle tip a large enough electrical potential is necessary to overcome the surface tension of the polymer solution at the air-liquid interface to make the electrospinning process possible. At a critical electric potential the polymer solution droplets are deformed into a conical shape known as a Taylor cone. As a result of the high voltage applied to the polymer solution, the surface tension of the solvent is overcome and a thin polymer jet is ejected from the Taylor cone towards the collector plate where a nonwoven mat of nanofibers is collected. The polymer jet travels through the air in a whipping motion due to bending instabilities resulting from the high surface charge and solvent continuously evaporate from the jet surface. With each whip the volume of the polymer jet decreases while the entangled polymer chains are elongated forming the very fine nanofibers deposited on the collector.

A number of parameters such as solution viscosity, polymer and solution conductivity, electric field strength, spinning distance, feed rate, temperature and humidity govern the process and the morphology of the fibers obtained. The influences of these parameters on the final product will not be reviewed in detail and the reader is referred to the reviews by Ramakrisna *et al.* and others[55–57], for further information. Instead, the focus will be on the advantages of nanofibers in composite materials and their use as filtration media.

Nanofibers have, as their most obvious advantage, the fact that they have a very large surface to volume ratio. In the case of nonwoven ENMs they also lead to very small pore size distribution, which implies a relatively low MWCO. The MWCO of these membranes are typically in the UF range and make ENMs a very attractive option for air and water filtration, on their own, or as part of composite membrane materials[58–61]. In addition, nanofibers spun from solution allow for modification with antimicrobial functional groups such as quaternary ammonium compounds (QACs) prior to or after electrospinning[62]. Antimicrobial nanofibers capable of disinfection can be achieved through addition of biocides to the spinning solution that are incorporated into the fibers during the electrospinning process[63]. ENMs have also been successfully functionalized with compounds such as quorum sensing (QS) sensing molecules such as furanones[64] and enzymes that are capable of degrading extracellular polymeric substances (EPS) or catalyse biological reactions turning the ENM surface into a biocatalyst support[65,66].

Based on the fact that ENMs can be manufactured from a wide range of polymers that can be chosen with specific post-manufacturing surface modifications in mind, the possibilities for functional membranes with superior filtration efficiency that can resist fouling appears to be endless.

Bibliography

(1) Mansouri, J.; Harrisson, S.; Chen, V. *J. Mater. Chem.* **2010**, *20*, 4567.

(2) Allgeier, S. *Membrane Filtration Guidance Manual, EPA, USA*; 2005.

(3) Ersahin, M. E.; Ozgun, H.; Dereli, R. K.; Ozturk, I.; Roest, K.; van Lier, J. B. *Bioresour. Technol.* **2012**, *122*, 196.

(4) Nandi, B. K.; Uppaluri, R.; Purkait, M. K. *Appl. Clay Sci.* **2008**, *42*, 102.

(5) Melo, L. F.; Bott, T. R. *Exp. Therm. Fluid Sci.* **1997**, *14*, 375.

(6) Hojo, K.; Nagaoka, S.; Ohshima, T.; Maeda, N. *J. Dent. Res.* **2009**, *88*, 982.

(7) Harding, J. L.; Reynolds, M. M. *Trends Biotechnol.* **2014**, *32*, 140.

(8) Rouaix, S.; Causserand, C.; Aimar, P. *J. Memb. Sci.* **2006**, *277*, 137.

(9) Vrijenhoek, E. M.; Hong, S.; Elimelech, M. *J. Memb. Sci.* **2001**, *188*, 115.

(10) Esty, A.; Gilbert, J. *Dartmouth Medicine*. 2010, pp. 27–31.

(11) Cloete, T. E. *Mater. Corros.* **2003**, *54*, 520.

(12) Flemming, H.-C. *Exp. Therm. Fluid Sci.* **1997**, *1777*, 382.

(13) Al-Amoudi, A.; Lovitt, R. W. *J. Memb. Sci.* **2007**, *303*, 4.

(14) Meyer, B. *Int. Biodeterior. Biodegradation* **2003**, *51*, 249.

(15) Davies, D. *Nat. Rev. Drug Discov.* **2003**, *2*, 114.

(16) Singer, H.; Mu, S.; Pillonel, L. **2002**, *36*, 4998.

(17) Cloete, T. E.; Jacobs, L.; Brözel, V. S. *Biodegradation* **1998**, *9*, 23.

(18) Ang, W. S.; Yip, N. Y.; Tiraferri, A.; Elimelech, M. *J. Memb. Sci.* **2011**, *382*, 100.

(19) Auriol, M.; Filali-Meknassi, Y.; Tyagi, R. D.; Adams, C. D.; Surampalli, R. Y. *Process Biochem.* **2006**, *41*, 525.

(20) Petrovic, M.; Montserrat, S.; Alda, M. J. L. De; Barcelo, D. *Environ. Toxicol. Chem.* **2002**, *21*, 2146.

(21) Puspitasari, V. L.; Rattier, M.; Le-Clech, P.; Chen, V. *Desalin. Water Treat.* **2010**, *13*, 441.

(22) Banerjee, I.; Pangule, R. C.; Kane, R. S. *Adv. Mater.* **2011**, *23*, 690.

(23) Roy, D.; Knapp, J. S.; Guthrie, J. T.; Perrier, S. *Biomacromolecules* **2008**, *9*, 91.

(24) Charnley, M.; Textor, M.; Acikgoz, C. *React. Funct. Polym.* **2011**, *71*, 329.

(25) Kostina, N. Y.; Rodriguez-Emmenegger, C.; Houska, M.; Brynda, E.; Michálek, J. *Biomacromolecules* **2012**, *13*, 4164.

(26) Rodriguez-Emmenegger, C.; Kylián, O.; Houska, M.; Brynda, E.; Artemenko, A.; Kousal, J.; Alles, A. B.; Biederman, H. *Biomacromolecules* **2011**, *12*, 1058.

(27) Khulbe, K. C.; Feng, C.; Matsuura, T. *J. Appl. Microbiol.* **2009**, *115*, 855.

(28) Rios, P. F.; Dodiuk, H.; Kenig, S.; McCarthy, S.; Dotan, A. *J. Adhes. Sci. Technol.* **2007**, *21*, 399.

(29) Patel, K. R.; Tang, H.; Grever, W. E.; Simon Ng, K. Y.; Xiang, J.; Keep, R. F.; Cao, T.; McAllister, J. P. *Biomaterials* **2006**, *27*, 1519.

(30) Ho, C.-C.; Prodan, B. N. R.; Kiessling, B.; Co, C. C. *J. Memb. Sci.* **2011**, *366*, 342.

(31) Kane, R. S.; Deschatelets, P.; Whitesides, G. M.; York, N. *Langmuir* **2003**, *19*, 2388.

(32) Cheng, G.; Xue, H.; Zhang, Z.; Chen, S.; Jiang, S. *Angew. Chem. Int. Ed. Engl.* **2008**, *47*, 8831.

(33) Flemming, H. *Biofilm Highlights* **2011**, *5*, 81.

(34) Cloete, T. E. *Int. Biodeterior. Biodegradation* **2003**, *51*, 277.

(35) Klemm, D.; Heublein, B.; Fink, H.-P.; Bohn, A. *Angew. Chem. Int. Ed. Engl.* **2005**, *44*, 3358.

(36) Kauffman, G. B. *J. Chem. Educ.* **1993**, *70*, 887.

(37) Borbély, É. *Acta Polytech. Hungarica* **2008**, *5*, 11.

(38) Roy, D.; Semsarilar, M.; Guthrie, J. T.; Perrier, S. *Chem. Soc. Rev.* **2009**, *38*, 2046.

(39) Carlmark, A.; Larsson, E.; Malmström, E. *Eur. Polym. J.* **2012**, *48*, 1646.

(40) Krouit, M.; Bras, J.; Belgacem, M. N. *Eur. Polym. J.* **2008**, *44*, 4074.

(41) Hufendiek, A.; Trouillet, V.; Meier, M. A. R.; Barner-Kowollik, C. *Biomacromolecules* **2014**, *15*, 2563.

(42) Hansson, S.; Tischer, T.; Goldmann, A. S.; Carlmark, A.; Barner-Kowollik, C.; Malmström, E. *Polym. Chem.* **2012**, *3*, 307.

(43) Gupta, K. C.; Khandekar, K. *Biomacromolecules* **2003**, *4*, 758.

(44) Ibrahim, M. M.; Flefel, E. M.; El-Zawawy, W. K. *J. Appl. Polym. Sci.* **2002**, *84*, 2629.

(45) Matyjaszewski, K.; Xia, J. *Chem. Rev.* **2001**, *101*, 2921.

(46) Lee, S. B.; Koepsel, R. R.; Morley, S. W.; Matyjaszewski, K.; Sun, Y.; Russell, A. J. *Biomacromolecules* **2004**, *5*, 877.

(47) Carlsson, L.; Malmström, E.; Carlmark, A. *Polym. Chem.* **2012**, *3*, 727.

(48) Vlcek, P.; Janata, M.; Latalova, P.; Dybal, J.; Spirkova, M.; Toman, L. *J. Polym. Sci. Part A Polym. Chem.* **2007**, *46*, 564.

(49) Daly, W. H.; Evenson, T. S.; Iacono, S. T.; Jones, R. W. *Macromol. Symp.* **2001**, *174*, 155.

(50) Willcock, H.; O'Reilly, R. K. *Polym. Chem.* **2010**, *1*, 149.

(51) Pfukwa, R.; Pound, G.; Klumperman, B. *Polym. Prepr.* **2008**, *49*, 117.

(52) Roy, D.; Guthrie, J.; Perrier, S. *Macromolecules* **2005**, 10363.

(53) Teo, W.-E.; Inai, R.; Ramakrishna, S. *Sci. Technol. Adv. Mater.* **2011**, *12*, 013002.

(54) Persano, L.; Camposeo, A.; Tekmen, C.; Pisignano, D. *Macromol. Mater. Eng.* **2013**, *298*, 504.

(55) Teo, W. E.; Ramakrishna, S. *Inst. Phys. Publ.* **2006**, *17*.

(56) Doshi, J.; Reneker, D. H. *J. Electrostat.* **1995**, *35*, 151.

(57) Huang, Z.; Zhang, Y.; Kotaki, M.; Ramakrishna, S. *Compos. Sci. Technol.* **2003**, *63*, 2223.

(58) Homaeigohar, S.; Elbahri, M. *Materials (Basel).* **2014**, *7*, 1017.

(59) Yoon, K.; Hsiao, B. S.; Chu, B. *J. Mater. Chem.* **2008**, *18*, 5326.

(60) Mondrzyk, A.; Fischer, J.; Ritter, H. *Polym. Int.* **2014**.

(61) Yoon, K.; Hsiao, B. S.; Chu, B. *J. Memb. Sci.* **2009**, *326*, 484.

(62) Bshena, O.; Heunis, T. D.; Dicks, L. M.; Klumperman, B. *Futur. Med. Chem.* **2011**, *3*, 1823.

(63) Gule, N. P.; de Kwaadsteniet, M.; Cloete, T. E.; Klumperman, B. *Macromol. Mater. Eng.* **2012**, *297*, 618.

(64) Gule, N. P.; Bshena, O.; Kwaadsteinet, M. de; Cloete, T. E.; Klumperman, B. *Biomacromolecules* **2012**, *13*, 3138.

(65) Wang, Z.-G.; Wan, L.-S.; Liu, Z.-M.; Huang, X.-J.; Xu, Z.-K. *J. Mol. Catal. B Enzym.* **2009**, *56*, 189.

(66) Du Plessis, D. M.; Botes, M.; Dicks, L. M. T.; Cloete, T. E. *J. Chem. Technol. Biotechnol.* **2013**, *88*, 585.

Chapter 3

Surface modification of regenerated cellulose for improved anti-biofouling properties

Anti-biofouling properties were conferred to regenerated cellulose membranes by the surface grafting of hydrophilic polymers containing zwitterionic functionalities by an R-group approach of RAFT mediated polymerization. The membranes were characterized via XPS, FT-IR (Microscopy) and SEM to establish successful modification. Their anti-biofouling nature was determined through exposure to *Pseudomonas Aeruginosa* PA01. Modified membranes appeared to withstand adhesion of the foulants they were exposed to in comparison to controls of non-surface modified membranes.

3.1 Introduction:

Achieving permanently anti-cell adhesive surfaces has been the focus of a number of research projects geared at providing materials that are anti-biofouling[1]. It has been shown that grafting of hydrophilic polymers onto surfaces provides surfaces that do not allow for the initial adhesion of proteins and bacteria cells[2]. In addition, membrane surfaces that are both hydrophilic in nature and contain zwitterionic functional groups are less susceptible to cell adhesion and subsequent biofouling[3,4].

The prevention of initial adhesion or anchoring of bacteria cells prevents the proliferation of mature biofilms on membrane surfaces[5]. The formation of biofilms on surfaces of water filtration membranes is perceived to be inevitable and research in the fields of biochemistry and microbiology seeks to establish an in depth understanding of the mechanisms related to formation and proliferation of biofilms[6,7]. Biofilms constitute one of the leading factors in decrease of membrane lifespan and it leads to increased operational costs at the onset of fouling due to an effective loss of filtration efficiency requiring higher feed pressures for operation[8].

The impact of membrane fouling and decrease in membrane lifespan can temporarily be offset by means of adequate pretreatment of feed water to remove nutrients and biomolecules as well as backwashing and cleaning with surfactants and oxidizing agents[9]. Pretreatment of feed water significantly increases the cost of the process whereas oxidizing agents degrade the filtration membrane and not only the biofilm, leading to a decrease in lifespan. In addition, surfactants employed for cleaning the membrane during backwashing steps are among the major sources of endocrine disrupting compounds (EDCs) in waste water streams[10]. Thus the most feasible solution is to produce membranes that are inherently anti-biofouling or include a membrane surface modification step during manufacturing to produce surfaces that are not susceptible to biofilm formation.

Biofouling occurs readily on materials with hydrophobic surfaces and surface grafting of these materials with hydrophilic polymer chains has been reported to induce biofilm formation to a lesser extent[1]. The incorporation of zwitterionic structures in the backbone of surface grafted polymers reduces the fouling significantly. Grafted poly(*N*-vinylpyrrolidone) (PVP) has been evaluated as antifouling surface treatment compared to PEG and was found to be a promising alternative to PEG in biomedical applications[2]. Living radical polymerization, specifically ATRP, has been used extensively to graft polymer chains from surfaces, but as far as membrane filtration as well as surgical implants are concerned, the use of metal-based catalysts associated with this process is not ideal because of their cytotoxicity[11]. The advances made in end-group modification of RAFT-mediated polymers employing thiocarbonyl thio chain transfer agents have led to their use in the current study. RAFT polymers can easily undergo chain-end modification by hydrolysis, oxidation or reduction of the omega chain-end typically containing a thiocarbonyl thio moiety[12–14]. This allows for the incorporation of functional groups with properties targeted at rendering the surface less susceptible to biofouling. In this study we describe a process by which to achieve a grafted layer of PVP that contains zwitterionic groups, either at the chain-end or forming part of the backbone of surface-grafted polymer chains. The grafting occurs via an R-group approach of RAFT polymerization, after the cellulose membrane surface has been functionalized with a suitable thiocarbonyl thio moiety. This allows for grafting of polymers from the surface in a controlled fashion employing xanthate functional groups

covalently attached to the surface. The membranes were ultimately exposed to a bacteria culture and the extent of fouling was evaluated relative to a control.

3.2 Experimental:

3.2.1 Reagents

N-vinylpyrrolidone (NVP) [Sigma-Aldrich, 97 %] was dried over anhydrous magnesium sulfate and distilled under reduced pressure for purification. AIBN (Riedel-de Haën) was recrystallized twice from methanol and dried under high vacuum at room temperature. The following reagents were used without further purification: cellulose membranes (Sartorius Biolab Products, 0.45 µm); maleic anhydride (Merck, 99%); dioxane (Sigma-Aldrich, 99,8 %); KI (Sigma-Aldrich, 99 %); I_2 (Sigma-Aldrich, 99.9 %); H_2O (distilled) ; triethyl amine (TEA) [Sigm-Aldrich, 99.5 %]; dichloromethane (DCM); 2-bromopropionyl bromide (Sigma-Aldrich, 97%); 3-(*N*,*N*-dimethylamino)propyl-1-amine (DMAPA) [TCI, 99 %]; bromododecane [Sigma-Aldrich, 99,5 %]; bromodecane [Sigma-Aldrich, 97 %]; Tryptone Soy Broth (TSB) (Oxoid™) ; nutrient agar (Oxoid™); NaCl (biograde salt, Oxoid™); *Pseudomonas Aeruginosa* PA01

3.2.2 Characterization

3.2.2.1 ^{1}H NMR spectroscopy

^{1}H NMR spectroscopy was carried out on a VARIAN ^{UNITY}INOVA 400 MHz NMR instrument in *$CDCl_3$-d1*. All spectra were referenced to the *$CDCl_3$-d1* solvent peak at 7.26 *ppm* unless stated otherwise.

3.2.2.2 Size Exclusion Chromatography

SEC measurements were performed on a PL 50-Varian instrument equipped with a pre-column (8 x 50 mm) and 3 x PLgel 5 µm MIXED-C column with a 5 µm particle size and a separation range of 200- 2,000,000 g.mol^{-1}. The eluent used was DMAc (Sigma Aldrich, >99.9 %, HPLC grade) with 0.32 g/L LiBr (Sigma-Aldrich, 99 %) as stabilizer and the system was calibrated with narrowly distributed PMMA standards (PSS Std., Mainz). The experiments were run at a flow rate of 1.0 mL/min at 50 ^{o}C.

3.2.2.3 Attenuated Total Reflectance Fourier-Transform Infrared Spectroscopy ((ATR)FT-IR)

The spectra were recorded using a Thermo Scientific Nicolet iS10 FTIR (Thermo Scientific Inc. MA, USA) spectrometer for 64 scans with a resolution of 4 cm^{-1}. Data processing and atmospheric compensation was done using OMNIC software (Thermo Scientific Inc., MA, USA).

3.2.2.4 Fourier-Transform (FT)-IR Microscopy Imaging

The measurements were performed using a Bruker FT-IR microscope HYPERION 3000 coupled to a research spectrometer VERTEX 80. The HYPERION 3000 microscope is equipped with a single element MCT-detector (Mercury Cadmium Telluride) for the conventional mapping of the surface and a multi-element FPA-detector (Focal Plane Array) for imaging. The FPA-detector was used to obtain laterally resolved measurements. The multi-element FPA-detector consists of 64 x 64 elements that allow for simultaneous acquisition of 4096 spectra over a sample area of 32 x 32 µm in ATR mode. Processing in terms of baseline correction and atmospheric compensation was done, after acquisition, using OPUS software.

3.2.2.5 X-ray Photoelectron Spectroscopy (XPS)

XPS measurements were performed using a K-Alpha XPS spectrometer (ThermoFisher Scientific, East Grinstead, UK). Data acquisition and processing using the Thermo Avantage software is described elsewhere[15]. All samples were analyzed using a microfocused, monochromated Al Kα X-ray source (400 µm spot size). The K-Alpha charge compensation system was employed during analysis, using electrons of 8 eV energy, and low-energy argon ions to prevent any localized charge build-up. The spectra were fitted with one or more Voigt profiles (BE uncertainty: ±0.2eV) and Scofield sensitivity factors were applied for quantification[16]. All spectra were referenced to the C1s peak (C-C, C-H) at 285.0 eV binding energy controlled by means of the well-known photoelectron peaks of metallic Cu, Ag, and Au, respectively.

3.2.2.6 Fouling Studies

A pre-culture of *Pseudomonas aeruginosa* PA01 (Gram-negative bacteria) was prepared in 2 test tubes containing 5 mL of growth medium, Tryptone Soy Broth (TSB) [1.5 g/L], during a minimum aeration period of 18 hours at 26 °C. 1 mL of this pre-culture was diluted with 9 mL

saline [0.9% (w/v) $NaCl_{(aq)}$] and added to petri dishes containing functionalized and non-functionalized cellulose membranes along with an additional 15 mL of saline solution. The membranes were inoculated, under mild agitation, in the bacteria/saline solution for 2 hours, as well as overnight, at 26 °C. The samples were subsequently removed, rinsed twice with saline solution for 5 minutes in a petri dish. After rinsing, the membranes were removed carefully and allowed to drip dry before placing them in petri dishes of saline solution containing gluteraldehyde solution. The membranes were left at room temperature in the dark, without agitation, for 2 hours after which they were rinsed (and dehydrated) with aqueous ethanol solutions of 50%, 70%, 90% and finally 100% ethanol. The membranes were dried under high vacuum and sputter-coated with gold prior to imaging with scanning electron microscopy (LEO 1450VP Scanning Electron Microscope (SEM)). A dilution series was used to determine the amount of colony-forming units (CFU) each membrane was exposed to and was determined to be 10^4 CFU/mL.

3.3 Synthesis

3.3.1 Synthesis of macroRAFT Agent

1. Cellulose disks (5 x Ø 1.5 cm) were placed in a three-neck round-bottom flask with dry DCM (40 mL) and triethyl amine (0.75 g, 7.4 mmol). The reactor was cooled to 0 °C in an ice-bath and 2-bromopropionyl bromide (1.5 g, 6.95 mmol), dissolved in dry DCM (20 mL) was added drop-wise under magnetic stirring. The reaction was allowed to return to room temperature and left to react for 24 hours. The membranes were removed and rinsed with dry DCM and dried under a stream of nitrogen gas.

2. The membranes produced in Step 1 were added to a round-bottom flask containing potassium ethyl xanthagonate (1.24 g, 7.73 mmol) dissolved in dry ethanol (50 mL). The membranes were allowed to react for 24 hours at room temperature under magnetic stirring. The membranes were rinsed with dry ethanol and dried under a stream of nitrogen gas.

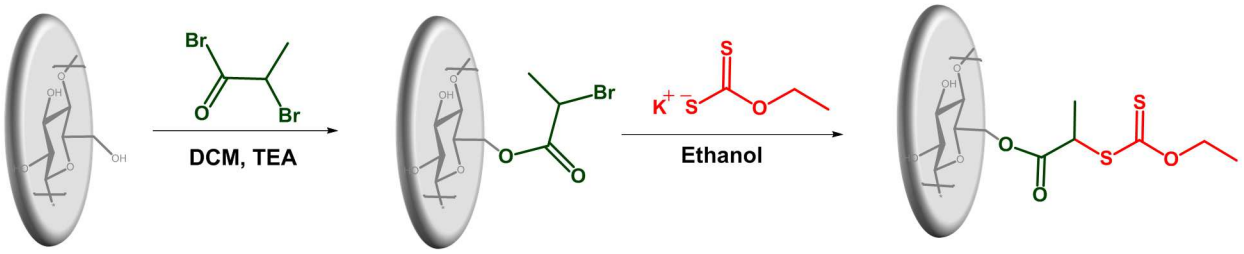

Scheme 3.1: Synthesis of macroRAFT agent

3.3.2 Grafting of PVP from macroRAFT Agent to produce cellulose-*g*-PVP

Grafting from xanthate-functionalized regenerated cellulose (macroRAFT; Ø1.5 cm) was done under a N_2 (g) atmosphere in a Schlenk tube at 60 °C after 3 FPT (freeze-pump-thaw cycles) or degassing with N_2 (g) for 30 minutes. Grafting was conducted in the presence of a sacrificial RAFT agent, *S*-(2-cyano-2-propyl)-*O*-ethyl xanthate [17]. To a Schlenk flask prior to FPT was added a macroRAFT disk, dioxane (10 mL, dry), NVP (0.5 g, 4.5 mmol), AIBN (1.3 mg, 8 µmol) and *S*-(2-cyano-2-propyl)-*O*-ethyl xanthate RAFT agent (5 mg, 25 µmol), targeting a DP = 180. The reaction was allowed to proceed for 18 hours. The polymer formed in solution was isolated by precipitation in diethyl ether and characterized via SEC and NMR.

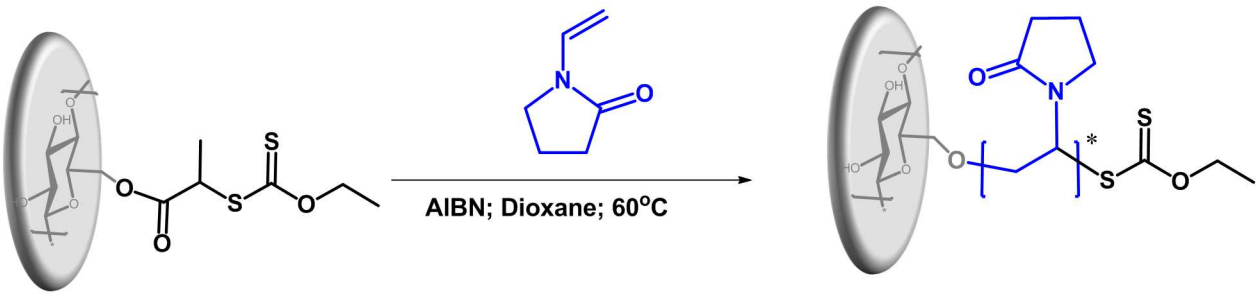

Scheme 3.2: Grafting reaction of poly (*N*-vinylpyrrolidone) from surface-modified regenerated cellulose

3.3.3 Grafting of cellulose-*g*-[PVP-*b*-(*N*-vinylpyrrolidone-*co*-maleic anhydride)] and zwitterionic modification

Maleic anhydride was incorporated into the grafted PVP polymer chains in two ways. 1) By grafting PVP in the presence of a sacrificial RAFT agent, isolating the membrane, rinsing and drying and then reacting with maleic anhydride dissolved in dioxane in the presence of AIBN. 2) By grafting PVP in the presence of a sacrificial RAFT agent and after a set period of time (4 hours) adding a shot of maleic anhydride dissolved in dioxane to the reaction mixture.

3.3.3.1 Reaction of cellulose-*g*-PVP with maleic anhydride

Cellulose-*g*-PVP was produced as described in Section 3.3.2. The membrane was isolated and rinsed extensively with dioxane before drying under high vacuum. The membrane was then placed in a round bottom flask with dioxane (5 mL) along with maleic anhydride (0.012 g, 0.122 mmol) and AIBN (0.005 g, 0.025 mmol) and allowed to react overnight at 60 °C after degassing with $N_{2(g)}$ for 15 minutes or 3 FPT cycles. The polymer formed in solution was isolated by precipitation in diethyl ether and characterized via SEC and NMR.

3.3.3.2 Cellulose-*g*-[PVP-*b*-(*N*-vinylpyrrolidone-*co*-maleic anhydride)]

Cellulose-*g*-PVP was produced as described in Section 3.3.2. After 4 hours since the start of the reaction, a shot of maleic anhydride (0.0122 g, 0.122 mmol) dissolved in dioxane was added after degassing with $N_{2(g)}$ and allowed to react overnight. The polymer formed in solution was isolated by precipitation in diethyl ether and characterized via SEC and NMR.

3.3.3.3 Zwitterionic modification

Surface-grafted membranes containing maleic anhydride units in the polymer backbone were reacted with 3-(*N*,*N*-dimethylamino)propyl-1-amine (DMAPA), dissolved in dioxane, at room temperature. DMAPA (0.0128 g, 0.125mmol) was added dropwise and allowed to react for 1 hour. To this mixture a stoichiometric amount, in a 1:1 ratio with DMAPA, of bromodecane or bromododecane was added dropwise. The reaction mixture was heated to 60 °C and the reaction was allowed to proceed overnight.

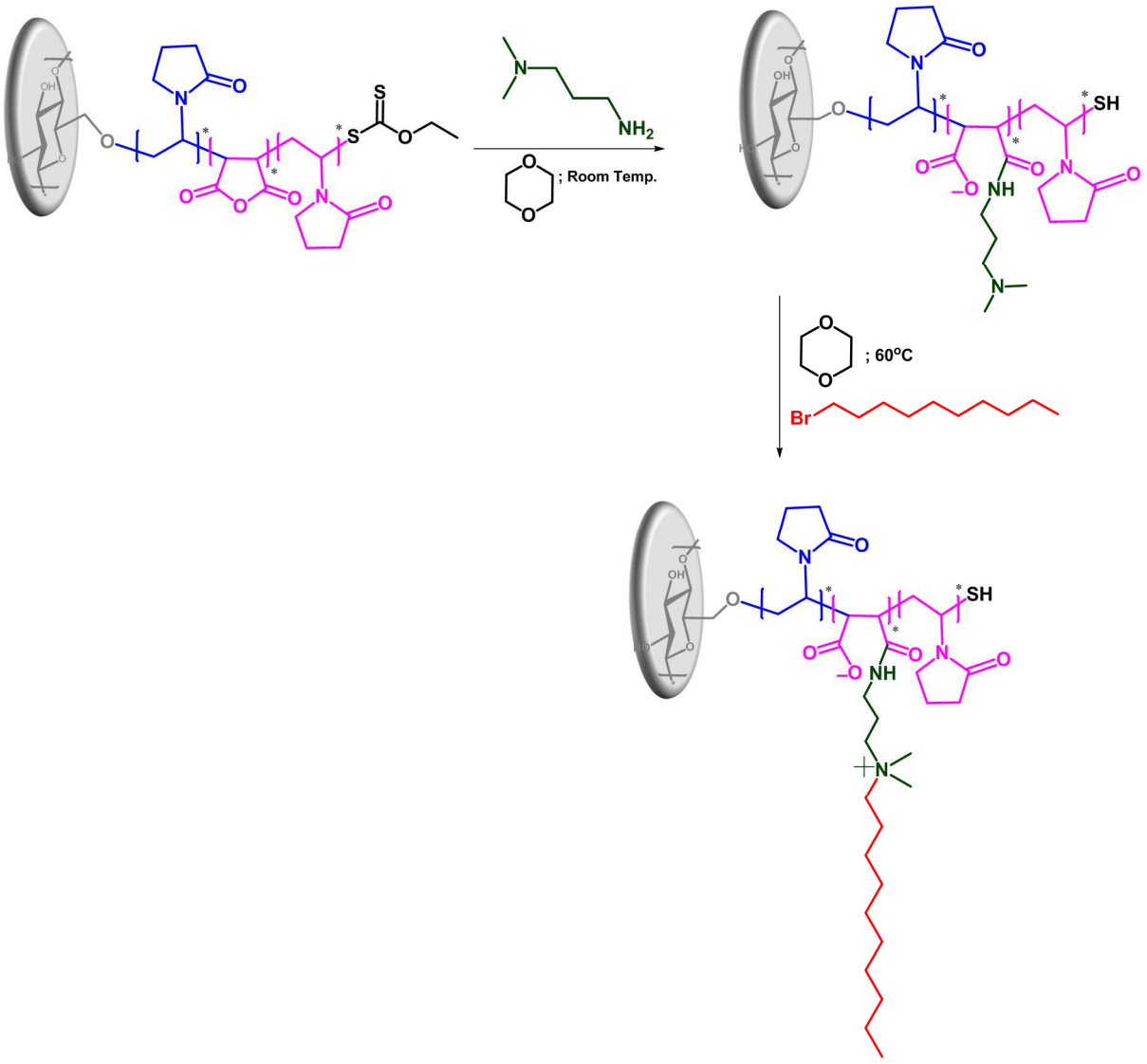

Scheme 3.3: Zwitterion modification of MAnh units in cellulose-*g*-[PVP-*b*-(*N*-vinylpyrrolidone-*co*-maleic anhydride)]

3.3.4 Control Experiments

3.3.4.1 Grafting of *N*-vinylpyrrolidone on pristine cellulose

Pristine cellulose (Ø1.5 cm) was reacted with *N*-vinylpyrrolidone (1 g, 9 mmol) under a N_2 (g) atmosphere in a Schlenk tube at 60 °C after 3 FPT cycles along with AIBN (0.08 g, 0.5 mmol) in dioxane (10 mL). The reaction was done in the absence of any sacrificial RAFT agent. FT-IR Microscopy was done to verify if any surface grafting took place.

3.3.4.2 Reaction of 3-(*N*,*N*-dimethylamino)propyl-1-amine (DMAPA) and bromododecane with pristine cellulose

Pristine cellulose (Ø1.5 cm) was reacted with 3-(*N*,*N*-dimethylamino)propyl-1-amine (DMAPA), dissolved in 10 mL dioxane, at room temperature. DMAPA (0.0128 g, 0.125 mmol) was added dropwise and allowed to react for 1 hour. To this mixture, a stoichiometric amount of bromododecane, in a 1:1 ratio with DMAPA, was added dropwise. The reaction was heated to 60 °C and allowed to proceed overnight. The membrane was rinsed thoroughly with dry organic solvents prior to XPS analysis to verify if any reactions between pristine cellulose and DMAPA and or bromododecane took place.

3.3.4.3 Reaction of 3-(*N*,*N*-dimethylamino)propyl-1-amine (DMAPA) and bromododecane with macroRAFT

The reaction procedure for reaction of DMAPA and aliphatic bromine with the macroRAFT was the same as for pristine cellulose, described in Section 3.3.5.2

3.4 Results and discussion:

The modification to introduce anti-biofouling surfaces was conducted using regenerated cellulose. As far as the authors know, the surface grafting of regenerated cellulose using an R-group approach in RAFT-LRP polymerization of PVP is reported for the first time. The R-group approach has been employed previously making use of filter paper[18], but no instance is reported for regenerated cellulose, which should also have abundantly accessible hydroxyl groups on the surface through which the chain transfer agent can be introduced[19]. The introduction of the chain transfer agent to the surface of a regenerated cellulose membrane to obtain the macroRAFT agent is shown in Scheme 3.1.

The macroRAFT agent was subsequently used for the surface grafting of *N*-vinylpyrrolidone in a solution polymerization in the presence of a sacrificial RAFT agent, *S*-2-cyano-2-propyl-*O*-ethyl xanthate. It is accepted that the rate of propagation of the surface grafted polymer and that of the one in solution are comparable and that the molar mass of the polymer isolated from solution gives a fairly accurate indication of the molar mass of the polymer grafted to the surface[20]. RAFT polymerization is a living radical polymerization technique that allows for the

chain extension of polymers after isolation. This implies that the isolated polymer can be chain-extended into a block copolymer when reacted with monomers in the presence of a thermal initiator under the right conditions. The incorporation of a maleic anhydride unit or a co-polymer block of poly(*N*-vinylpyrrolidone-*co*-maleic anhydride) is crucial for achieving zwitterionic surface structures. The way in which this is done is by 1) isolating the membrane and then adding MAnh in the presence of AIBN in dioxane or 2) adding a shot of MAnh dissolved in dioxane after allowing the grafting reaction (Scheme 3.2) to proceed for a period of time. After introduction of the MAnh, the membranes are isolated, rinsed and dried. They are then placed in dioxane and reacted with a diamine containing a primary amine on one end and a tertiary amine on the other (Scheme 3) The tertiary amine is then quaternized in a subsequent reaction step using an alkyl bromide to achieve a zwitterionic functional group at the end of each grafted poly(*N*-vinylpyrrolidone) chain.

Confirmation of surface grafting and subsequent zwitterionic modification was obtained via FT-IR microscopy as well as XPS measurements of the modified membranes.

3.4.1 FT-IR (ATR) Spectroscopy

FT-IR (ATR) spectra in Figure 3.1 show the successful modification of the cellulose membrane surface with grafted PVP. In the spectrum for the grafted cellulose membrane (black spectrum) the peak at 1640 cm^{-1} corresponds to the amide stretch vibration for the NVP monomer units in the backbone of the grafted polymer. This peak is not present in the pristine cellulose membrane (red spectrum) prior to grafting.

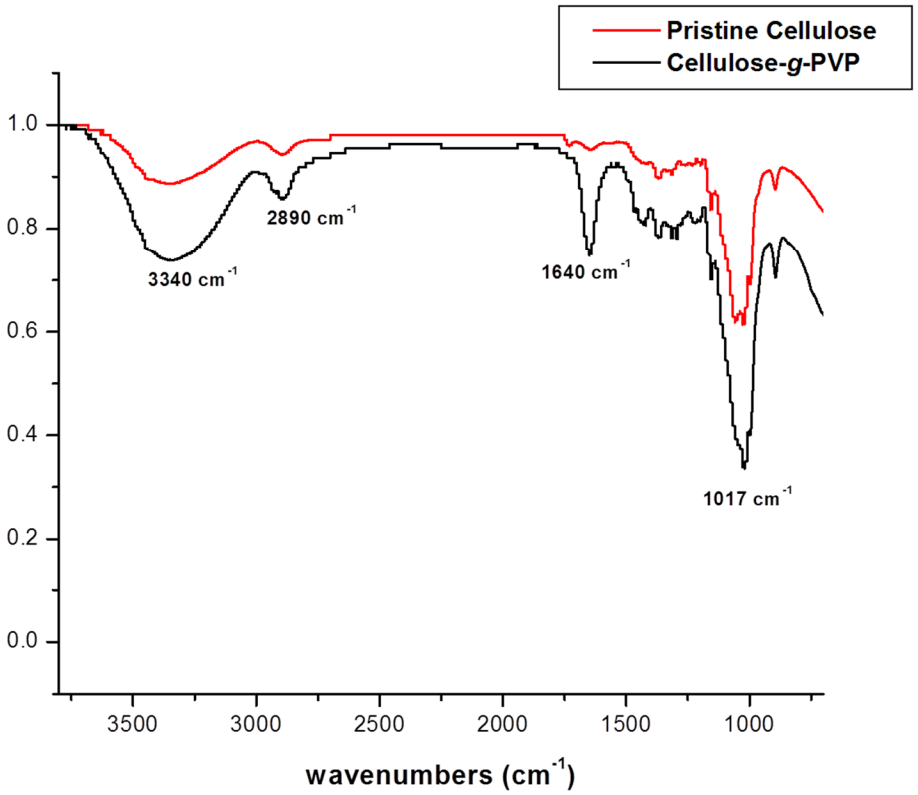

Figure 3.1: FT-IR (ATR) spectra of pristine cellulose (red) and surface-grafted cellulose membrane (black) with the amide stretch in the pyrrolidone ring visible at 1640 cm^{-1}

3.4.2 FT-IR Microscopy:

The FT-IR microscopy measurements were taken over an area of 32 µm x 32 µm to ensure that one could analyze a single cellulose fiber, having an average diameter of 10 µm and its surroundings. The spectra were acquired and then integrated to show the fingerprint regions of the carbonyl groups of the cellulose (1200 – 950 cm^{-1}) and the amide bonds in the PVP backbone (1700-1590 cm^{-1}). Figure 3.2 shows the FT-IR microscopy images for the macroRAFT agent containing no poly(*N*-vinylpryrrolidone). The cellulose fiber can be seen as the high red intensity in the upper left corner of the spectrogram A (Figure 3.2) when integrated for the fingerprint carbonyl region and in the same area in spectrogram B (Figure 3.2) it is clear that no amide (1700-1590 cm^{-1}) functionality is present on the surface of the membrane prior to surface grafting, which confirms the absence of PVP.

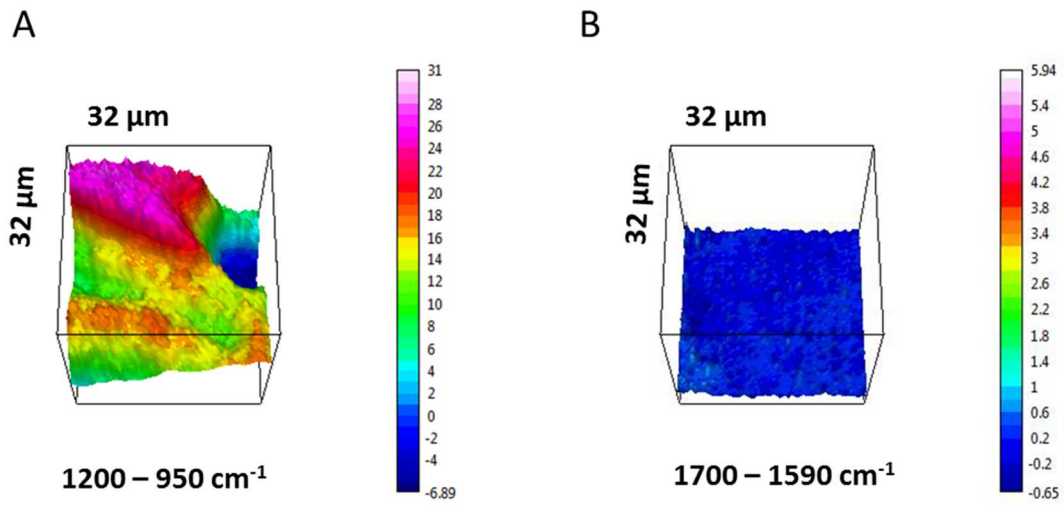

Figure 3.2: FT-IR microscopy on a 32 µm x 32 µm region of macroRAFT, integrated for the fingerprint region for cellulose (A) and the same image integrated for the amide region (B).

The spectrograms in Figure 3.3 are for the same 32 µm x 32 µm area on a membrane after it has been surface grafted with PVP through the use of the xanthate immobilized on the surface. Figure 3.3 shows the integration for the fingerprint region of cellulose (A) and for that of the fingerprint region for the amide in the pyrrolidone ring (B). In Figure 3.3 it is clear from the spectrograms of the same fiber that the fingerprint regions for both the cellulose and the amide bonds of the pyrrolidone ring overlap and this is a clear indication that the cellulose fiber was successfully modified via surface grafting of PVP and that the grafting occurred homogeneously over the area of the fiber measured. Based on this it is expected that it would be the same across the entire length of the fiber and that each fiber is entirely surface-grafted with PVP.

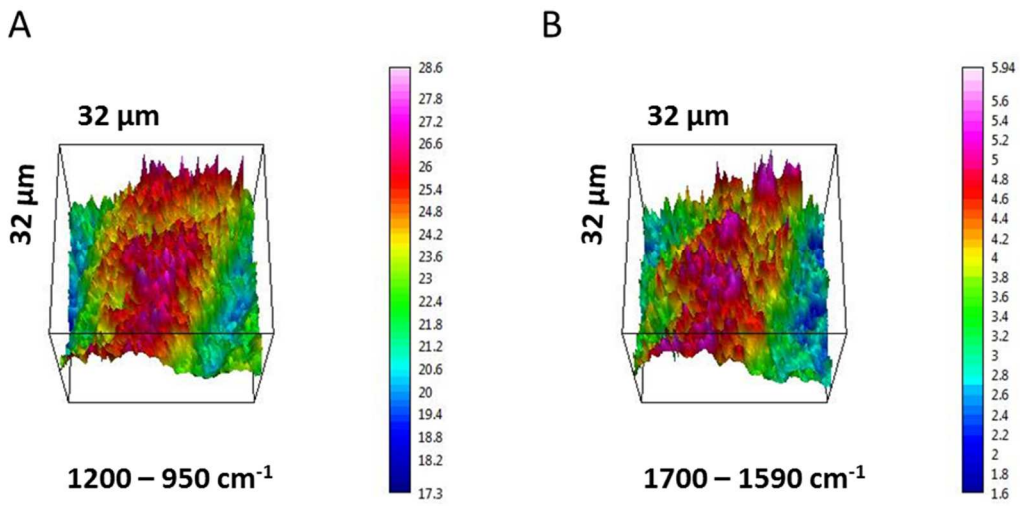

Figure 3.3: FT-IR microscopy on a 32 µm x 32 µm region of grafted cellulose, integrated for fingerprint region of cellulose (A) and the same image integrated for the fingerprint region of the amide of the pyrrolidone ring (B).

In Figure 3.4 it can be seen that no surface grafting occurred in the absence of the xanthate surface modification. The reason for this is that the thermal initiator used is unable to generate radicals on the surface of the cellulose and the polymerization of *N*-vinylpyrrolidone occurs only in solution. It is thus necessary to functionalize the cellulose with xanthate moieties prior to surface grafting. The xanthate groups on the surface are able to take part in the reversible chain transfer process that occurs in solution. During the polymerization they are transferred to propagating chains in solution which allows for insertion of *N*-vinylpyrrolidone into subsequent growing chains from the surface before deactivation by another xanthate CTA. This process continues throughout the polymerization reaction leading to control in molar mass of the polymer chains growing from the membrane surface.

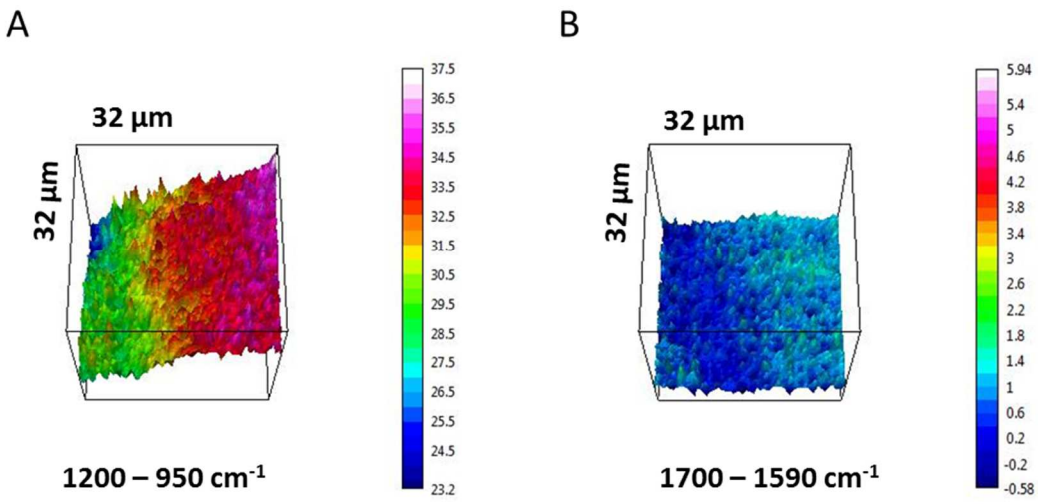

Figure 3.4: FT-IR microscopy on a 32 µm x 32 µm region of cellulose after conventional solution polymerization of NVP in its presence, integrated for fingerprint region of cellulose (A) and the same image integrated for the fingerprint region of the amide of the pyrrolidone ring (B).

From FT-IR microscopy it is thus confirmed that surface grafting of cellulose was successful when a surface-immobilized RAFT agent is used. The grafting density could however not be determined reliably via gravimetric analysis. This is due to large variations in masses obtained for surface grafted membranes. The large variation can be ascribed to the fact that commercial membranes of unknown composition were used. Since the reactions are conducted in organic solvent, it is possible that some components of the regenerated cellulose could dissolve and leach from the membrane during the reaction.

3.4.3 Size Exclusion Chromatography

The molar mass and dispersity (*Đ*) of grafted polymer chains in controlled polymerization systems are understood to be similar to the chains growing in solution at the same time. In order for this to happen, a sacrificial initiator (ATRP or Nitroxide-mediated polymerization) or chain transfer agent (RAFT) needs to be present in the system. In this study, polymers grown in solution during surface grafting from cellulose were isolated and characterized via SEC. The surface-grafted polymer was never analyzed via SEC since there was no guarantee that the polymers could be successfully cleaved and isolated for the same reason the grafting density

could not be successfully determined. In Figure 3.5, two chromatograms for polymers isolated from solution are shown. The experimental conditions were the same except for the addition of a shot of MAnh after 4 hours after the start of the reaction, to one of the reactors. The polymer isolated from solution for the latter experiment exhibited a bimodal distribution. The first peak was ascribed to being PVP homopolymer and the second to be a copolymer of PVP and MAnh. This was a rather unexpected result and reasons for this are discussed in more detail in Chapter 4 where the initialization behavior of copolymerization of NVP and maleic anhydride with two classes of RAFT agents is investigated. Based on the results discussed in Chapter 4, it is most likely that upon the addition of MAnh, acid-catalyzed dimerization of NVP and possibly other side reactions occur. This leads to the formation of polymers containing a different composition all together and both the grafted polymer and polymer in solution is not simply chain extended with a copolymer of NVP and MAnh. Subsequently a bimodal distribution observed in the SEC chromatogram (Figure 3.5) for the polymer chain extended with MAnh is observed. It is however not possible that such a large difference can be obtained in the copolymer nature as well as the hydrodynamic volume of the chain extended polymer vs. the PVP growing since the start of the reaction. Especially due to the fact that such a small amount of MAnh monomer is added to the reaction after the polymerization has been running for 4 hours. The best explanation for the trends observed is the fact that a significant amount of column interaction causes the copolymer with MAnh units to elute at a different time than the PVP homopolymer. It is thus suggested that a different highly polar eluent such as hexafluoroisopropanol (HFIP) be used to verify if better separation is achieved. In addition it would be worthwhile to conduct a dedicated investigation to establish the exact nature of the polymerization reaction as well as the composition of the distinct polymer fractions obtained. M_n values of PVP homopolymers isolated from grafting experiments however were fairly close to the theoretical M_n values with fairly low dispersity values ($Đ$) of about 1.4.

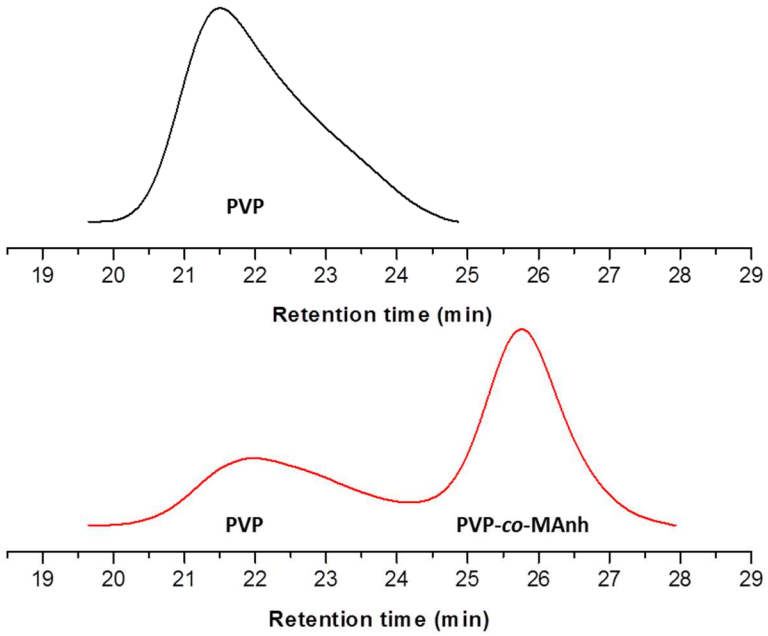

Figure 3.5: SEC chromatograms of polymers isolated from solution after surface-grafting of PVP (top) and grafting of PVP with *in-situ* chain extension with MAnh (bottom).

[**Note to examiner**: *The SEC measurements of the both the homo- and copolymers are currently being conducted at an external institution using HFIP as the mobile phase. The results were however not available at the time of submitting this thesis*]

3.4.4 X-ray Photoelectron Spectroscopy (XPS)

Commercial cellulose membranes were used exclusively throughout this study without detailed knowledge of the surface functionalities of these membranes except for the presence of –OH functionality. XPS analysis of all "pristine" cellulose membranes indicated the presence of a small amount of nitrogen (ca. at1%), possibly as a result of amine functional groups on the surface. Presence of nitrogen on the membrane surface could not be ascribed to surface contamination due to the significant amount as well as the fact that it was present in approximately the same percentage for all samples. The manufacturing process of these membranes remains proprietary information and the possible source of the amine groups on the membranes used in this study could not be verified.

Surface modification was done to obtain membranes with xanthate functional groups and the xanthate functionality was expected to be retained at the chain end of each grafted polymer chain. This implied that each modified membrane should contain a small percentage of sulphur on the surface, which was detected (ca. 1at% sulphur) whereas no sulphur was present in the case of the cellulose control. The S 2p spectrum of the cellulose modified with the macroRaft agent clearly shows 3 different components (Figure 3.6) S $2p_{3/2}$ at 162.0 eV is attributed to C=S and 163.0 eV to C-S, which proves the presence of xanthate groups[21]. The low intensity peak at 167.8 eV is probably due to some oxidation. Potassium ethyl xanthagonate was used in all reactions to obtain the xanthate functionality on the surface and as a result, potassium was present on the surface of the macroRAFT as well as surface-grafted membranes. Upon surface grafting employing the macroRAFT, the nitrogen content, due to the amide groups in PVP, increased to *ca.* 5 at%. This is in agreement with the FT-IR microscopy results, where it was shown that no significant presence of amide groups is observed prior to grafting of both the macroRAFT agent as well as the grafting experiments with pristine cellulose membranes without xanthate modification. As to be expected, there was no significant change in nitrogen content for experiments where chain extension with maleic anhydride was done *in-situ* or after first isolating membranes grafted with PVP and subsequently incorporating maleic anhydride groups at the chain ends. Reaction of surface-grafted membranes, containing maleic anhydride, with DMAPA and bromododecane resulted in the presence of 1.8 at% of quaternary nitrogen (N^+) species on the membrane surface.

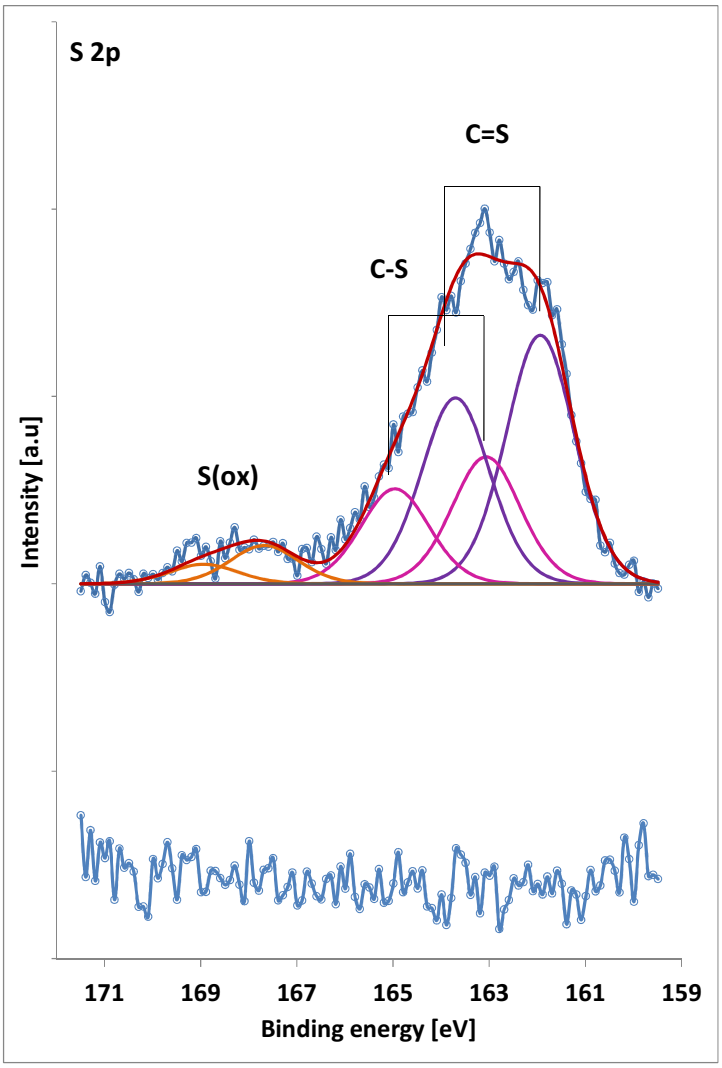

Figure 3.6: S 2p XP Spectra of the cellulose modified with the macroRAFT agent (top) and of pristine cellulose (bottom).

The N 1s spectrum of the grafted membrane (Figure 3.7) clearly shows two peaks, where the one at 399.6 eV with the highest intensity is attributed to the presence of amide and amine groups and the peak at 402.3 eV provides proof for the presence of the positively charged quaternary nitrogen[22]. Albeit in a much lower amount, the presence of quaternary ammonium compounds (0.6 at%) was also observed for the control reactions of bromododecane with macroRAFT and cellulose control. This could be due to the reaction of bromododecane with nitrogen-containing functional groups already present on the surface prior to any modification steps (*vide supra*).

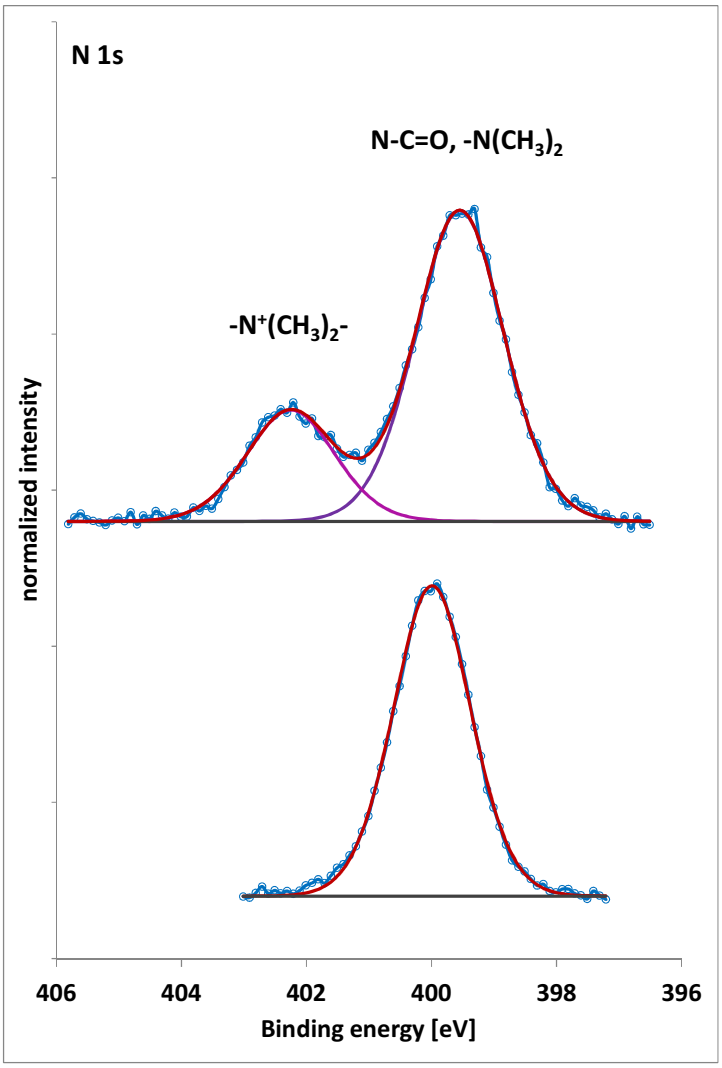

Figure 3.7: N 1s XP spectra of modified membrane containing zwitterion functionality cellulose-*g*-[PVP-*b*- (*N*-vinylpyrollidone-*co*-*N*-DMAP-maleimide-Q12)] (top) and of cellulose-*g*- PVP (bottom)

3.4.5 Scanning Electron Microscopy (SEM)

All surface-grafted membranes *versus* a control of non-functionalized membranes were exposed to bacteria (*Pseudomonas aeruginosa* PA01) under mild agitation for 2 hours as well as overnight. *P. aeruginosa* was chosen due to the fact that Gram-negative bacteria are notoriously more difficult to kill then Gram-positive bacteria. Since mature biofilms not only lead to decrease in the flux and increased production costs, but also release harmful bacteria, prevention of adhesion and biofilm formation due to *P. aeruginosa* will go a long way towards

anti-fouling and sanitary membrane filtration processes. SEM analysis of surfaces after exposure to *P. aeruginosa* indicated that a gel or slimy layer was present for all of the control membranes (Figure 3.8, image A and B). In the case of the surface-grafted cellulose membranes, this slimy layer was not present.

The slimy layer present on the cellulose fibers of the control membrane was not unequivocally verified to be a biofilm, but from the images it is clear that some form of fouling does occur on the membranes containing no surface modification. Future work is geared at optimizing the experimental procedure to grow and fully characterize a biofilm on the control surface and compare that to the degree of biofilm formation (or absence thereof) on the surface-modified membranes. Due to the short exposure times, a mature biofilm was not expected, but the presence and adhesion of the bacteria cells, however, was. The fact that no bacteria cells adhered to the control surface could be as a result of insufficient time allowed for the production and attachment of EPS (extracellular polymeric substances) on the surface.

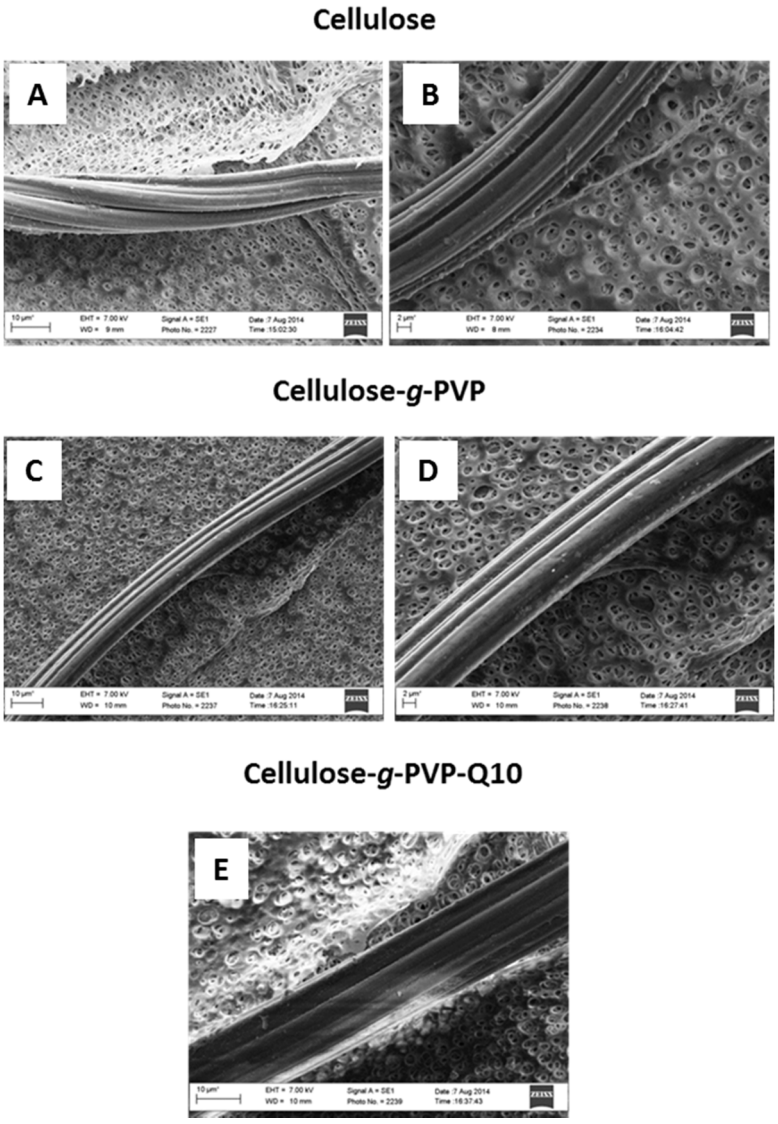

Figure 3.8: SEM images of anti-fouling nature before exposure to *P. aeruginosa* of modified cellulose fibers. The images represent from top to bottom, pristine cellulose (A and B), cellulose surface-grafted with PVP (C and D) and cellulose with surface-grafted PVP and zwitterionic functionalization (E).

EPS is commonly understood to provide the primary means of attachment of biofilms to a surface as well as keeping the biofilm together. In this case not enough time might have been allowed for this to happen and since no additional growth media was added to bacteria suspensions during incubation, they are expected not to proliferate significantly during overnight exposure.

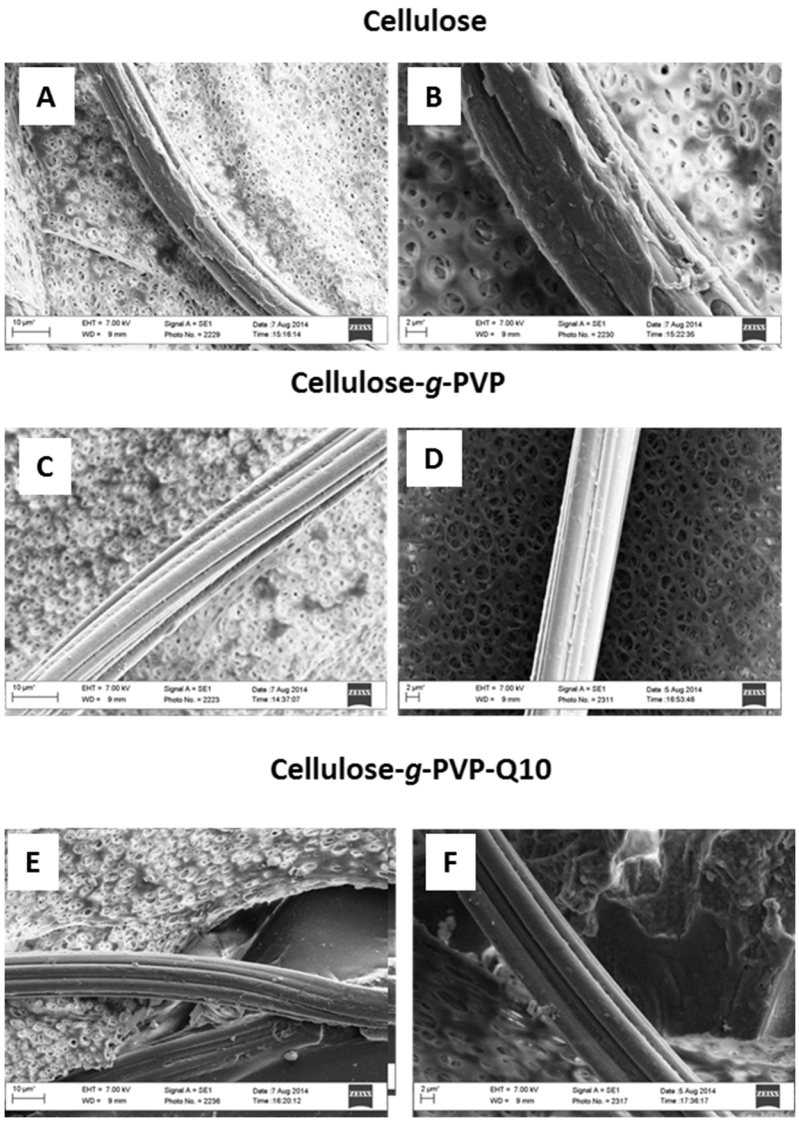

Figure 3.9: SEM images of anti-fouling nature of modified cellulose fibers after exposure to *P. aeruginosa*. The images represent from top to bottom, pristine cellulose (A and B), cellulose surface grafted with PVP (C and D) and a cellulose fiber with surface grafted PVP and zwitterionic functionalization (E and F).

The membranes containing grafted PVP including the zwitterionic modification were evaluated in the same way as the membranes containing only surface-grafted PVP. Compared to a control of non-functionalized cellulose, no visible fouling was observed for the surface-modified membranes. Zwitterionic functional groups on membrane surfaces have been shown to

significantly increase the antifouling nature of surfaces and in the current evaluation, no fouling was observed. In the current evaluation, no significant difference was observed between the antifouling behavior for membranes containing only surface-grafted PVP and those including the zwitterionic modification. It can thus be said that both modifications lead to anti-adhesive surfaces, but the ability of each membrane modification to withstand biofouling over time still needs to be assessed.

3.5 Conclusions:

This study showed the successful surface grafting of regenerated cellulose with *N*-vinylpyrrolidone through an R-group approach of RAFT-mediated polymerization using xanthate moieties immobilized on the surface. Maleic anhydride units were incorporated throughout the copolymer or as end groups of the grafted polymer and were subsequently converted to zwitterionic structures via reaction with mixed amine compounds and an aliphatic bromide. These membranes were characterized via conventional surface characterization techniques and their antifouling properties were evaluated through exposure to Gram-negative bacteria (*Pseudomonas aeruginosa* PA01) and imaged via SEM. The membranes with surface modification of hydrophilic polymers and zwitterionic structures contained therein fared better than the control of pristine cellulose. No fouling of surface-modified membranes was observed. Future work will involve the surface grafting, targeting various polymer chain lengths on the surface and testing the fouling behavior of multiple Gram-positive and Gram-negative bacteria on these modified surfaces.

Bibliography:

(1) Banerjee, I.; Pangule, R. C.; Kane, R. S. *Adv. Mater.* **2011**, *23*, 690.

(2) Liu, X.; Xu, Y.; Wu, Z.; Chen, H. *Macromol. Biosci.* **2013**, *13*, 147.

(3) Hadidi, M.; Zydney, A. L. *J. Memb. Sci.* **2014**, *452*, 97.

(4) Zhao, X.; Chen, W.; Su, Y.; Zhu, W.; Peng, J.; Jiang, Z.; Kong, L.; Li, Y.; Liu, J. *J. Memb. Sci.* **2013**, *441*, 93.

(5) Cordeiro, A. L.; Werner, C. *J. Adhes. Sci. Technol.* **2012**, *25*, 2317.

(6) Bester, E.; Wolfaardt, G. M.; Aznaveh, N. B.; Greener, J. *Int. J. Mol. Sci.* **2013**, *14*, 21965.

(7) Cloete, T. E. *Mater. Corros.* **2003**, *54*, 520.

(8) Flemming, H. *Biofilm Highlights* **2011**, *5*, 81.

(9) Vrouwenvelder, J. S.; Kruithof, J. C.; Van Loosdrecht, M. C. M. *Water Sci. Technol.* **2010**, *62*, 2477.

(10) Barnabé, S.; Brar, S. K.; Tyagi, R. D.; Beauchesne, I.; Surampalli, R. Y. *Sci. Total Environ.* **2009**, *407*, 1471.

(11) Zamfir, M.; Rodriguez-Emmenegger, C.; Bauer, S.; Barner, L.; Rosenhahn, A.; Barner-Kowollik, C. *J. Mater. Chem. B* **2013**, *1*, 6027.

(12) Chong, Y. K.; Moad, G.; Rizzardo, E.; Thang, S. H. *Macromolecules* **2007**, *40*, 4446.

(13) Pfukwa, R.; Pound, G.; Klumperman, B. *Polym. Prepr.* **2008**, *49*, 117.

(14) Willcock, H.; O'Reilly, R. K. *Polym. Chem.* **2010**, *1*, 149.

(15) Parry, K. L.; Shard, a. G.; Short, R. D.; White, R. G.; Whittle, J. D.; Wright, a. *Surf. Interface Anal.* **2006**, *38*, 1497.

(16) Scofield, J. H. *J. Electron Spectr. Relat. Phen.* **1976**, *8*, 129.

(17) Pound, G. Reversible Addition Fragmentation Chain Transfer (RAFT) Mediated Polymerization of N -vinylpyrrolidone, Stellenbosch University, 2008.

(18) Roy, D.; Guthrie, J.; Perrier, S. *Macromolecules* **2005**, 10363.

(19) Tizzotti, M.; Charlot, A.; Fleury, E.; Stenzel, M.; Bernard, J. *Macromol. Rapid Commun.* **2010**, *31*, 1751.

(20) Hansson, S.; Antoni, P.; Bergenudd, H.; Malmström, E. *Polym. Chem.* **2011**, *2*, 556.

(21) Hufendiek, A.; Trouillet, V.; Meier, M. A. R.; Barner-kowollik, C. **2014**.

(22) Boudou, J.-P.; Schimmelmann, A.; Ader, M.; Mastalerz, M.; Sebilo, M.; Gengembre, L. *Geochim. Cosmochim. Acta* **2008**, *72*, 1199.

Chapter 4

Initialization behavior of RAFT-mediated copolymerization of *N*-vinylpyrrolidone (NVP) and maleic anhydride (MAnh)

4.1 Introduction

RAFT-mediated polymerization is a versatile way of producing polymer chains with tunable end group functionalities in a controlled fashion[1,2]. RAFT polymerization falls in the class of living radical polymerization (LRP) techniques that give control over the molecular weight with low dispersity of the molecular weight distribution of the polymer chains. Controlled polymerization of various monomers is possible via RAFT by employing thiocarbonyl thio chain transfer agents (CTAs) or RAFT agents[3]. In addition it allows for complex molecular architectures to be achieved through design of RAFT agents and the living radical nature of the technique[2]. There is no universal RAFT agent and the choice of R and Z groups in the thiocarbonyl thio skeleton is important for controlled polymerization of specific monomers. Xanthates (Z group) are known to control the polymerization of *N*-vinylpyrrolidone (NVP) very well, but the degree of control and fast initialization are dependent on the R group[4,5]. The concept of initialization was introduced by McLeary *et al.* to explain the previous "rate retardation" or inhibition phenomena observed for RAFT polymerization where little to no monomer conversion is observed for a significant period of time after the start of the reaction[6–8]. Initialization is considered to be a process by which all RAFT agent molecules are first converted into single monomer adducts prior to further propagation and chain growth. In the case of RAFT copolymerization it has also been shown that for a given R and Z group combination, initialization, or the formation of single monomer adducts can be selective towards one of the two monomers[9]. In the current investigation, two RAFT agents were chosen for the copolymerization of NVP and maleic anhydride (MAnh). *S*-(2-cyano-2-propyl)-*O*-ethyl xanthate (X6) was chosen for its known ability to control NVP homo polymerization and selective addition to NVP was expected during the initialization period of the reaction. Ethyl 2-(((butylthio)carbonothioyl)thio)propanoate (T1) was chosen due to the fact that trithiocarbonate RAFT agents have been shown to control the copolymerization of MAnh

with monomers such as styrene. Due to the relatively electron-poor character of the propionate R-group, initialization is expected to occur mainly via addition to NVP. The formation of an R-NVP-MAnh-Z adduct in one activation-deactivation cycle is very well possible due to the expected fast cross-propagation. It is understood that MAnh does not homopolymerize and that after initialization, the formation of an alternating copolymer is expected from the equimolar comonomer mixture. However, NVP polymerization in bulk and solution is prone to side reactions in particular the formation of unsaturated dimers observed if any maleic acid is present in the system[10]. In turn, gradient terpolymers of NVP, MAnh and styrene have been successfully synthesized[11]. The objective was thus to verify the effect of MAnh on the polymerization of NVP when added in low concentrations and when present in a 1:1 ratio with NVP. A thorough understanding of the RAFT copolymerization of MAnh and NVP will provide possibilities of end-capping of PVP with a functional monomer such as MAnh or incorporating single units of MAnh into the homo- or block copolymer chains at predetermined intervals. Such sequence control[12–14] over spacing of functional monomers in a polymer backbone will open new possibilities for complex macromolecular architectures to be achieved for PVP polymers.

4.2 Experimental

4.2.1 Reagents

N-vinylpyrrolidone (NVP) [Sigma-Aldrich, 97 %] was dried over anhydrous magnesium sulfate and distilled under reduced pressure for purification. AIBN (Riedel-de Haën) was recrystallized twice from methanol and dried under high vacuum at room temperature. The following reagents were used without further purification: MAnh (Merck, 99 %), dimethyl sulfoxide (DMSO-*d6*, Merck, 99.8 %), dimethylformamide (DMF). Synthesis of *S*-(2-cyano-2-propyl)-*O*-ethyl xanthate (X6) was carried out as described by Pound *et al.* (Scheme 4.1)[15]. The starting compound, 2-(((butylthio)carbonothioyl)thio)propanoic acid for the synthesis of ethyl 2-(((butylthio)carbonothioyl)thio)propanoate (T1) was obtained from a colleague and used as received for the synthesis of T1 (Scheme 4.2).

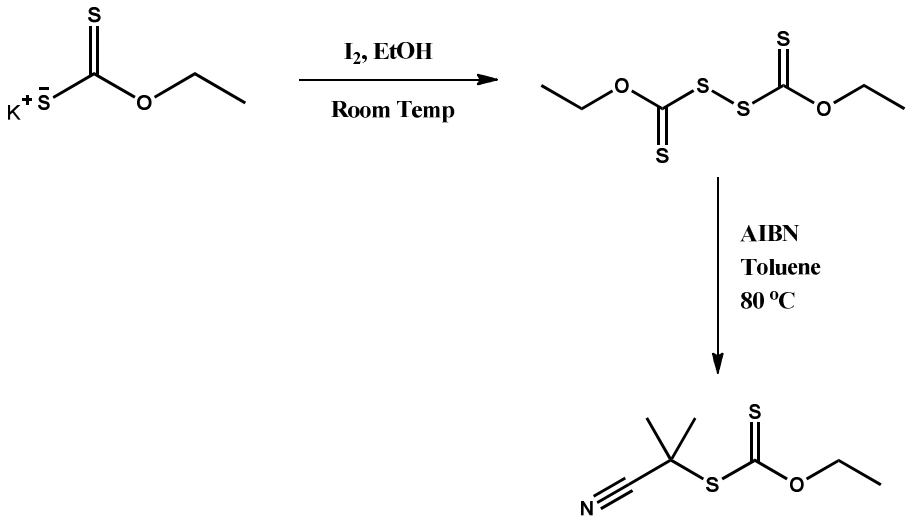

Scheme 4.1: Synthesis of *S*-(2-cyano-2-propyl)-*O*-ethyl xanthate (X6)

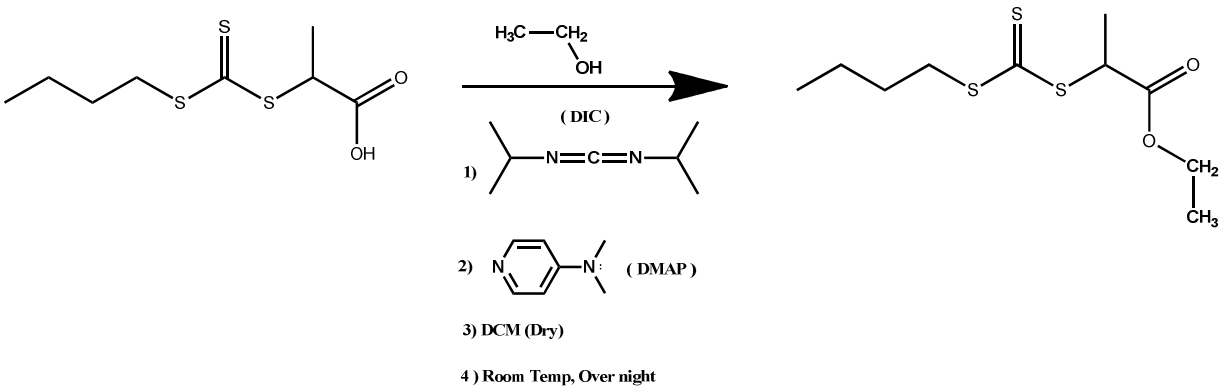

Scheme 4.2: Synthesis of ethyl 2-(((butylthio)carbonothioyl)thio)propanoate (T1)

4.2.2 In-situ ^{1}H-NMR investigation of RAFT mediated homo- and copolymerization of NVP / MAnh

A typical in-situ ^{1}H-NMR experiment was done with a monomer to RAFT ratio of 10:1 and a RAFT to AIBN ratio of 3:1. The amounts of reagents, including a reference of DMF (20 µL), were accurately weighed and homogenized and subsequently transferred to an NMR tube. The reaction mixture was degassed through 3 freeze-pump-thaw (FPT) cycles and after the final FPT cycle, the head space of the NMR tube was filled with $Ar_{(g)}$. All the experiments were conducted at 60 °C and followed online via ^{1}H-NMR (400 MHz VARIAN ^{UNITY}INOVA spectrometer) by acquiring a ^{1}H-NMR spectrum every 5 min (after equilibration at 60 °C for

ca. 3 minutes) over the total reaction time of 300 min. A reference experiment was conducted of the copolymerization of NVP and MAnh in a 1:1 ratio and in the absence of a RAFT agent under the same experimental conditions. Processing and integration of spectra was done using ACD/NMR Processor Academic Edition (ACD Labs 12.01). All FID files were processed all at once as a group. Automatic phase and baseline correction were applied to the Fourier-transformed spectra and manual integration of the peaks was done for all experiments. The concentration profile for the signals of interest was determined relative to the DMF peak that served as an internal reference. Manual integration was done for the vinyl protons of each monomer and for the RAFT agent protons on the Z and R groups respectively and the RAFT-monomer adducts formed during the reaction, respectively.

4.3 Results and discussion

It was expected that each RAFT agent would exhibit selectivity for one particular monomer during the initialization period, at the start of the polymerization. Thereafter the copolymerization was presumed to continue in a controlled fashion. In terms of the homopolymerization of NVP with X6, well defined initialization behavior is observed in the first 100 minutes of the polymerization (Figure 4.1), which is in agreement with the formation of a single monomer adduct as described by Pound *et al.*[4] There is a gradual consumption of NVP throughout the duration of the experiment with an equimolar amount of NVP relative to the RAFT agent consumed at the start of the reaction until all of the RAFT agent is converted to the single monomer adduct of NVP and X6. In the ^{1}H-NMR spectra (Figure 4.1), the formation of the single monomer adduct of NVP and X6 can be seen around 4.6 ppm as a distinct and well-defined quartet for the methylene protons of the xanthate Z-group. This becomes a multiplet towards the end of the reaction indicating that the 1st monomer adduct is converted to higher oligomeric species. This is also evident from the concentration profile of the monomer adduct (Figure 4.1) where there is a decrease in the amount of adduct towards the end of the reaction past 200 min.

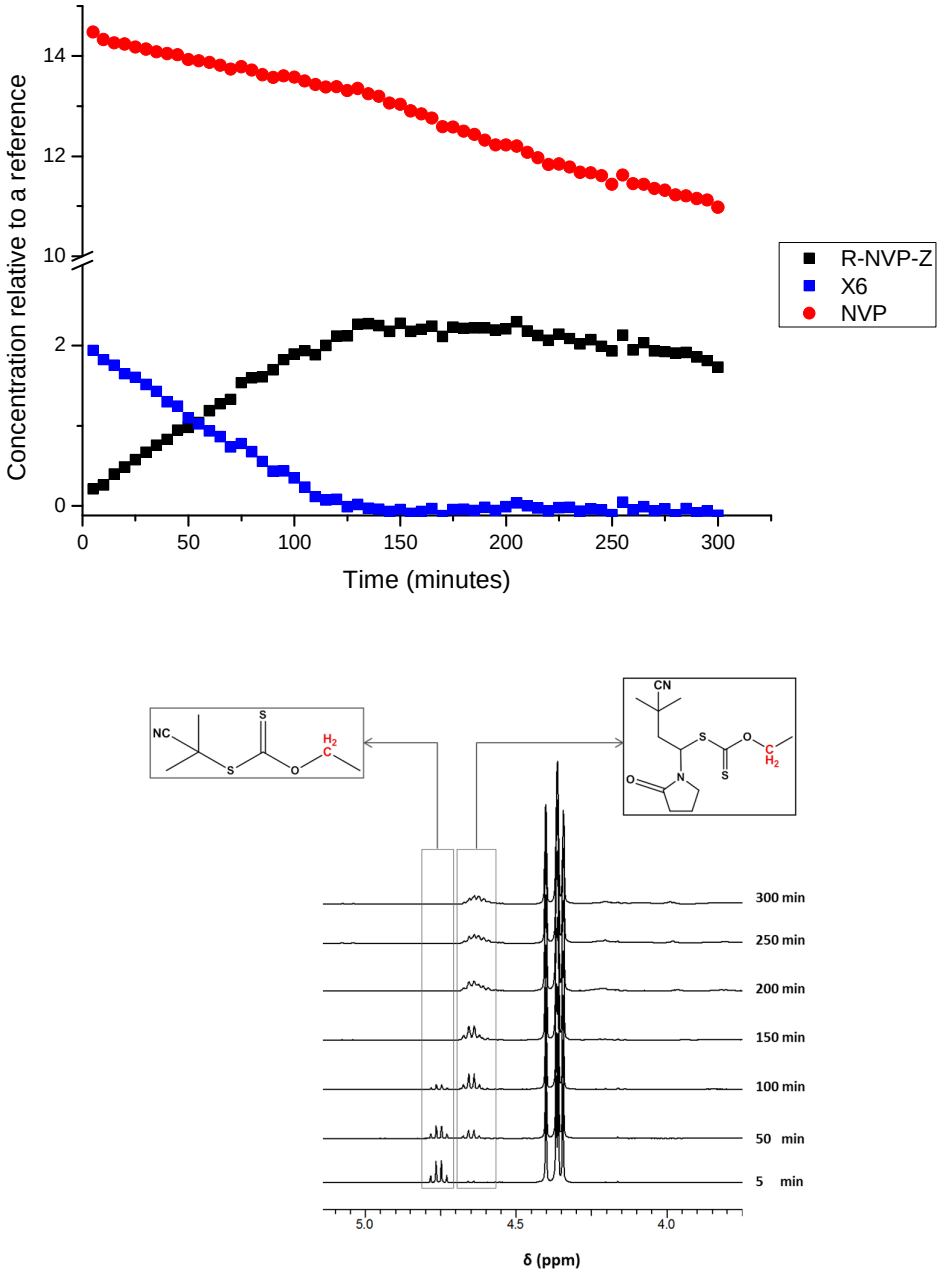

Figure 4.1: Concentration profiles of NVP and X6 over time (top) and the formation of the single monomer adduct visible in the ^{1}H-NMR spectra (bottom) during an initialization experiment for the homopolymerization of NVP.

From the concentration profiles in Figure 4.2 initialization of NVP using T1 was also observed. Here initialization occurred in a shorter time period, around 50 minutes, but not as efficiently as in the case with X6. In the ^{1}H-NMR spectra in Figure 4.2 it can be seen that although R-NVP-Z adducts with T1 are formed there is also some evidence for peaks related

to the formation of the unsaturated dimer of NVP at around 6.8 ppm. The R-group of T1 contains an ester group and as previously reported by Pound *et al*. this (or small amounts of residual acid-functional RAFT agent precursor) could catalyze the formation of unsaturated dimers of NVP[10]. The concentration profile for dimer formation over time is not shown, but evidence thereof can be seen in the ^{1}H-NMR spectra (Figure 4.2) as a doublet forming around 6.8 ppm. In addition, the rate of polymerization of NVP slows down considerably after initialization and no significant propagation is observed or any visible decrease in the R-NVP-Z adducts concentration. This could be related to possible side reactions taking place including reaction with the unsaturated dimers formed during the polymerization.

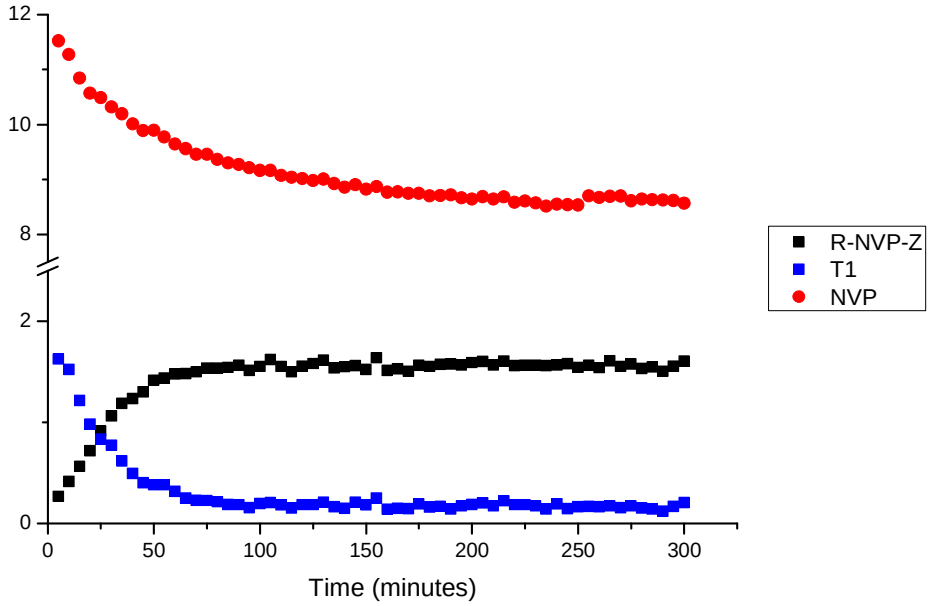

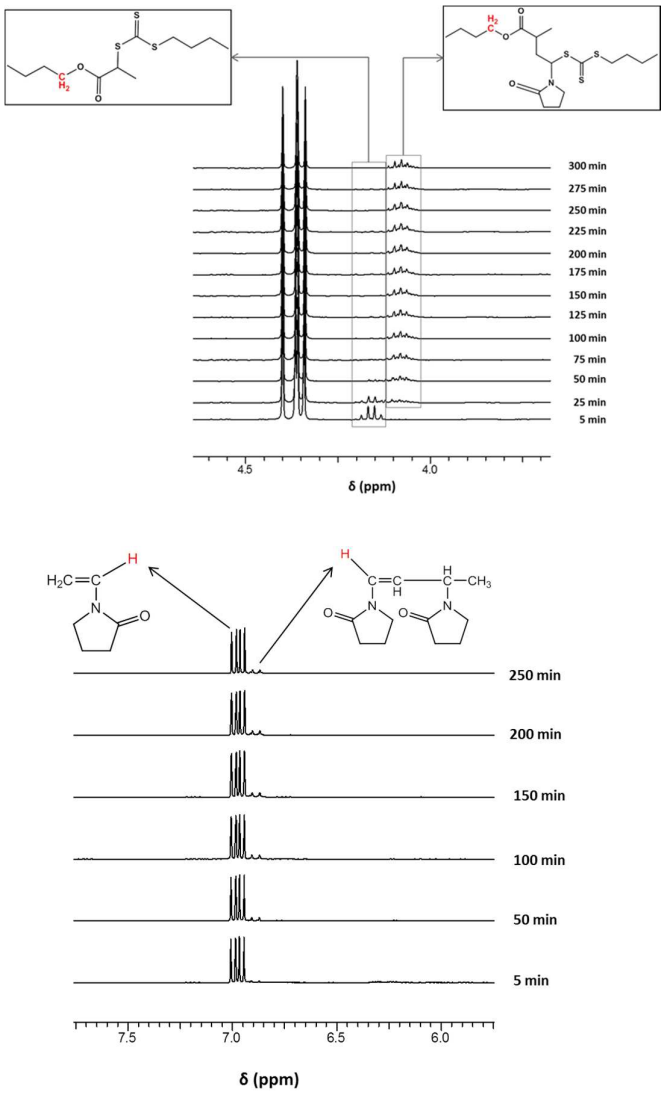

Figure 4.2: Concentration profiles of NVP and T1 over time (top) as well as the ^{1}H-NMR spectra showing the formation of the 1st monomer adduct of NVP and T1 (middle) and the formation of unsaturated dimers of NVP (bottom) during an initialization experiment for the homopolymerization of NVP.

During RAFT mediated homo-polymerizations of NVP, besides the slight amount of dimer formation during the polymerization of NVP in the presence of T1, successful initialization at the start of both homo-polymerizations suggest good control over the polymerization should be achieved with both X6 and T1. This however was determined not be the case for the copolymerization experiments conducted and no initialization occurred. Concentration profiles for copolymerization of NVP/MAnh with X6 show only a gradual consumption of the RAFT agent (Figure 4.3) and a very high rate of conversion for the NVP. The high rate of NVP

consumption suggests that it is polymerizing under conventional free radical conditions and that no RAFT equilibrium is established in order to achieve control over the polymerization. However, the fast reaction rate of NVP can largely be ascribed to unsaturated dimer formation since the decrease in NVP coincides with a rapid increase in the concentration of unsaturated dimers of NVP in the reaction mixture. Not all of the NVP is converted into unsaturated dimers however and the formation of R-NVP-Z adducts with X6 is observed, although not shifted as far downfield from the methylene protons of the xanthate Z-group (Figure 4.3). The only species formed in a relatively significant concentration are unsaturated dimers of NVP as well as R-NVP-Z adducts. This suggests that dimer and R-NVP-Z adduct formation are the two key mechanisms of NVP consumption. The fact that dimerization occurs can be ascribed to the presence of a small amount of MAnh being present in its ring-opened maleic acid form or that the carbonyl groups contained in the maleic anhydride monomer catalyzing the dimerization. The former is most likely to be the cause of dimerization. However, the concentration profiles in Figure 4.3 are derived directly from the integrals relative to a reference in the spectra. In this experiment, the concentration at the end of the experiment is roughly half of the initial concentration of NVP. Since the dimer consists of two monomer units, it would mean that almost all of the NVP was converted to dimers. So the peaks assigned to be single monomer adducts, may in fact not be R-NVP-Z adducts, but could possibly be due to RAFT agent adding to initiator derived radicals of the unsaturated dimers. No evidence was obtained for the formation of such species and a dedicated experiment would be necessary to verify whether dimers can take part in further reactions and the RAFT agent would add to initiator derived dimer radicals. From the concentration profiles in Figure 4.3 it is also clear that a small amount of MAnh is consumed during the reaction. However, the consumption of MAnh proceeds at a higher rate than the RAFT agent. This potentially means that the RAFT agent does not preferentially add to MAnh and that some of the MAnh adds to initiator-derived radicals or to oligomers with terminal NVP radical units. This would result in terminated maleic anhydride species containing one monomer unit or being incorporated sporadically into a growing NVP radical terminated chain. This is presumed to be the case and ongoing work is seeking to verify this.

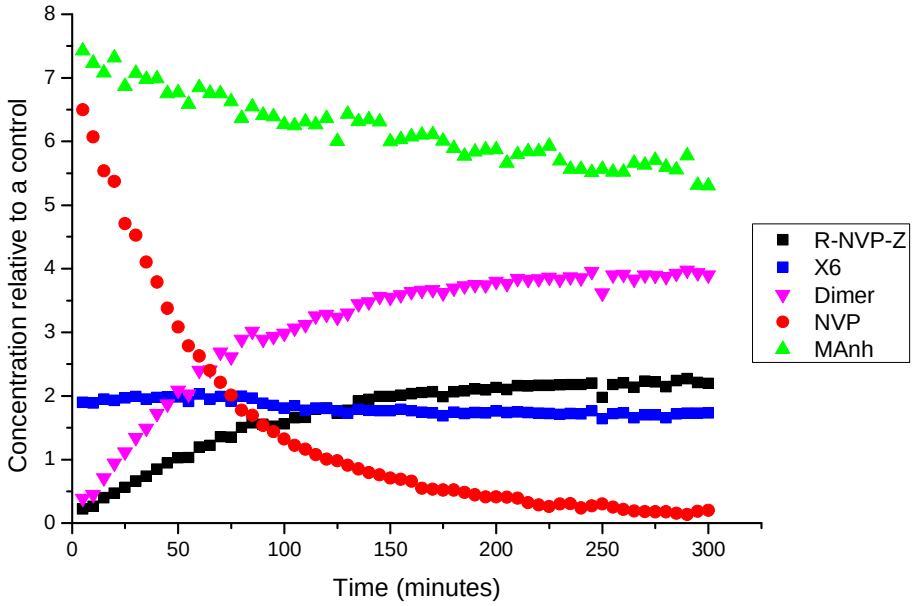

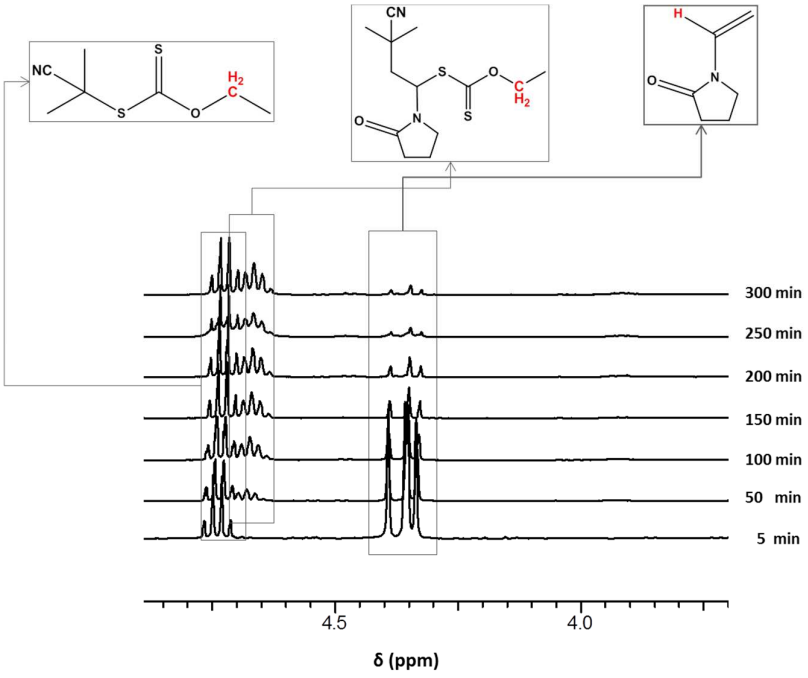

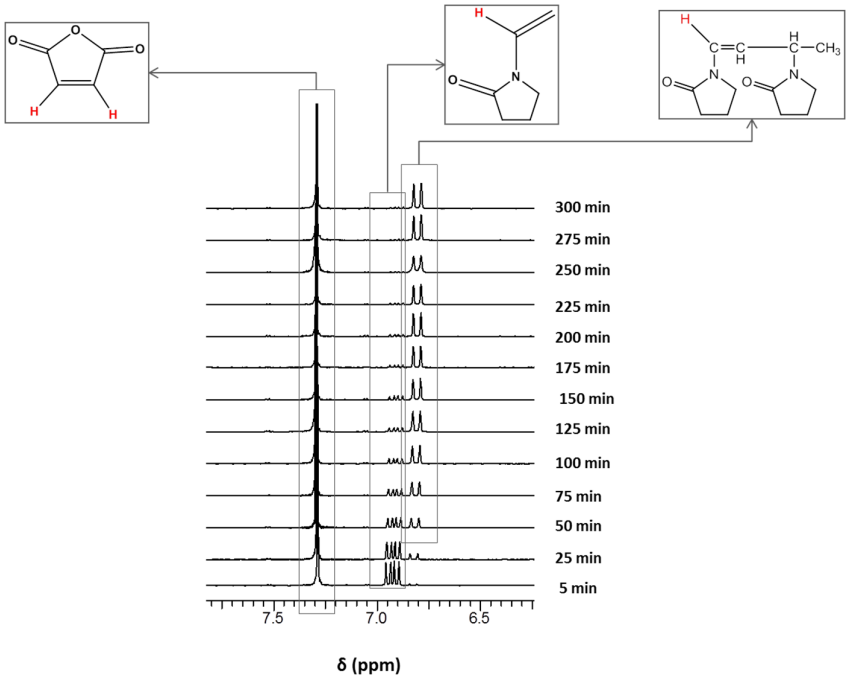

Figure 4.3: Concentration profiles of NVP, MAnh and X6 over time and the ^{1}H-NMR spectra showing the formation of R-NVP-Z adducts at 4.6 ppm (middle) and the formation of unsaturated NVP dimers at around 6.8 ppm (bottom) during an initialization experiment for the equimolar copolymerization of NVP and MAnh.

Copolymerization of NVP/MAnh in the presence of T1 also resulted in no initialization or control over the copolymerization. Again, only a gradual decrease in RAFT agent is observed and no initialization is evident from the concentration profiles in (Figure 4.4) A gradual consumption of MAnh is observed in both copolymerization reactions but in the presence of T1, the consumption of MAnh occurs at a slightly higher rate compared to the reaction with the copolymerization in the presence of X6. This suggests that during reaction, the R group of the RAFT agent adds to an initiator-derived MAnh radical to from a stable compound or that the R group of the fragmented RAFT agent preferentially adds to MAnh to form a stable species that does not fragment. No evidence for the formation or termination of intermediate radicals of these species was however obtained and it will be worthwhile to investigate this in future studies. It is also evident that the formation of unsaturated NVP dimers accounts for a large part of the NVP consumed. There are some NVP "missing" from the profile. This again could be due to either NVP reacting with the unsaturated dimers formed during the reaction or that they might be reacting under conventional free radical polymerization conditions with MAnh. Also, unlike in the copolymerization using a xanthate

RAFT agent, no adducts are formed during the copolymerization with T1 and virtually none of the trithiocarbonate RAFT agent is consumed during the polymerization. This highlights the importance of investigating the role the unsaturated dimers play during polymerization. Specifically, to verify whether they can form radicals that adds to either of the monomers or to the RAFT agent.

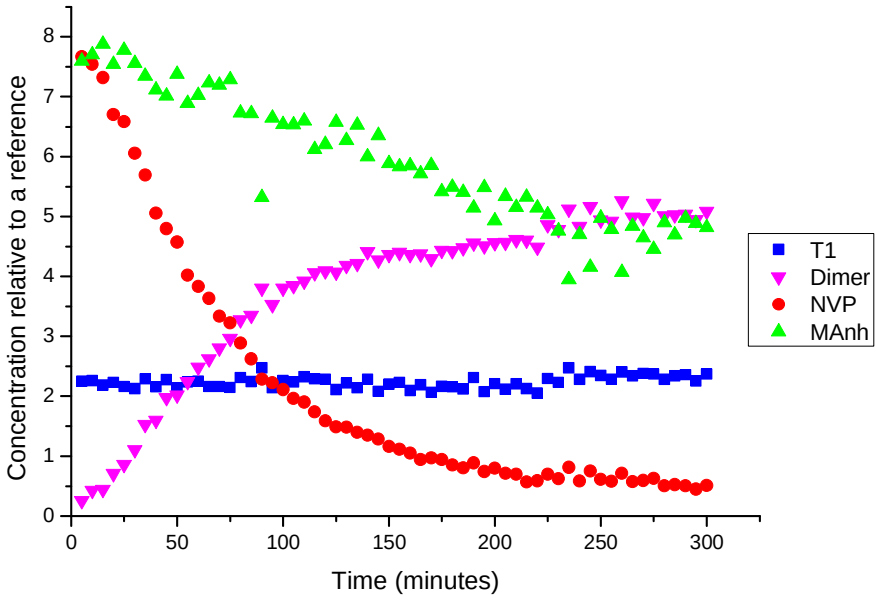

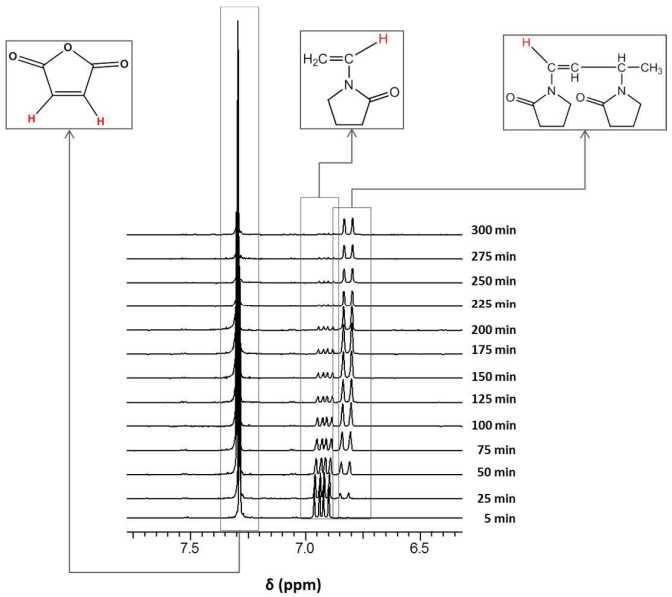

Figure 4.4: Concentration profiles of NVP, MAnh and T1 over time (top) and ^{1}H-NMR spectra showing the formation of unsaturated dimer of NVP (bottom) during an initialization experiment for the equimolar copolymerization of NVP and MAnh.

In order to establish what the influence of MAnh is on the reaction kinetics of the RAFT copolymerizations, experiments were conducted with a smaller amount of MAnh as part of the formulation. For these experiments a ratio of RAFT: MAnh of 1 : 0.5 was used (NVP:RAFT =10). This would provide information on whether MAnh influences the kinetics at even very low concentrations. From the concentration profiles (Figures 4.5 and 4.6) it can be seen that this is indeed the case. Prior to complete consumption of MAnh, the NVP consumption proceeds at a much faster rate than after all the MAnh have been converted. This suggests that in the early stage of the reaction, as indicated from the copolymerization reactions discussed above, that NVP is either polymerizing under free radical conditions or NVP consumption is due to the acid catalyzed dimerization of NVP[10]. The latter case being the most likely due to the presence ^{1}H NMR signals for NVP dimers present in the spectra (Figure 4.5). Once the MAnh is consumed completely, what appears to be an initialization step for NVP polymerization starts to occur. This can be deduced from the increased rate of RAFT consumption coinciding with an immediate decrease in the rate of NVP consumption, during which the formation of R-NVP-Z adducts are observed in the ^{1}H NMR spectra (Figure 4.5).

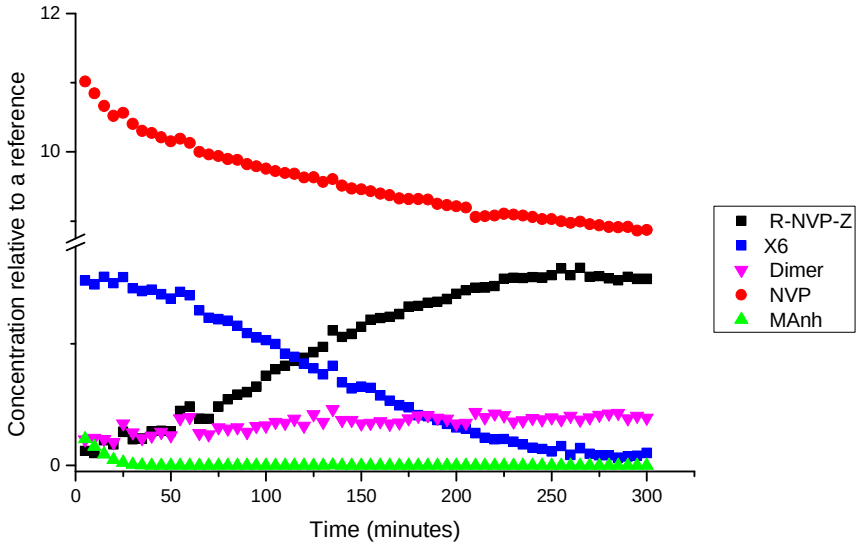

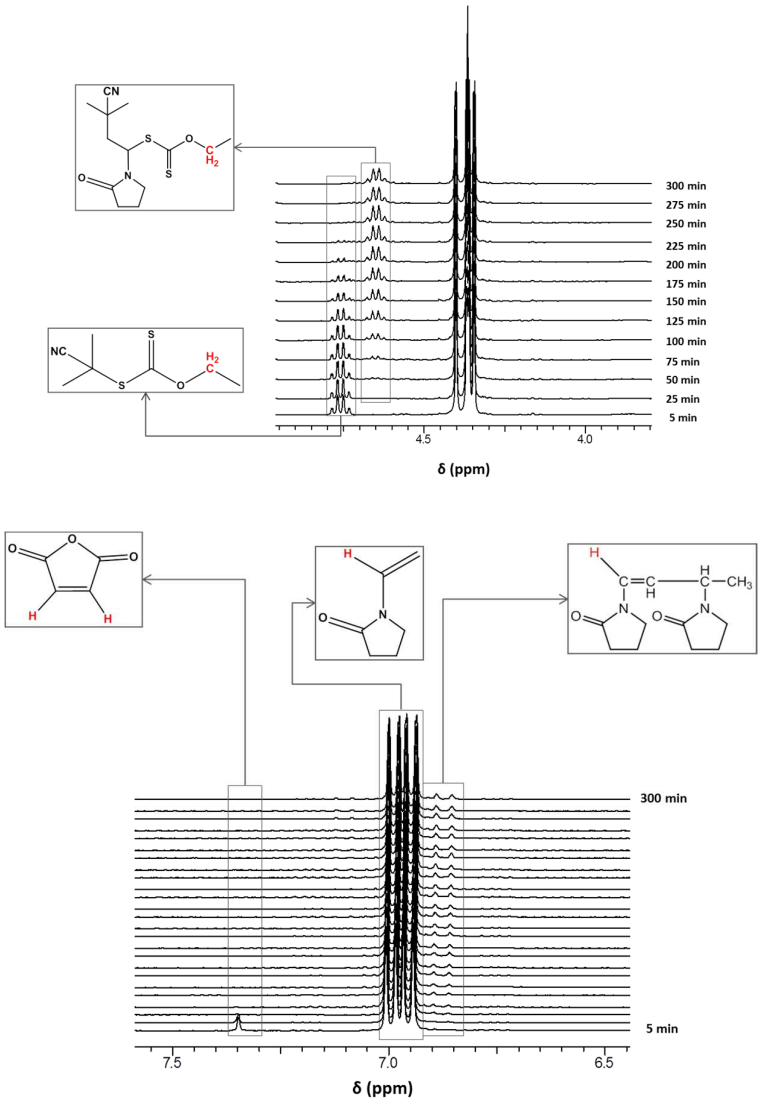

Figure 4.5: Concentration profiles of NVP, MAnh and X6 over time (A) and ^{1}H-NMR spectra showing the formation of R-NVP-Z adducts (middle) and the formation of a small amount of unsaturated NVP dimers (bottom) during an initialization experiment for the copolymerization of NVP with a small amount of MAnh.

The polymerization of NVP with T1 in the presence of a small amount of MAnh proceeds in a similar fashion as the one with X6. In Figure 4.6 the consumption of NVP occurs at a high rate until all the MAnh is consumed whereafter the rate of NVP consumption immediately drops whilst coinciding with what appears to be an initialization step and the formation of R-NVP-Z adducts. A significantly larger amount of dimers are formed in the case of T1. This could be due to a combination of the acid catalyzed dimerization by both the MAnh as well as the RAFT agent based on the fact that some dimer formation occurs for NVP homopolymerization with only T1 present in the reaction mixture. Again the fates of the

dimers are uncertain for the experiments with only a small amount of MAnh present. Also, the fact that an initialization steps starts and the dimerization stops almost immediately after the complete consumption of MAnh suggests that the MAnh is in fact incorporated into the polymer chains and no longer capable of catalyzing any dimer formation. The decrease in MAnh concentration for the copolymerization suggests the same, in that MAnh is incorporated into the polymer chain. But in the copolymerization reactions there is a much higher concentration of MAnh that leads to the competing dimerization reaction occurring for a longer period and essentially leads to a depletion of the NVP before significant chain growth can be achieved.

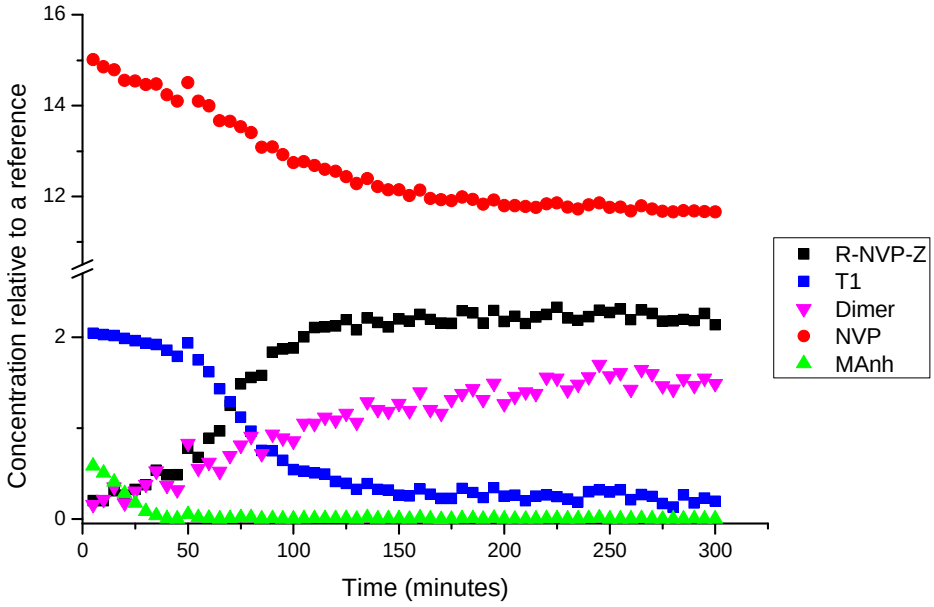

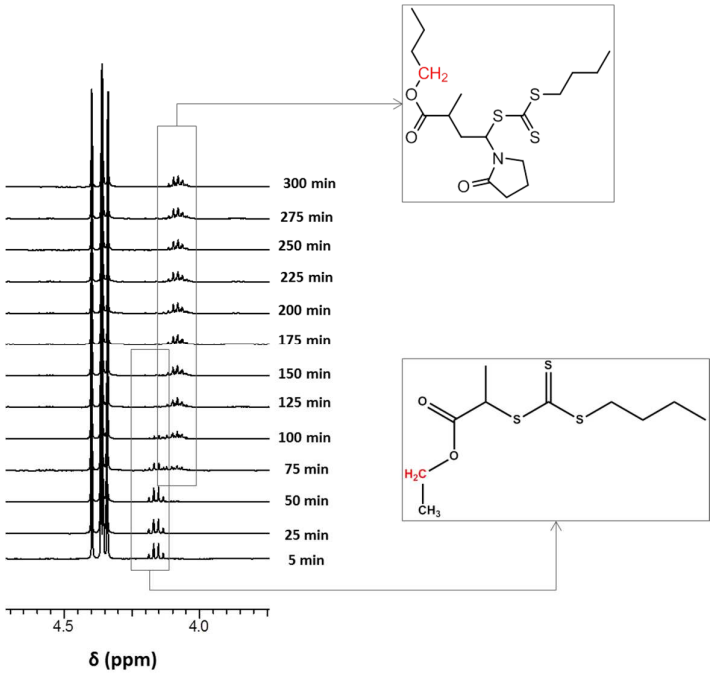

Figure 4.6: Concentration profiles of NVP, MAnh and T1 over time (top) and ^{1}H-NMR spectra showing the formation of R-NVP-Z adducts (bottom) during an initialization experiment for the copolymerization of NVP with a small amount of MAnh.

4.4 Conclusions

Initialization of the RAFT hompolymerization of NVP was achieved through the use of both a xanthate (X6) and a trithiocarbonate (T1). No initialization is however observed for the copolymerization of NVP and MAnh in the presence of both X6 and T1. Subsequently, no control of the polymerization is achieved employing these RAFT agents for the copolymerization of a 1:1 ratio of NVP and MAnh. The polymerization is subject to side reactions, the most dominant appearing to be as a result of acid-catalyzed dimerization of NVP due to the presence of MAnh. However, at small percentages of MAnh in the system, the dimerization of NVP is only present at the very beginning of the reaction until all the MAnh is consumed after which a normal initialization period commences. The fact that there is a significant decrease in the concentration of MAnh during the copolymerizations in a 1:1 ratio with NVP and the fact that it is completely converted during the copolymerizations where it is added in only a relatively low amount suggest that copolymers of NVP and MAnh are accessible via RAFT polymerization. This implies that some form of sequence control should be possible in producing copolymers with short segments of NVP-*co*-MAnh by either

adding small amounts of MAnh at the start, middle or towards the end of the copolymerization reaction. At the current stage it is however not optimized and control over the polymerization should be screened for different monomer ratios of NVP and MAnh as well as for different R and Z groups of xanthate and trithiocarbonate RAFT agents.

Future work should therefore involve elucidating all possible structures based on the ^{1}H NMR signals in combination with mass spectrometry analysis of the oligomers formed during the early stages of the polymerization reactions. It will also be worthwhile to perform designated experiments to evaluate the role unsaturated dimers of NVP play during the polymerization. By synthesizing and isolating unsaturated NVP dimers, they can subsequently be added in different ratios to NVP homopolymerizations as well as NVP copolymerizations with MAnh in order to characterize the polymers formed under both conventional free radical and RAFT polymerization conditions.

Bibliography

(1) Moad, G.; Rizzardo, E.; Thang, S. H. *Aust. J. Chem.* **2012**, *65*, 985.

(2) Moad, G.; Rizzardo, E.; Thang, S. H. *Chem. Asian J.* **2013**, *8*, 1634.

(3) Moad, G.; Rizzardo, E.; Thang, S. H. *Polymer (Guildf).* **2008**, *49*, 1079.

(4) Pound, G.; McLeary, J. B.; McKenzie, J. M.; Lange, R. F. M.; Klumperman, B. *Macromolecules* **2006**, *39*, 7796.

(5) Destarac, M. *Polym. Rev.* **2011**, *51*, 163.

(6) Barner-Kowollik, C.; Quinn, J. F.; Vana, P.; Davis, T. P. *Macromolecules* **2002**, *35*, 8300.

(7) Mcleary, J. B.; Mckenzie, J. M.; Tonge, M. P.; Sanderson, R. D.; Klumperman, B. *Chem. Commun. (Camb).* **2004**, *6*, 1950.

(8) McLeary, J. B.; Calitz, F. M.; McKenzie, J. M.; Tonge, M. P.; Sanderson, R. D.; Klumperman, B. *Macromolecules* **2004**, *37*, 2383.

(9) Van Den Dungen, E. T. A.; Rinquest, J.; Pretorius, N. O.; McKenzie, J. M.; McLeary, J. B.; Sanderson, R. D.; Klumperman, B. *Aust. J. Chem.* **2006**, *59*, 742.

(10) Pound, G.; Eksteen, Z.; Pfukwa, R.; Mckenzie, J. M.; Lange, R. F. M.; Klumperman, B. *J. Polym. Sci. Part A Polym. Chem.* **2008**, *46*, 6575.

(11) Hu, Z.; Zhang, Z. *Macromolecules* **2006**, *39*, 1384.

(12) Lutz, J.-F. *Polym. Chem.* **2010**, *1*, 55.

(13) Badi, N.; Lutz, J.-F. *Chem. Soc. Rev.* **2009**, *38*, 3383.

(14) Lutz, J.-F.; Ouchi, M.; Liu, D. R.; Sawamoto, M. *Science.* **2013**, *341*, 1238149.

(15) Pound, G. Reversible Addition Fragmentation Chain Transfer (RAFT) Mediated Polymerization of N -vinylpyrrolidone, PhD Thesis, Stellenbosch University, 2008.

Chapter 5

Facile immobilization of enzymes on electrospun poly(styrene-*alt*-maleic anhydride) nanofibres[†]

Facile immobilization of horseradish peroxidase (HRP) and glucose oxidase (GOX) was achieved on electrospun nanofibres made of an alternating copolymer of styrene (Sty) and maleic anhydride (MAnh). The immobilized enzymes were used to perform a cascade reaction oxidizing D-glucose by GOX to yield H_2O_2 and employing HRP to catalyze the reaction between the generated H_2O_2 and Ampliflu Red to yield Resorufin. The average activity of the immobilized HRP was determined to be 21% of that of the free enzyme.

Enzymes can be immobilized on suitable polymeric materials with retention of their catalytic activity[1]. Immobilization is typically achieved through a site-specific reaction between reactive moieties of the chosen material and an amino acid residue on the enzyme[2]. These catalytically active, immobilized enzymes are able to catalyze degradation or neutralization reactions of certain toxins in wastewater[3]. Treatment processes of the wastewater at common municipal sewage treatment plants are not efficient with regards to the removal of trace amounts of biologically active pollutants from the water[4–6]. Immobilized enzyme systems are extremely sensitive for detecting these toxins as well as providing a means of bioremediation by degrading or neutralizing the pollutant species[3]. Most endocrine disrupting toxins found in the wastewater are from drug residues excreted by humans, one example being estrogen, commonly found in female oral contraceptives[5]. These biologically active species remain to a certain extent in the treated sewage water and are subsequently introduced into the environment with adverse effects on animal life and, via the process of bioaccumulation, ultimately on human health[4,6]. Apart from providing a means of detection and remediation of toxins in wastewater, immobilized enzymes are also essential for bioreactors in which directional synthesis can take place via cascade reactions[3]. Currently, the production of polymeric surfaces for immobilization of enzymes typically entails laborious synthetic techniques for surface modification in order to ensure the availability of

[†] The text in this chapter was adapted from a manuscript published in Polymer Chemistry (2011): **Cloete, W. J.; Adriaanse, C.; Swart, P.; Klumperman, B. *Polym. Chem.* 2011, *2*, 1479**.

reactive moieties for immobilization. In this chapter, a facile method for the immobilization of enzymes on nanofibrous membranes is described. We used conventional radical copolymerization for the synthesis of the copolymer without the necessity for surface modification of the resulting polymeric membrane. Electrospinning produces sub-micron polymer fibres that form membranes with extremely high surface areas on which enzymes can be immobilized[4]. The high surface areas increase the amount of enzymes that can be immobilized and cause a concomitant increase in the catalytic activity of the enzymes per unit area of the membrane[1,3].

We successfully immobilized two enzymes (horseradish peroxidase and glucose oxidase)[7] on a membrane consisting of unmodified polymeric fibres. This was accomplished by making use of the reactive maleic anhydride units of poly(Sty-*alt*-MAnh) copolymer[8–12]. Both enzymes contain a number of accessible amine functional groups from their lysine residues. These primary amines can react in an amidation reaction with the maleic anhydride units on the polymer backbone to become covalently bonded to the polymer fibre. Poly(Sty-*alt*-MAnh) was chosen for this study because of several properties which make it ideal for electrospinning into sub-micron fibres from the solution[13]. Specifically, it is soluble in common organic solvents and reasonably high molar masses can easily be obtained via free radical polymerization. Conventional free radical polymerization was thus employed to make an alternating copolymer from styrene and maleic anhydride. The reaction was carried out in solution in a 1:1 molar ratio under inert conditions using AIBN as an initiator at 60 °C. The polymer was characterized in a THF solution by means of size exclusion chromatography (SEC, Figure S5.2) using linear polystyrene calibration standards and a refractive index detector (M_w = 253 × 10^3 Da, $Đ$ = 4.6).

Electrospinning of the polymer was done from a 1:2 DMF/acetone solution (15 wt%) with the collector at a distance of 15 cm and offset of 4 cm from the needle tip that was connected to a high voltage supply (25 kV, 400 microamps, 10 Watts, high output voltage supply) set at 15 kV and the polymer solution was fed at 0.01 mL min^{-1} by means of a feed pump (Harvard, Model 33 Twin Syringe Pump). SEM analysis was done on a series of fibres, spun from the same solution, but with varying flow rates and field strengths (Tables S5.1-5.2; Figures S5.3- S5.6). The conditions described above were found to be optimal for producing visibly uniform fibres of the desired diameter. A mesh of these fibres with a diameter of ca. 500 nm (Figure. 5.1) was employed for the immobilization of HRP and GOX. Earlier work in our labs showed that the fiber diameter as studied by SEM has a tendency to increase upon

protein immobilization. Measurements after immobilization were not performed in the present study.

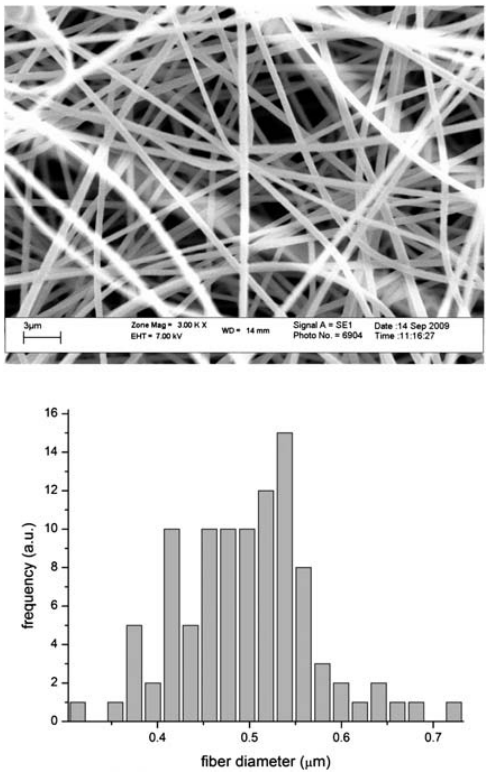

Figure 5.1: SEM image of poly(Sty-*alt*-MAnh) copolymer fibres and the fibre diameter as determined via analSIS doco by Olympus Soft Imaging Solutions GmbH.

The fibres were immersed in 10 mL of a 4 mg mL^{-1} solution of HRP in PBS buffer (pH 7.4)[1]. Incubation of the enzyme solution with the fibres took place at ambient conditions for 1 hour in a Petri dish with the solution rotated/shaken by means of a Belly Dancer laboratory shaker. The fibres were removed and washed three times for 10 minutes at a time, with a PBS/Tween (0.01% Tween-20) solution. This buffer solution, containing the mild detergent, Tween-20, was used to get rid of any non-specific binding or adsorption of the enzyme to the polymer fibres. A substrate solution consisting of 2,2'-azino-bis(3-ethylbenzthiazoline-6-sulfonic acid)-ABTS and H_2O_2 in PBS was introduced to the fibre-immobilized enzymes and a colour change was observed relative to a control (Figure 5.2). The controls used in the study consisted of poly(Sty-*alt*- MAnh) fibres incubated for 1 hour in the same PBS buffer solution without the enzyme as well as crosslinked fibres with no remaining anhydride moieties, incubated with and without the enzyme.

Figure 5.2 The colour change of substrate solution ABTS/PBS/H_2O_2, left is the control with no enzyme immobilized and right is the poly(Sty-*alt*- MAnh) with covalently bonded HRP.

The crosslinked membranes were obtained by electrospinning under the same conditions as before onto a 0.3 M ethylene diamine solution in isopropanol. The crosslinked membrane obtained was no longer soluble in acetone or DMF indicating that the electrospun fibres were fully crosslinked. An excess of amine was used in the crosslinking reaction to ensure that the fibres no longer contained any accessible reactive maleic anhydride moieties.

The substrate solution introduced to the fibres on which the enzyme was immobilized turned from light green to dark blue. This indicated the presence of covalently bonded HRP on the poly(Sty-*alt*-MAnh) fibres since HRP catalyzes the reaction between ABTS and H_2O_2, in a PBS buffer solution, turning ABTS (light green) into $ABTS^+$ (dark blue). The expected colour change was not observed for the fibres without incubation with the HRP or for the crosslinked fibres after incubation with and without the HRP.

In order to see if a simple cascade reaction could be done with immobilized enzymes, two further experiments were conducted. In the first experiment, HRP (4 mg mL^{-1}) and GOX (10 mg mL^{-1}) were immobilized together on a membrane while dissolved in PBS buffer solution. Incubation and wash steps were repeated as previously described. A substrate solution made up of Ampliflu Red/D- glucose in PBS buffer was introduced and the subsequent colour change observed (Figure 5.3)[1]. The proposed mechanism for this colour change was that GOX oxidized D-glucose leading to the evolution of H_2O_2. Then, the immobilized HRP catalyzed the reaction between evolved H_2O_2 and Ampliflu Red to yield Resorufin. To test whether this reaction cascade had indeed occurred, in the second experiment, HRP and GOX

were immobilized on two separate membranes. We first introduced Ampliflu Red substrate solution onto the membrane with the GOX to produce H_2O_2. The resulting solution was then transferred to the membrane on which the HRP was immobilized. The same colour change was observed as in the previous experiment, indicating that the HRP successfully catalyzed the reaction between the evolved H_2O_2 and Ampliflu Red to yield Resorufin. To confirm the immobilization of HRP with the retention of enzymatic activity, the immobilization was repeated. Instead of adding the substrate after immobilization of HRP onto the fibres, the fibres were incubated in a buffered solution of primary and secondary antibodies followed by testing with an appropriate substrate solution *(vide infra).*

Figure 5.3 The colour change of substrate solution going from Ampliflu Red to Resorufin. On the left is the control with no immobilized enzyme and on the right the immobilized membrane with glucose oxidase and horseradish peroxidase.

The HRP was first incubated as previously discussed with subsequent wash steps. Then the fibres were incubated in casein buffer (10 mM Tris, pH 7.6, 0.15 M NaCl, 0.5 % casein, 0.02 % thiomersal) for 20 minutes in order to block all nonspecific sites where antibodies may bind. Anti-HRP antibodies (1:10 000 in casein buffer) were incubated along with the fibres at 37 °C for 2 hours. After washing with 0.1 % Tween-20 solution as before, a secondary antibody (Sigma, anti-rabbit IgC, catalogue: A3687), conjugated to alkaline phosphatase (1:20 000), was added to the fibres and incubated at 37 °C for 2 hours. This was followed by four wash cycles, where after 5-bromo-4-chloro-3-indolyl phosphate p-toluidine salt/nitro blue tetrazolium (BCIP-T/NBT) substrate was added at room temperature. A positive result was obtained with the substrate solution changing from light yellow to dark purple (Figure 5.4), indicating that the enzyme was successfully immobilized with retention of its catalytic

activity.

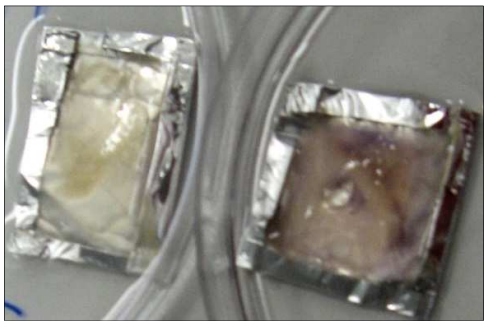

Figure 5.4 The colour change of subatrate solution BCIP-T/NBT, left is the control with no enzyme antibody immobilized and right is the fibres after incubation with HRP, primary and secondary antibodies.

The controls used in this experiment consisted of the same controls used for the previous experiments and the introduction of the BCIPT/NBT substrate solution yielded a negative result for the crosslinked membranes as well as the fibres on which no enzymes were immobilized. In order to assess the activity of the immobilized enzymes, a dedicated experiment was conducted. In this experiment, the HRP was immobilized from 10 mL of a diluted solution in PBS (1.0 mg mL^{-1}) onto a 1 cm^2 membrane of poly(Sty-*alt*- MAnh) nanofibres and washed four times with 0.01% Tween-20 solution in PBS. The concentration of active HRP was determined via an assay with ABTS and H_2O_2 solution in a citrate buffer at pH 5.0. The substrate solution was composed of 6 mg ABTS and 6 mL H_2O_2 (30%) in 12 mL of citrate buffer. The concentration in the various samples was measured by UV absorbance at 405 nm and calibrated against a calibration curve of known enzyme concentrations. From the difference in the HRP concentration in the solution before and after the immobilization, it was calculated that 1.96 mg HRP was bound to the fiber surface. The activity of the immobilized enzymes was equivalent to 0.42 mg HRP, i.e. 21% activity relative to the free enzyme. This can mean that either HRP loses some of its activity upon immobilization or that the active site of a fraction of the enzyme is inaccessible to the substrate. The retention of enzymatic activity compares favorably with earlier reported values on enzymes immobilized on poly(ethylene-*g*-(STY-*co*- MAnh))[11].

Conclusions

This study qualitatively showed that using the reactive maleic anhydride residues on electrospun poly(Sty-*alt*- MAnh) fibres provides a facile method to immobilize enzymes such as HRP and GOX. Two methods confirmed the covalent attachment of HRP to the electrospun fibres. First, wash steps with Tween-20 solution were unable to remove the enzyme from the membrane. Second, poly(Sty-*alt*- MAnh) fibres that were treated with ethylene diamine and consequently had no reactive MAnh moieties were unable to immobilize HRP. The binding efficacy of the HRP and the retention of its catalytic activity were successfully verified by means of incubation with primary and secondary anti-HRP antibodies. The reported immobilization method is highly recommended as a viable alternative for enzyme immobilization on high surface area polymeric materials. No modification of the surface or functionalization thereof is necessary prior to immobilization of the enzymes. This facile method of immobilization with retention of catalytic activity makes it ideal as a detection method for toxins and possible bio-remediation. It also provides an opportunity for kinetic studies of directional biochemical reactions by spectroscopic means, since cascade reactions can easily be conducted after enzyme immobilization. Further studies on recyclability and possible enzyme leaching of the membranes are underway in our labs.

Bibliography

(1) Logan, T. C.; Clark, D. S.; Stachowiak, T. B.; Svec, F.; Fre, J. M. J. **2007**, *79*, 6592.

(2) Gauthier, M. a; Klok, H.-A. *Chem. Commun. (Camb).* **2008**, 2591.

(3) Ignatova, M.; Stoilova, O.; Manolova, N.; Mita, D. G.; Diano, N.; Nicolucci, C.; Rashkov, I. *Eur. Polym. J.* **2009**, *45*, 2494.

(4) Kasprzyk-Hordern, B.; Dinsdale, R. M.; Guwy, A. J. *Water Res.* **2009**, *43*, 363.

(5) Hollender, J.; Zimmermann, S. G.; Koepke, S.; Krauss, M.; McArdell, C. S.; Ort, C.; Singer, H.; von Gunten, U.; Siegrist, H. *Environ. Sci. Technol.* **2009**, *43*, 7862.

(6) Auriol, M.; Filali-Meknassi, Y.; Tyagi, R. D.; Adams, C. D.; Surampalli, R. Y. *Process Biochem.* **2006**, *41*, 525.

(7) Wilhelm, T.; Wittstock, G. *Angew. Chem. Int. Ed. Engl.* **2003**, *42*, 2248.

(8) Mannino, S.; Brenna, O.; Buratti, S.; Cosio, M. S. *Electroanalysis* **1997**, *9*, 1337.

(9) Goldstein, L. In *Methods in Enzymology*; Gertrude, L. .; Perlmann, E., Eds.; Academic Press, 1970; Vol. 19, pp. 935–962.

(10) Beddows, C. .; Gil, M. .; Guthrie, J. T. *Polym. Bull.* **1985**, *14*, 199.

(11) Beddows, C. G.; Gil, H. G.; Guthrie, J. T. *Biotechnol. Bioeng.* **1985**, *27*, 579.

(12) Lee, M.-Y.; Srinivasan, A.; Ku, B.; Dordick, J. S. *Biotechnol. Bioeng.* **2003**, *83*, 20.

(13) Tang, C.; Ye, S.; Liu, H. *Polymer (Guildf).* **2007**, *48*, 4482.

Supplementary Information:

Facile immobilization of enzymes on electrospun poly(styrene-alt- maleic anhydride) nano fibres.

Synthesis of poly(Sty-*alt*-MAnh)

An alternating copolymer of styrene (extracted with KOH, dried over $MgSO_4$, distilled in vacuo) and maleic anhydride (Merck 99%) was synthesized by conventional free radical chemistry in a 1:1 molar ratio styrene : maleic anhydride. 15 g Styrene monomer was dissolved in 200 mL MEK (SASOL Chemicals, 99.75%) along with 14.12 g maleic anhydride and 0.1182 g AIBN (Riedel-DeHaën ; SIGMA-ALDRICH; Recrystallized from CH_3OH). The reaction mixture was degassed with N_2 (gas) for 30 min and reacted over-night under reflux at 60 °C. The polymer was precipitated in 500 mL iso-propanol (SASOL Chemicals, 85%).

The polymer was dried in a vacuum oven at room temp, overnight to remove unreacted monomer and solvent. The total amount of polymer recovered was 27.03 g (%Yield = 92.80%). ^{1}H-NMR (Varian Unity Inova, 400MHz) in d6-DMSO was used to verify if the co-polymer was in fact synthesized and size exclusion chromatography (SEC) was done to establish the molar mass.

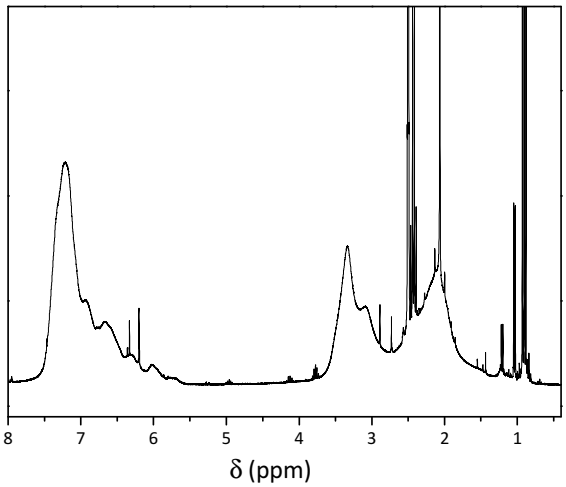

Figure S5.1: ^{1}H-NMR of poly(Sty-*alt*-MAnh) δ(d6-DMSO) [ppm]: J=6.5-7.5 Hz, benzyl unit; J=3- 3.5,2H, anhydride unit; J=2.1, (CH2-CH(C6H5))

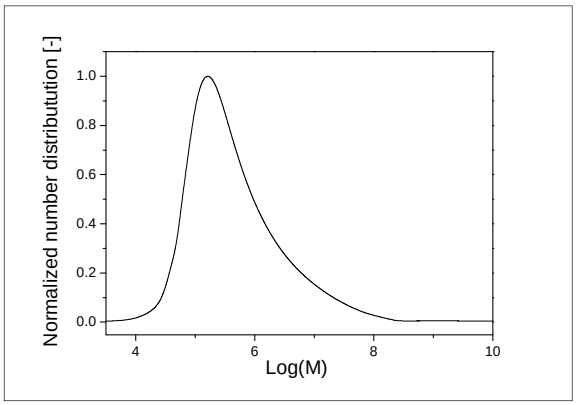

Figure S5.2: SEC analysis done in THF (M_w = 252 887 Da, $Đ$ = 4.6)

Electrospinning

The polymer was dissolved in a 1:2 DMF:acetone solution (15 wt%). The collector (aluminium foil) was set up 15 cm below needle tip with an offset of 4 cm to the centre of the collector. The polymer solution was fed through a Teflon tube (Hamilton, P/N 8651/00) from a glass syringe mounted in a syringe pump (Harvard, Model 33 Twin Syringe Pump) to the needle (Hamilton, 26 Gauge). The needle was positioned at an angle of ca. 30°. A flow rate of 0.01 mL/min and the high voltage supply (Voltage supply: 25 kV, 400 micro Amps, 10 Watt, high output voltage supply) set at 15 kV appeared to be the optimum parameters for spinning. Table S5.1 contains all the parameters used in the different electrospinning experiments.

Table S5.1: Same experimental setup but different flow rates for electrospinning

Experiment:	**WC013**				
Sample:		**#1**	**#2**	**#3**	**#4**
Parameters:	**Volts**	**15 kV**	**15 kV**	**15 kV**	**15 kV**
	Distance	**15 cm**	**15 cm**	**15 cm**	**15 cm**
	Flow Rate	**0.01 mL/min**	**0.02 mL/min**	**0.03 mL/min**	**0.04 mL/min**
	Offset	**4 cm**	**4 cm**	**4 cm**	**4 cm**
	Concentration	**15 wt% SMA**	**15 wt% SMA**	**15 wt% SMA**	**15 wt% SMA**

Table S5.2: Same experimental setup but electrospinning done at different voltages *SEM* analysis was done after vacuum gold coating of some of the resulting fibres at *500X* and *3000X* magnification respectively.

Experiment:	**WC014**			
Sample:		**#1**	**#2**	**#3**
Parameters:	**Volts**	**10 kV**	**15 kV**	**20 kV**
	Distance	**15 cm**	**15 cm**	**15 cm**
	Flow Rate	**0.01 mL/min**	**0.01 mL/min**	**0.01 mL/min**
	Offset	**4 cm**	**4 cm**	**4 cm**
	Concentration	**15 wt% SMA**	**15 wt %SMA**	**15 wt% SMA**

SEM analysis was done after vacuum gold coating of some of the resulting fibres at *500X* and *3000X* magnification respectively.

The following images were obtained from the SEM analysis:

WC013_Sample1

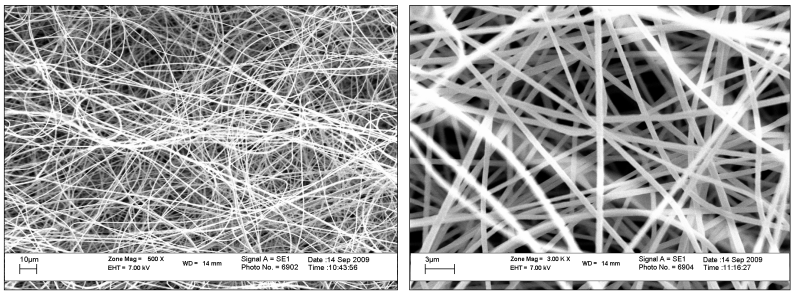

Figure S5.3: *Poly(Sty-alt- MAnh)* fibres Zone Magnification *X500* and *X3000*

WC013_Sample2

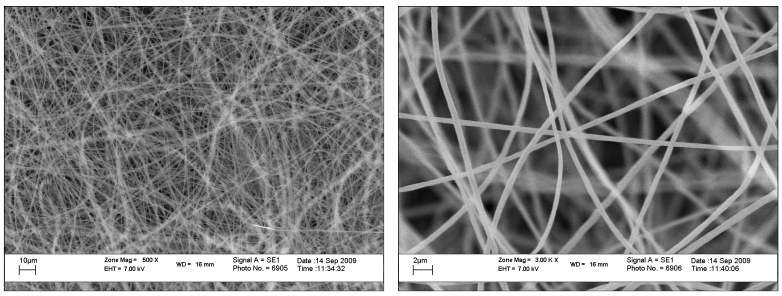

Figure S5.4: *Poly(Sty-alt- MAnh)* fibres Zone Magnification *X500* and *X3000*

WC014_Sample3

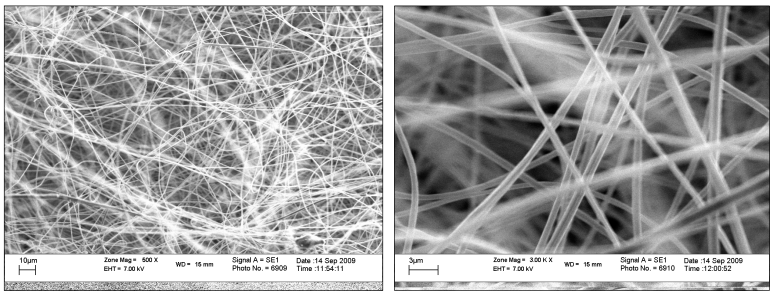

Figure S5.5: *Poly(Sty-alt- MAnh)* fibres Zone Magnification *X500* and *X3000*

WC013_Sample4

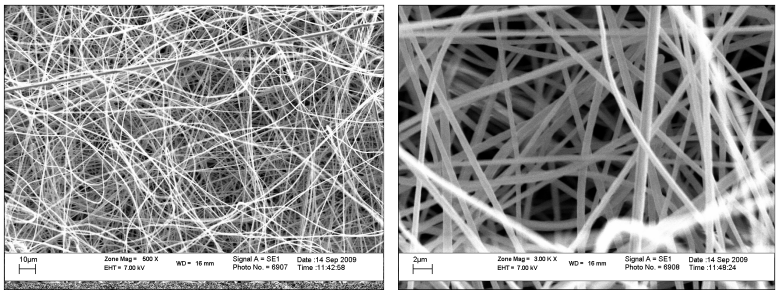

Figure S5.6: *Poly(Sty-alt- MAnh)* fibres Zone Magnification *X500* and *X3000*

From the images it is clear that fairly uniform fibres were obtained and that different spinning conditions, all resulted in fibre diameters *ca*. 300 nm.

Immobilization of *Horseradish Peroxidase (HRP)* on *poly(Sty-alt-MAnh)*

A 4 mg/mL solution was made up by dissolving *HRP* in *PBS* buffer (8 g NaCl; 0.2 g KCl; 11.5 g Na_2HPO_4; 0.2 g KH_2PO_4; pH 7.4) and placed along with the electro spun fibres in a petri dish and incubated for one hour on a Belly Dancer laboratory shaker. The fibres were subsequently washed three times for 10min at a time with PBS-Tween buffer solution (*PBS, 0.01% Tween 20*). The substrate solution *ABTS/H_2O_2* (*6 mg ABTS (2, 2'-azino-bis(3-ethylbenzthiazoline-6-sulphonic acid)*) and *37% H_2O_2, 6 µL* in *12 mL* citrate buffer *0.1 M*, *pH 5*) was then introduced to the fibres and a colour change was observed. The colour change was noted relative to what happens when the *ABTS/H_2O_2* is introduced to fibres where no *HRP* was immobilized and incubated for the same time period in the *PBS* buffer.

Figure S5.7: Colour change (dark blue) observed relative to a control with no immobilized enzyme and the two substrate solutions used in the left picture after half an hour.

Immobilization of Horseradish peroxidise (*HRP)* and Glucose oxidase (*GOX)* on *poly(Sty-alt-MAnh)*

The same approach was taken as above for the immobilization of *HRP*. The *GOX* was immobilized by incubating the fibres in a petri dish with a *10 mg/mL* solution of *GOX-PBS* (*PBS pH 7.55*). The membranes was washed 3 times for *10 min* at a time with *PBS-Tween* (*PBS, 0.01% Tween 20*) The substrate solution of final concentration *100 µL/mL Ampliflu Red/PBS* was made up of two solutions, *1 mg/mL Dextrose (D-glucose)/PBS* and *10 mmol/L Ampliflu Red/PBS*. The substrate solution was introduced to the membranes and the colour change observed relative to a control. Two experiments were done, one where both *HRP* and *GOX* were immobilized on one membrane and another where *HRP* and *GOX* were immobilized on two separate membranes. In the experiment where the enzymes were immobilized on separate membranes the substrate solution (*Ampliflu Red/PBS/Dextrose*) was introduced to the *GOX* membrane first; the solution was then transferred from there to the membrane with *HRP* and the subsequent colour change was observed relative to a control.

Figure S5.8: Colour change (pink) observed relative to a control with no immobilized enzyme and the two substrate solutions after half an hour.

Binding efficiency of *HRP*

The binding efficacy of *HRP*(*BBI Enzymes, Sample for Stellenbosch University*) to the *Poly(Sty-alt- MAnh)* fibres was determined with the use of antibodies. Primary antibodies (*Anti-HRP*) were raised in rabbits with an immunization schedule of *56 days*. The *HRP* was first incubated as previously discussed with subsequent wash steps. Then the fibres were incubated in casein buffer (*10 mM TRIS, pH 7.6, 0.15 M NaCl, 0.5 % Casein, 0.02 % Thiomersal*) for *20 minutes* in order to block all non-specific sites where the antibodies may bind. For the controls only *PBS* was added. After *60 minutes* the *HRP* solution was discarded/decanted and the fibres were washed four times, four minutes each, with PBS buffer containing *0.1% Tween-20* (*PBS-Tween*). *Anti-HRP* antibodies (*1:10 000 in casein buffer*) was incubated with these fibres at *37 ℃* for *2 hours* followed by wash steps as mentioned previously.

Figure S5.9: Colour change observed after incubation of primary and secondary *Anti-HRP* antibodies and the introduction of the *BCIP-T/NBT* substrate solution.

A secondary antibody (*Sigma, anti-rabbit IgG, catalogue number: A3687*), conjugated to alkaline phosphotase (1: 20 000), was then added to the fibres and incubated at 37 °C for 2 hours, also followed by four washes with *PBS-Tween* as before, where after a *5-bromo-4-chloro-3-indolyl phosphate p-toluidine salt /nitro blue tetrazolium (BCIP-T/NBT)* substrate, *33 ml* of *BCIP-T* (*50 mg/mL in DMF*) and *44 ml* of *NBT* (*75 mg/mL in 70% DMF*) in *10 ml* of alkaline phosphotase buffer (*100 mM TRIS, pH 9.5, 100 mM NaCl, 10 mM* $MgCl_2$), was added to the *poly(Sty-alt- MAnh)* fibres and incubated at room temperature. The colour change was observed relative to the controls.

BCIP-T (Fermentas Life Sciences [Fermentas], Catalogue number R0821)

NBT (Fermentas Life Sciences [Fermentas], Catalogue number R0841)

Chapter 6

Degradation of proteins and starch by combined immobilization of protease and α-amylase on a single electrospun nanofibrous membrane

Combined immobilization of enzymes allowed for the degradation of complex solutions of starch and proteins. The effect of protease and α-amylase, immobilized on electrospun nanofibrous membranes made from poly(styrene-*alt*-maleic anhydride), on the degradation of proteins and starch solutions was evaluated on their own as well as in combination with each other. An *azocasein* assay showed that the immobilized protease (7.54 mg/cm^2) degraded proteins at a rate of 7.78 x 10^{-4} µmol.min^{-1}.mg protein^{-1}.cm^{-2}. Immobilized α-amylase degraded starch solutions at a rate of 0.808 µmol.min^{-1}.mg protein^{-1}.cm^{-2}, for an enzyme loading of 39.7 mg/cm^2, as determined using a *Megazyme* α-amylase assay kit. Immobilization of protease and α-amylase together on the same membrane led to an increase in enzyme activity for α-amylase from 0.808 µmol.min^{-1}.mg protein^{-1}.cm^{-2} on its own, to a value of 2.37 µmol.min^{-1}.mg protein^{-1}.cm^{-2} in combination with protease. There was however a sharp decrease in activity of the co-immobilized protease. The threefold increase in activity for the α-amylase and the observed decrease in protease activity for co-immobilized enzymes were not anticipated and the reason for this is under investigation.

6.1 Introduction

Enzymes play an important role in catalysing reactions at relatively mild conditions, such as ambient temperatures and pressures as are common in biological systems. For this reason, enzymes are also widely used in modern biotechnologies. Isolation of enzymes from microorganisms enables production of large quantities of robust enzymes, functionalized for specific applications, and suitable to meet industrial demands. Commercial enzymes are supplied as solutions or as freeze-

dried powders that can be reconstituted into a solution by the end user. They may also be immobilized by adsorption or covalent attachment to polymers and high surface area substrates that find application in fine-chemical synthesis, fabrication of biosensors and diagnostics, food processing, protein digestion and bioremediation[1].

Immobilized enzymes have advantages over free enzymes in solution because they can be used repeatedly. However, certain immobilization substrates may compromise the function of the immobilized enzymes, depending on the characteristics of the substrate. Enzyme immobilization on mesoporous ceramics, for instance, leads to loss of catalytic activity because the enzymes are contained within the support and diffusion of the substrate solution to and from the active sites of the enzyme is restricted[1]. Nonwoven nanofibrous mats can overcome this disadvantage because their high porosity and interconnectivity allow mass transfer of substrate solution, and their high surface to volume ratio provides a relatively larger surface area for immobilization. In addition, nanofibers can be spun from a variety of polymers with modifiable functionality, enabling the design and manufacture of tailor-made surfaces for covalent enzyme immobilization.

Sheng-Feng Li *et al.* [2] described the use of immobilized enzymes on high surface area nanofibrous materials for converting raw materials into value added products. They made use of immobilized *Candida rugosa* lipase on PAN fibres for the hydrolysis of soybean oil into free fatty acids. Conversion of vegetable oils into chemical feedstock, using enzymes, illustrates the feasibility of adopting this technology and its preferential use over batch solution processes that are often employed. Immobilization of enzymes on high surface area substrates will increase their economic feasibility for industrial use. For instance, the major drawback of converting starch into maltose using *α*-amylase is the fact that it is performed in a batch reaction[3]. This process is not economically desirable because the enzymes involved can only be used once. Immobilized enzymes allow for reuse of the enzyme which is one of the key expenses and most vital component of the process.

Enzymes are not only used in processes to convert bio-matter into value added products, but also find widespread use in the remediation of biofouling that occurs in filtration processes and

bioreactors. Biofouling is a common phenomenon in environments where water is prevalent for extended periods[4]. Enzymes, such as proteases and amylases, are used for the remediation of biofilms and the degree of biofouling decreases drastically in the presence of these enzymes[5]. The formation of biofilms increases production costs as a result of the need for frequent cleaning and costly pre-treatment of the feed to the reactor or filtration module, and has clinical implications in that mature biofilms lead to the proliferation and spreading of pathogenic bacteria. Towards the goal of creating anti-biofouling coatings and surfaces, Cordeiro *et al.* showed that immobilized enzymes are able to counteract biofouling and they conclude that co-immobilization of different enzymes is the best route to effective, inherently anti-biofouling surfaces[6].

Currently, the best strategy to prevent the formation of biofilms is to inhibit initial adhesion of microorganisms. Due to the complexity of natural systems, the immobilization of more than one enzyme on the same surface is required. Combinations of enzymes have been evaluated in so-called clean-in-place (CIP) systems related to the food industry. The size, shape and nature of biofilms and extracellular polymeric substances (EPS) are on-going fields of investigation in parallel to finding suitable enzyme combinations for their degradation. Screening different combinations of immobilized enzymes may lead to a more feasible option than CIP for the remediation of complex solutions of biological foulants.

Maleic anhydride residues can be used to immobilize enzymes on nanofibers to provide a solid support for enzyme immobilization[6–11]. Our research group has developed a facile approach to enzyme immobilization on electrospun nanofibers containing maleic anhydride residues. This approach does not require rigorous modification or activation steps prior to immobilization, and therefore may provide a low-cost alternative for industrial applications[12]. Here, we extend the previous work by immobilizing commercial enzymes to lead the way for the manufacturing of membranes that are inherently anti-biofouling or for use in membrane reactors and food processing. The primary role of protease in nature is the proteolysis of proteins, to break them down into smaller polypeptides and amino acids. In turn, α-amylase hydrolyses starch into mono- and oligosaccharides. In this chapter we assess the ability of two enzymes, a commercial protease

(*Esperase*) and α-amylase (*Dextrozyme*), immobilized on electrospun nanofibrous materials, to degrade proteins and starch in solution, on their own and in combination.

6.2 Materials and methods

6.2.1 Reagents

All reagents were used as received and all buffer solutions were previously prepared and used as stock solutions and diluted as needed.

6.2.2 Enzyme assays

Commercially available enzyme kits were used to assess the enzyme activities of both the free as well as immobilized enzymes. The *Ceralpha method (AOAC Method 2002.01)* and the *Megazyme* α-amylase (*Megazyme International, Ireland*) kits were used to determine the enzyme activity of the protease and α-amylase respectively. The assays were chosen so that each substrate, upon conversion, leads to the evolution of a UV active dye. The amount of UV active dye in each supernatant was measured with a *Cary 60 UV-Vis* spectrophotometer (*Agilent Technologies*) and used to quantitatively determine and compare the enzyme activity of both the free as well as immobilized enzymes.

6.3 Experimental

The synthesis of poly(styrene-*alt*-maleic anhydride) and subsequent electrospinning into nanofibres was done as previously described by Cloete *et al.* [12]. Protein immobilization was achieved by incubating a 4 cm^2 fibre mat in 5 mL protein solution (*ca.* 43 mg/mL for protease and *ca.* 296 mg/mL for α-amylase, used as supplied without dilution) for 1 hour at room temperature with agitation. As control, bovine serum albumin (10 mg/mL) was also immobilized on a separate mat as well as with both protease and α-amylase. The amount of bovine serum albumin immobilized was

used to verify if immobilization of protease and α-amylase can be achieved in combination with an arbitrary additional protein. This was necessary since the enzyme solutions used in this study were commercial enzyme solutions and were used as received, meaning the enzymes were not isolated from the commercial solution and reconstituted prior to immobilization. Samples of each protein solution used (1 mL) were collected prior to incubation and the protein concentration was determined as described below. After incubation, each fibre mat was extensively washed with phosphate buffered saline (PBS, pH 7.0) containing *0.1% Tween 20* (4 x 5 min) to remove non-covalently bound protein. Four 1 mL samples of the PBS-Tween solution were collected and the protein content was determined, together with the original protein solution prior to incubation with the membrane, using the *Pierce BCA* protein assay kit with bovine serum albumin as standard. The amount of immobilized protein was calculated as the difference in protein content prior to and following immobilization. The same immobilization procedure described above was used for all enzyme and control solutions.

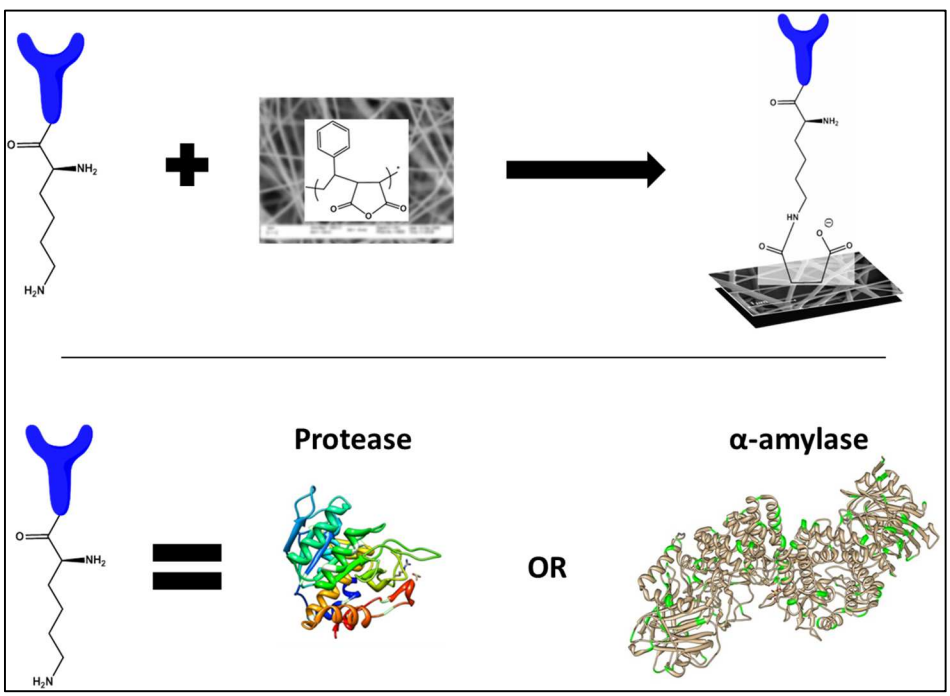

Figure 6.1: General scheme for enzyme immobilization on poly(styrene-*alt*-maleic anhydride) nanofibers. The lysine residues on the enzymes through which immobilization is expected to take place are highlighted in white for the protease and green for the α-amylase.

The *Ceralpha method* (*AOAC Method 2002.01*) was used to quantify α-amylase activity of the immobilized enzyme using the *Megazyme α*-amylase kit (*Megazyme International, Ireland*) as per manufacturer instructions. Briefly, a sufficient volume of substrate solution, containing *para-nitrophenyl maltoheptaoside*, was equilibrated to 40 °C, separate from the fibre mat samples. After 5 min, *ca.* 800 µL of the substrate was added to each fibre mat and incubated for exactly 10 min at 40 °C. After incubation, enzyme activity was quenched by addition of 8 mL 1% Tris-base. The samples were thoroughly mixed and the absorbance of the supernatant was read at 400 nm in a *Cary 60 UV-Vis* spectrophotometer (*Agilent Technologies*) against a sample blank. The sample blank was prepared by incubating *ca.* 200 µL liquid enzyme solution with 8 mL *1%* Tris-base prior to addition of the substrate. Incubation was performed as with the fibre mat samples. Total enzyme activity was calculated using *Equation 1* where ΔA represents the change in absorbance at 400 nm following incubation, V the total reaction volume in mL, ε is the millimolar extinction coefficient of *para-nitrophenol* (18.1 $mM^{-1}.cm^{-1}$), *t* the total incubation time of *10* min for a specific area of the fibre mat.

$$U/mg\ protein/cm^2 = \frac{(\Delta A \times V)}{(t \times \varepsilon \times \left(\frac{[protein]}{cm^2}\right))} \qquad (1)$$

During protease immobilization studies, the protease was evaluated for retention of enzymatic activity using an assay adapted from Sheng-Feng Li *et al.* (2009)[2]. *Azocasein* substrate solution (*2.5 mL of 2.5% stock in* 50 *mM borax buffer, pH 9.5*) was added to the electrospun fibre mat containing *0.6 mg* immobilized protein. The reaction was quenched with 2.5 mL of 10*% trichloroacetic acid* (*TCA*) in deionized water, after 5 min incubation at 30 °C. The solutions were held at a constant *pH of* 9.5 in order to simulate the conditions under which *Esperase* is used in laundry detergents. After centrifugation of each reaction mixture, the UV absorbance of the supernatant was read at 340 *nm* on a *Cary 60 UV-Vis* spectrophotometer. The rate at which the immobilized protein hydrolysed the *azocasein* substrate was calculated using *Equation 1,* where (Δ*A*) represents the change in

absorbance at 340 nm, (V) the reaction volume (in mL), (ε) is the extinction coefficient of the product of azocasein hydrolysis at 340 nm and has a value of 38 $mM^{-1}.cm^{-1}$ and (t) is the reaction time of 5 min.

In order to verify whether more than one type of enzyme can be immobilized on the same nanofibrous membrane simultaneously, both *Dextrozyme* and *Esperase*, inhibited with *phenylmethylsulfonyl fluoride* (*PMSF*) [Thermo Scientific], were added to a buffered solution in a similar fashion to the immobilization of individual enzymes. *PMFS* reversibly inhibits the catalytic activity of the protease, preventing the degradation of the α-amylase during immobilization. Subsequent to immobilization, the *PMFS* was removed along with any non-covalently bound enzyme during the wash steps with *Tween-20*. The removal of *PMFS* from the active centre regenerates the catalytic activity of the protease. The enzymatic activity of *Dextrozyme* was assayed as described using *para-nitrophenyl maltoheptaoside* as substrate and calculated in the same way as before using *Equation 1.*

6.4 Results and Discussion

Both enzymes were effectively immobilized and partially retained their activity, continuing to degrade proteins and starches while immobilized on the electrospun nanofibrous mat (Table 6.1). The retention of enzymatic activity is largely dependent on whether or not it is immobilized a way that the active centre of the enzyme is accessible to the substrate. So although a large number of enzymes can be immobilized, the overall enzymatic activity of immobilized enzymes will be lower than that of the free enzyme in solution. The proposed mechanism for enzyme immobilization in the current approach is through nucleophilic addition of primary amines contained in the lysine residues that make up part of the amino acids in the enzyme structure. The crystal structures described for various enzymes and those seen in Figure 6.1 are not necessarily indicative of enzyme conformation in solution[13]. This implies that prior to immobilization each enzyme may be present in more than one conformation and the vast amount of available lysine residues are equally likely to undergo the amidation reaction to the reactive MAnh units. This could result in random

orientations of immobilized enzymes with some leaving no access of the substrate to the active site of the enzyme[14]. The actual immobilization may also cause conformational changes leading to a loss of activity due to decreased ability of the substrate molecules to diffuse to the active centre of the enzyme. Furthermore, protease and α-amylase were successfully immobilized in combination with each other on the same membrane and assays showed that both enzymes retain their catalytic activity (Table 6.1). Surprisingly, α-amylase activity increased significantly when the two enzymes were immobilized in combination on the same membrane (2.37 U.mg protein^{-1}.cm^{-2} in combination with protease compared to 0.808 U.mg protein^{-1}. cm^{-2} for the individually immobilised α-amylase) whilst the protease activity dropped by *ca.* 85 %. The increase in enzyme activity of co-immobilized enzymes has previously been reported for cholesterol oxidase (COD) and horseradish peroxidase (HRP) after covalent attachment via gluteraldehyde to a perlite support material after surface modification with 3-aminopropyltriethoxysilane. In this case COD and HRP make use of the same substrate namely H_2O_2 and the increase in activity once co-immobilized could be due to enhanced mass transfer effects and the proximity of the immobilized enzymes[15]. This was proposed to be the reason for increased activity co-immobilized glucoamylase and glucose isomerase, which again makes use of the same substrate[16]. In the case of changes in activity for enzymes employing different substrates, an increase or decrease in activity can not readily be explained through mass transfer and proximity alone. The reason for the increase in activity of the α-amylase as well as the large decrease in activity for the protease once they are co-immobilized onto SMA nanofibers is under investigation. Experimental verification of whether this is the case when α-amylase and protease are immobilized in combination with other enzymes and possibly different substrate materials is pending.

Table 6.1: Enzymatic activity of enzymes immobilized on poly(styrene-*alt*-maleic anhydride) nanofibrous mats.

Enzyme	Enzyme loading[a]	Activity[b]	Free Enzyme Activity[b]	% Retention[c]
protease	7.54	7.78×10^{-4}	8.87×10^{-4}	87.0 %
α-amylase	39.7	0.808×10^{0}	8.81×10^{0}	9.00 %
protease + α-amylase	N/A	1.54×10^{-5}	8.87×10^{-4}	1.73 % (protease)
	N/A	2.37×10^{0}	8.81×10^{0}	27.0 % (α-amylase)

***a* in *mg/cm²* ;**

b* in *µmol.min.mg.cm⁻²

***c* is the activity retained after immobilization vs. the activity of the free enzyme**

In order to compare the respective enzymes in terms of their catalytic activity, assays were chosen so that the same quantitative variable could be measured for both enzymes: UV detection of the amount of free azo dye in the case of the azocasein substrate solution (to detect protease activity), and the release of *para-nitrophenol* when using *para-nitrophenyl maltoheptaoside* as substrate (to detect α-amylase activity). Each substrate used for the assays contained a UV active compound conjugated to the substrate through either a peptide or glucose bond that can be cleaved by the enzyme. These assays proved highly efficient for the investigation of the rate at which immobilized enzymes degrade or convert the substrate. UV intensity, related directly to the concentration of UV active species in the supernatant after centrifugation, was used to quantify the enzyme activity and correlate it with the retention of activity of immobilized protease and α-amylase. This method worked well for the enzymes immobilized in this study ensuring a quantitative means for comparison of enzyme activity for different enzymes immobilized on their own as well as in combination with each other.

6.4 Conclusions

The results in this chapter demonstrate that commercial α-amylase and protease can be immobilized on poly(styrene-*alt*-maleic anhydride) nanofibrous mats with partial retention of their catalytic activity towards the degradation of starch and proteins. Co-immobilization of α-amylase and protease led to a significant increase in α-amylase activity alongside a significant decrease in activity for the protease compared to each one immobilized on its own. Recommended future work includes the investigation of more combinations of enzymes immobilized on a single nanofibrous mat and the evaluation of membranes with immobilized enzymes for continuous use in the digestion of complex solutions of biomolecules as well as their ability to withstand biofouling. A combination of immobilized enzymes targeted at the digestion or degradation of a variety of proteins and other biomolecules will go a long way in providing surfaces that prevent the attachment and proliferation of microbial foulants. This opens the door to design single membranes that can perform cascade reactions or single membranes to digest complex solutions of proteins and other biomolecules. Nanofibrous mats as filtration media are feasible and promising materials for use as filtration membranes[17,18]. The design of tailor-made nanofibrous filter materials with immobilized enzymes may provide a solution for the prevention of biofouling by excluding organic fouling agents or converting and metabolizing nutrients that sustain biofilm growth. The ultimate application would be a means of pre-treatment of the feed in water purification, such as in remediation of effluents and waste streams, or for use in bioreactors to convert starch and oils into feedstock for the food industry.

Bibliography

(1) Wang, Z.-G.; Wan, L.-S.; Liu, Z.-M.; Huang, X.-J.; Xu, Z.-K. *J. Mol. Catal. B Enzym.* **2009**, *56*, 189.

(2) Li, S.-F.; Wu, W.-T. *Biochem. Eng. J.* **2009**, *45*, 48.

(3) Bayramoğlu, G.; Yilmaz, M.; Arica, M. Y. *Food Chem.* **2004**, *84*, 591.

(4) Coetser, S. E.; Cloete, T. E. *Crit. Rev. Microbiol.* **2005**, *31*, 213.

(5) Cordeiro, A. L.; Werner, C. *J. Adhes. Sci. Technol.* **2012**, *25*, 2317.

(6) Cordeiro, A. L.; Hippius, C.; Werner, C. *Biotechnol. Lett.* **2011**, *33*, 1897.

(7) Kim, B. C.; Nair, S.; Kim, J.; Kwak, J. H.; Grate, J. W.; Kim, S. H.; Gu, M. B. *Nanotechnology* **2005**, *16*, S382.

(8) Zaharieva, E. I.; Georgiev, G. G.; Konstantinov, C. I. *Biomaterials* **1996**, *17*, 1609.

(9) Ye, P.; Xu, Z.; Wu, J.; Innocent, C.; Seta, P. **2006**, 1041.

(10) Pompe, T.; Zschoche, S.; Herold, N.; Salchert, K.; Gouzy, M.-F.; Sperling, C.; Werner, C. *Biomacromolecules* **2003**, *4*, 1072.

(11) Cordeiro, A. L.; Lenk, T.; Werner, C. *J. Biotechnol.* **2011**, *154*, 216.

(12) Cloete, W. J.; Adriaanse, C.; Swart, P.; Klumperman, B. *Polym. Chem.* **2011**, *2*, 1479.

(13) Rivas-Pardo, J. A.; Herrera-Morande, A.; Castro-Fernandez, V.; Fernandez, F. J.; Vega, M. C.; Guixé, V. *PLoS One* **2013**, *8*, e66687.

(14) Elnashar, M. M. M. In *Biotechnology and Biopolymers*; Elnasher, M. M. ., Ed.; 2011; pp. 3–32.

(15) Torabi, S.-F.; Khajeh, K.; Ghasempur, S.; Ghaemi, N.; Siadat, S.-O. R. *J. Biotechnol.* **2007**, *131*, 111.

(16) Ge, Y.; Wang, Y.; Zhou, H.; Wang, S.; Tong, Y.; Li, W. *J. Biotechnol.* **1999**, *67*, 33.

(17) Yoon, K.; Kim, K.; Wang, X.; Fang, D.; Hsiao, B. S.; Chu, B. *Polymer (Guildf).* **2006**, *47*, 2434.

(18) Yoon, K.; Hsiao, B. S.; Chu, B. *J. Memb. Sci.* **2009**, *326*, 484.

Appendix A: Derivation of Enzyme Activity Equation (*Equation 1*)

A single unit of enzyme activity is defined as the amount of product formed (in µmol) per minute. In this case the measured quantity is the change in absorbance. In order to convert absorbance to a concentration one needs to use the Beer-Lambert law,

$$\mathbf{A = \varepsilon C L ,}$$

where ε is the millimolar extinction coefficient for each product (18.1 $mM^{-1}.cm^{-1}$ para-nitrophenol and 38 $mM^{-1}.cm^{-1}$ for the the azo-dye), C the concentration in mM and L the light path length of the cuvette used (1 cm in our case).

Therefore: $\mathbf{C = (A/\varepsilon L)}$

A standard unit (U) of enzyme activity is defined as **1 µmol** product formed per minute. Consequently one needs to convert concentration in mM to µmol.

Since $1x10^{-3}$ M * $1x10^{-3}$ L = $1x10^{-6}$ Mol, 1 µmol is equal to 1 mM * 1 mL

In order to convert concentration from mM to µmol one needs to multiply with the total assay volume (substrate + TCA (5 mL) in the case of protease and substrate + 1% tris (8.8 mL) in the case of amylase)

To convert to a unit of enzyme activity one needs to divide by the assay time (5 min for protease and 10 min for amylase)

Therefore: $\mathbf{U = (A^* V)/(\varepsilon * t)}$

The definition of specific enzyme activity (Specific U) is the amount of enzyme that produces 1 µmol product per minute under assay conditions. As a result one needs to divide by the concentration of immobilized enzyme used in the assay (U/[mg protein]).

$$\mathbf{U/[mg\ protein]} = \mathbf{(A^*\ V)/(\varepsilon * t * [mg\ protein])}$$

Specific activity / cm^2:

$$\mathbf{(U/[mg\ protein])/\ cm^2 = (A^*\ V)/(\varepsilon * t * [mg\ protein]/\ cm^2))}$$

This formula above is universal for both assays used in this study, and yields comparable results for enzyme activities of different enzymes. Since the formulae are similar, the order of enzyme activity will be similar as it should be. This enables us to compare the results more directly since the units for each enzyme assay are the same.

Chapter 7

Conclusions and Future work

Membrane filtration as a means for the production of potable water is becoming increasingly important. However, membrane processes are expensive and often not economically feasible in developing countries. Much of the expense is due to the requirement of pre-treatment of feed water to prevent biofilm formation. Biofilms can cause irreversible damage to membranes by clogging membrane pores. Various strategies exist for the remediation of biofilms but none of the current strategies are 100% effective. Current strategies include periodic cleaning with surfactants and biocides to kill and remove biofilms as well as backwashing and air scrubbing. These treatments, besides being largely ineffective, also lead to large increases in production costs and can pollute downstream water bodies where the long-term prevalence of surfactants and biocides leads to residual toxicity to marine life and biocide-resistant bacteria.

New developments in the design and control of complex polymers via living radical polymerization techniques, coupled with increasingly powerful surface characterization tools such as FTIR microscopy, enable surface modification and the production of versatile, functional surfaces. ATRP has been most commonly used for the surface grafting of cellulose to improve its anti-biofouling properties. RAFT polymerization, however, has the advantage of requiring no heavy metal catalysts and allows for chain end modification to increase the functionality of the modified surface. ATRP requires the use of heavy metal catalysts that cannot be removed completely post-polymerization, the residual metals may lead to corrosion of filtration systems and, due to their cytotoxicity, are unsuitable for biomedical applications.

Surface characterization techniques such as FTIR microscopy and XPS allow for both visualization of grafting efficiency as well as quantification of the extent of grafting on the surface. Azo-dyes conjugated to substrate molecules in enzyme activity assays allow for direct quantification of enzyme activity via UV spectroscopy by detecting the UV absorption of free azo-dye after conversion. Furthermore, in-situ ^{1}H-NMR measurements track the conversion of reagents and formation of polymeric species formed during polymerization

reactions in real-time. This data can then be used to form an understanding of the reaction kinetics and underlying mechanisms of the polymerization reaction.

In this thesis, some of the current problems in membrane filtration are addressed by synthesizing and characterizing anti-cell adhesive and reactive surfaces as novel antifouling materials for membrane filtration.

Chapter 3 deals with the surface grafting of regenerated cellulose with hydrophilic copolymers containing zwitterionic functionalities. Employing the reactive hydroxyl groups on the surface of the membranes, successful grafting of copolymers of *N*-vinylpyrrolidone (NVP) and maleic anhydride (MAnh) was achieved through an R-group approach of RAFT mediated polymerization. The MAnh contained in the polymer backbone or endgroups of the polymer were converted to zwitterionic compounds and upon exposure to bacteria cultures, these membranes were found to prevent adhesion of extracellular polymeric substances (EPS) and bacteria cells.

In Chapter 4, the underlying mechanism of the copolymerization of NVP/MAnh via RAFT polymerization is investigated. Better knowledge of this mechanism will allow the design and synthesis of a hydrophilic polymer with various advantages over the widely used PEG while incorporating a functional comonomer MAnh through which additional chemical modification can easily take place. Based on initialization studies done through in-situ ^{1}H-NMR experiments, no control is achieved for 1:1 monomer ratios of NVP/MAnh using two types of RAFT agents. The lack of control was due to the acid-catalyzed dimerization of NVP occurring at a much faster rate than the RAFT equilibrium could be established. The copolymerization was affected at even small amounts of MAnh but once consumed an initialization step for NVP was observed. This means that at low concentrations of MAnh, copolymerizations of MAnh/NVP can be controlled via trithiocarbonate and xanthate chain transfer agents. The resulting copolymer will contain short segments of NVP-*co*-MAnh in addition to a block of NVP homopolymer. Depending on the addition of MAnh, at the start, middle or towards the end of the polymerization NPV-*co*-MAnh segments can be built in at predetermined positions in the copolymer chains.

In Chapters 5 and 6, the facile immobilizationis described of enzymes on poly(styrene-co-maleic anhydride) nanofibers produced via electrospinning. The immobilization occurs through nucleophilic addition of primary amines on the enzyme to reactive maleic anhydride

units in the copolymer backbone. The covalently immobilized enzymes retain their activity and allow for cascade reactions to be performed on the surface as well as the degradation of complex solutions of proteins and starches. The combined immobilization of protease and α-amylase (Chapter 6) led to an unexpected increase in activity for the α-amylase but at the same time resulting in a significant decrease in protease activity.

Several overarching principles emerged during this study. Employing an R-group approach of RAFT mediated polymerization for the surface grafting of cellulose served as a proof of principle that any surface containing hydroxyl groups can effectively be modified with functional copolymers. Since any synthetic membrane can be modified in a similar fashion by introducing hydroxyl functionalities through plasma treatment or oxidation of the surface, this technique can be widely applied. To date, RAFT agents have not been widely available for use on an industrial scale. Various RAFT agents are now becoming commercially available, increasing the feasibility of this surface modification approach for manufacturing of antifouling membranes.

Electrospun nanofibrous membranes as part of composite membranes are becoming increasingly viable as a solution to provide ultrafiltration at lower operating pressure. Immobilization of enzymes on these high surface area materials may lead to membranes that are both inherently antifouling as well as capable of degrading pollutants that cannot be removed by conventional filtration processes.

Strategies for membrane filtration - recommendation

In summary, the results obtained from the strategies explored in this thesis bode well for the future of manufacturing inherently anti-biofouling membranes and may very well lead to making membrane filtration a more economically feasible means for potable water production, especially in the developing world.

Recommendations for membrane filtration include a two-step process: Firstly, reactive surfaces such as electrospun membranes with immobilized enzymes should be used as a pre-treatment to filtration processes (RO and UF) in order to remove and degrade organic foulants. Then, in turn, anti-cell adhesive modification of RO and UF membranes will assist in removing all organic remnants in solution without being susceptible to biofilm formation. The techniques developed in this study are easily scalable and should be employed as a final

step in the existing membrane manufacturing processes. This will allow for easy adoption by existing manufacturers and lead to fast tracking the roll-out of inherently antibiofouling materials for membrane filtration.

Future work

It will be worthwhile to test the anti-cell adhesive membranes produced in Chapter 3 under simulated conditions of actual filtration processes to assess their antibiofouling in both cross-flow and dead-end filtration processes.

The R-group approach of RAFT mediated polymerization of functional hydrophilic copolymers should be employed on different synthetic materials commonly used as filtration membranes, such as nylon and polysulfone in addition to further *in situ* ^{1}H-NMR studies for the optimization and understanding of the reaction conditions.

Design processes in which the surface grafting can be achieved on an industrial scale and investigate the economic feasibility of doing so.

This study showed that more than one enzyme can be immobilized on the same surface and it will be worthwhile to investigate more enzyme combinations targeting various degradation reactions in complex biological solutions.

Finally, include the nanofibers with immobilized enzymes in the composite membranes for water filtration and test their efficacy in pre-treatment of feed water to degrade foulants and pollutants that are currently difficult or impossible to remove from feed water streams.